PAPER-BASED TEST STRIP FOR PESTICIDE ANALYSIS

WANCHALEARM MANCHAN

A THESIS SUBMITTED IN PARTIAL FULFILLMENT OF
THE REQUIREMENTS FOR MASTER DEGREE OF SCIENCE
IN CHEMISTRY
FACULTY OF SCIENCE
BURAPHA UNIVERSITY
2024

แผ่นตรวจวัดแบบกระดาษสำหรับวิเคราะห์ยาฆ่าแมลง

วันเฉลิม มั่นจันทร์

วิทยานิพนธ์นี้เป็นส่วนหนึ่งของการศึกษาตามหลักสูตรวิทยาศาสตรมหาบัณฑิต
สาขาวิชาเคมี
คณะวิทยาศาสตร์ มหาวิทยาลัยบูรพา
2567

PAPER-BASED TEST STRIP FOR PESTICIDE ANALYSIS

WANCHALEARM MANCHAN

A THESIS SUBMITTED IN PARTIAL FULFILLMENT OF
THE REQUIREMENTS FOR MASTER DEGREE OF SCIENCE
IN CHEMISTRY
FACULTY OF SCIENCE
BURAPHA UNIVERSITY
2024

The Thesis of Wanchalearm Manchan has been approved by the examining committee to be partial fulfillment of the requirements for the Master Degree of Science in Chemistry of Burapha University

Advisory Committee

Principal advisor

.....

(Associate Professor Dr. Yupaporn Sameenoi)

Examining Committee

..... Principal examiner
(Dr. Nadnudda Rodthongkum)

..... Member
(Assistant Professor Dr. Napa Tangtreamjitmun)

..... Member
(Associate Professor Dr. Yupaporn Sameenoi)

..... Dean of the Faculty of Science
(Associate Professor Dr. Usavadee Tuntiwaranuruk)
.....

This Thesis has been approved by Graduate School Burapha University to be partial fulfillment of the requirements for the Master Degree of Science in Chemistry of Burapha University

..... Dean of Graduate School
(Associate Professor Dr. Witawat Jangiam)
.....

65910105: MAJOR: CHEMISTRY; M.Sc. (CHEMISTRY)

KEYWORDS: PAPER-BASED TEST STRIP /ORGANOPHOSPHAT AND CARBAMATE PESTICIDE/ENZYME INHIBITION ASSAY

WANCHALEARM MANCHAN : PAPER-BASED TEST STRIP FOR PESTICIDE ANALYSIS. ADVISORY COMMITTEE: YUPAPORN SAMEENOI, Ph.D. 2024.

A paper-based test strip for analysis of organophosphate (OPs) and carbamate (CBs) pesticide using enzyme inhibition acetylcholinesterase (AChE) has been developed. The device was constructed by immobilizing the AChE enzyme and Ellman's Reagent (DTNB) onto the detection zones of the paper devices. Biopolymers were employed for reagent coating and stabilizing to extend shelf life of the devices. In the absence of pesticides, the enzyme AChE catalyzed the formation of thiocholine (TC) that reacts with DTNB to produce a yellow product (TNB^-). After incubation with organophosphate pesticide, the activity of AChE was inhibited and produced less TC, and hence, reduced yellow product. Color intensity was analyzed by scanning the picture and measuring the intensity using ImageJ software. The developed paper-based test strip can analyze OPs and CBs pesticides without complicated methods and expensive laboratory instrument. Excellent limits of detection were obtained for all four pesticide representatives. Limits of detection as low as 1.34 µg/mL, 1.21 ng/mL, 1.36 µg/mL and 1.48 ng/mL were detected for malathion, dichlorvos, carbaryl and carbofuran, respectively. The developed paper-based test strip can be successfully used to detect pesticide contamination in dried seafood product samples (dried fish, dried squid, and dried shrimp) and the results were validated with those obtained from the traditional method (LC-MS/MS). The DSP level obtained from the two methods were not significant difference at 95% confidence level (two tailed $P>0.05$) indicating the high accuracy of the developed paper-based test strip. Therefore, the developed test can be used as an alternative method for the analysis of OP and CB pesticides offering low cost, rapid and on-site analysis, without complicated laboratory instrument.

ACKNOWLEDGEMENTS

This thesis was successfully completed with the great support of Associate Professor Dr. Yupaporn Samenoi, my advisor, and and Miss Benjarat Thasaengthong who provided advice, consultation, and meticulous corrections. They consistently supported and encouraged me, pushing forward ideas with care. I am extremely grateful and would like to express my deepest gratitude on this occasion.

Great appreciation is offered to all committee members for thesis defense, Asst. Prof. Dr. Napa Tangtreamjitmun and Dr. Nadnudda Rodthongkum and for proposal examination, Asst. Prof. Dr. Napa Tangtreamjitmun and Asst. Prof. Dr. Anan Athipornchai.

I would like to express my gratitude to all the faculty members of the Department of Chemistry, Faculty of Science, Burapha University, for their dedicated instruction in chemistry content and laboratory work, which has helped me grow into a competent and skilled scientist and and this research was supported by (i) Fundamental Fund: Grant no.25/2566 and (ii) the Center of Excellence for Innovation in Chemistry (PERCH-CIC)

Finally, I would like to express my gratitude to my beloved family and all my classmates who have supported me in every way, providing constant encouragement. I also wish to extend the benefits and knowledge gained from this thesis to all who have contributed to my growth and learning.

Wanchalearm Manchan

TABLE OF CONTENTS

Page

LIST OF TABLE

Page

LIST OF FIGURE

Page

CHAPTER 1
INTRODUCTION

1.1 Statement and significance of the problems

Pesticide has been extensively used worldwide to increase food security. Dried seafood products (DSPs) were one of the foods that have been reported to be contaminated by pesticides. The DSPs are widely favored in Thailand and other Asian countries due to their extended shelf life and good taste. DSPs are also a crucial source of protein, vitamins (B, D, and A), and essential minerals, including calcium, phosphorus, and iron, that are necessary for the body. Various methods, such as baking and sun drying, are employed to convert fresh seafood into DSPs. After the production process, DSPs are kept in warehouses awaiting export. During storage, it is necessary to use pesticides to protect DSPs from pests and insects (Kumar, Yadav, Saxena, Paul, & Tomar, 2021). As a result, pesticide contamination in DSPs is commonly detected and reported worldwide (Zhao & Talha, 2022). The most widely used pesticides are organophosphate (OPs) and carbamate (CBs) pesticides (Zhao & Talha, 2022).

OPs and CBs are responsible for over 200,000 fatalities worldwide each year due to the consumption of pesticide-contaminated food (Calista, Haikael, Athanasia, Neema, & Judith, 2022). These substances cause acute toxicity by inhibiting acetylcholinesterase (AChE) activity, leading to accumulating the neurotransmitter acetylcholine (ACh) in the body. This accumulation can cause organ failure and even lead to death (Sinha et al., 2021). Long-term exposure to these pesticides can affect various functions in the body, such as the nervous system, immune system, and hormone balance. High quantities of pesticides can cause life-threatening effects. In humans, acute poisoning symptoms appear within minutes and include headache, dizziness, nausea, vomiting, constricted pupils, excessive sweating, lacrimation, and salivation. The toxin also causes muscle weakness and spasms, changes in heart rate, and can lead to seizures and coma (Kamel & Hoppin, 2004).

Currently, several methods can be used to analyze OP and CB pesticide levels, such as liquid chromatography-mass spectrometry (LC-MS) and gas chromatography-mass spectrometry (GC-MS) (da Silva Sousa, do Nascimento, de Oliveira Gomes, & do Nascimento, 2021), high-performance liquid chromatography (HPLC) (X. Liu et al., 2022), enzyme activity inhibition assays (Zhai et al., 2022), and enzyme-linked immunosorbent assays (ELISAs) (X.-L. Yin et al., 2021). These techniques are efficient in analyzing OP and CB content since they can be quantified at low concentrations at the nanomolar level and have a low limit of detection (LOD). However, these methods have several limitations, such as high analysis cost, expensive instruments and laboratory-based and time-consuming analysis, need for highly trained technicians, and incapability to be performed on-site.

Currently, there are pesticide test kits available in the market such as the Government Pharmaceutical Organization (GPO) pesticide test kit, which is cheaper than the instrumental techniques mentioned above. However, this test kit involves several vials (Figure 1-1) (Janyawat T. Vuthijumnonk & Warawaran Shimbhanao, 2019) with multiple analysis steps that require heating solutions, long analysis time and trained personnel. It can only determine if the tested samples contain harmful or safe levels of pesticides (Yes or No), making it a low analytical sensitivity method. Moreover, the price of the test kit is quite expensive compared to other field test kits (1,300 baht per 10 samples). These limitations make it difficult for the consumer to access currently available field test kits for pesticides.

Therefore, the goal of this work is to develop the on-site pesticide test that is affordable, user-friendly and can provide rapid sample-to-answer analysis. The paper-based devices with enzyme inhibition assay are employed to accomplish this goal. Paper-based devices have the following advantages over other field test kits and traditional laboratory analytical methods including: (I) the device is made of low-cost material such as paper making it affordable for use in developing countries (II) paper-based device have excellent surface area and porosity making it easy to immobilize enzymes and chemicals and maintains catalytic stability of the enzymes as well (III) paper-based device is small and light making it portable to do on-site test.

Figure 1-1 Pesticide testing kit commercialized by GPO (Janyawat T Vuthijumnonk & Warawaran Shimbhanao, 2019)

Analysis of pesticides using the developed paper-based device relies on enzyme inhibition assay. As shown in Figure 1-2, the process involves the hydrolysis of acetylthiocholine (ATC) in water by acetylcholine esterase enzyme (AChE), which produces thiocholine (TC) and acetic acid (CH_3COOH). TC then reacts with 5,5'-dithio (2-nitrobenzoic acid) (DTNB) yielding a yellow color product of 5-thio-2-nitrobenzoic acid (TNB^-) as observed in a control area (C) of the paper-based device. In the presence of OP and CB pesticides, the activity of AChE enzyme is inhibited, resulting in a decrease in the catalytic hydrolysis of ATC and hence, less production of TC. As a result, the yellow color of the TNB^- product is reduced. The amount of pesticide in the sample can be monitored by observing the reduction of color in the test zone (T) of the paper-based devices relative to the control zone (C).

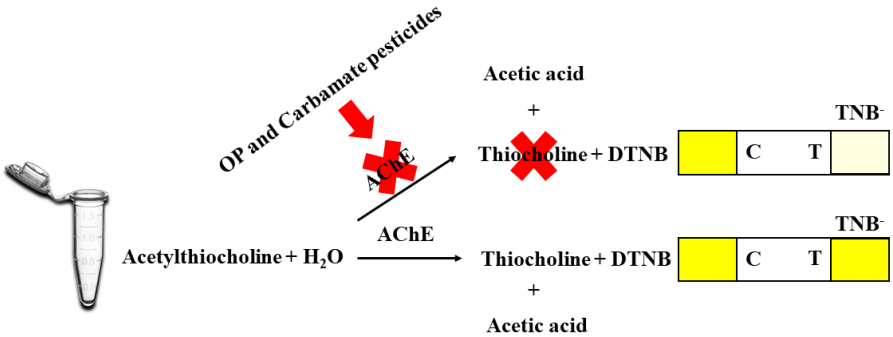

Figure 1-2 Principles of pesticide determination by enzyme inhibition assay on the paper-based devices

1.2 Objective

To develop a colorimetric paper-based test strip for the determination of pesticides in food samples using enzyme inhibition assay.

1.3 Contribution to knowledge

1. The developed paper-based test strip can be used to detect pesticides in food sample effectively.
2. The developed method provides user-friendly, rapid and accurate analysis with low-cost, and on-site applicability.
3. The general public can afford the developed test to monitor the contamination of pesticide in foods because of its low-cost and user-friendly to conduct the test.

1.4 Scope of study

1. Develop the paper-based test strips for OP and CB pesticide analysis using an enzyme inhibition assay.
2. Study the optimized conditions of the enzyme inhibition method for the analysis of pesticides using paper-based test strips.
3. Study the analytical performance characteristics of the developed paper-based assay including linear range, reproducibility (%RSD) and limit of detection (LOD) for pesticides analysis using OP and CB pesticide standards.
4. Study accuracy of the developed method by determining the percentage recovery from pesticide analysis in food samples. The method performance was investigated by comparing the accuracy of the developed method with the traditional method from the analysis of pesticides in food samples.

CHAPTER 2
LITERATURE REVIEWS

2.1 OP and CB pesticides

Pesticides are substances that are toxic and harmful to humans. They are widely used in agriculture to protect crops from pests and insects during planting, harvesting, and storage before they are ready for market (N. D. Chau, Z. Sebesvari, W. Amelung, & F. G. Renaud, 2015; N. D. G. Chau, Z. Sebesvari, W. Amelung, & F. G. Renaud, 2015). The residue of these chemicals can be detected in food items like fruits and vegetables, as a study found residues in over 21 plant samples, including a combination of imported products from Thailand (Skretteberg et al., 2015). Currently, pesticides are extensively used worldwide and provide significant economic and market benefits, as illustrated in Figure 2-1. However, they also pose significant health risks to humans and can contaminate various environmental elements such as soil, water, and air (Yadav et al., 2015).

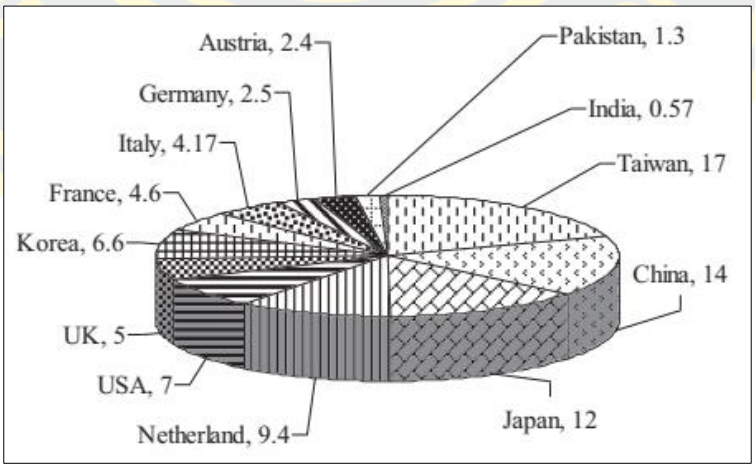

Figure 2-1 Distribution of pesticides worldwide (kg/m^2) (Yadav et al., 2015)

OP and CB pesticides are two widely used groups of pesticides due to their effectiveness in controlling insects and pests (S. Nouanthavong, D. Nacapricha, C. S. Henry, & Y. Sameenoi, 2016). Examples of OP pesticides are shown in Figure 2-2 including tetraethyl pyrophosphate, parathion, methyl-paraoxon, chlorpyrifos-oxon, fenthion, fenitrothion, malathion, dichlorvos and diazinon (Lorke & Petroianu, 2019). The examples of CB pesticides are shown in Figure 2-3 including isoprocarb, carbofuran, fenobucarb, carbaryl and methomyl (Mustapha, Halimoon, Johar, & Abd Shukor, 2019).

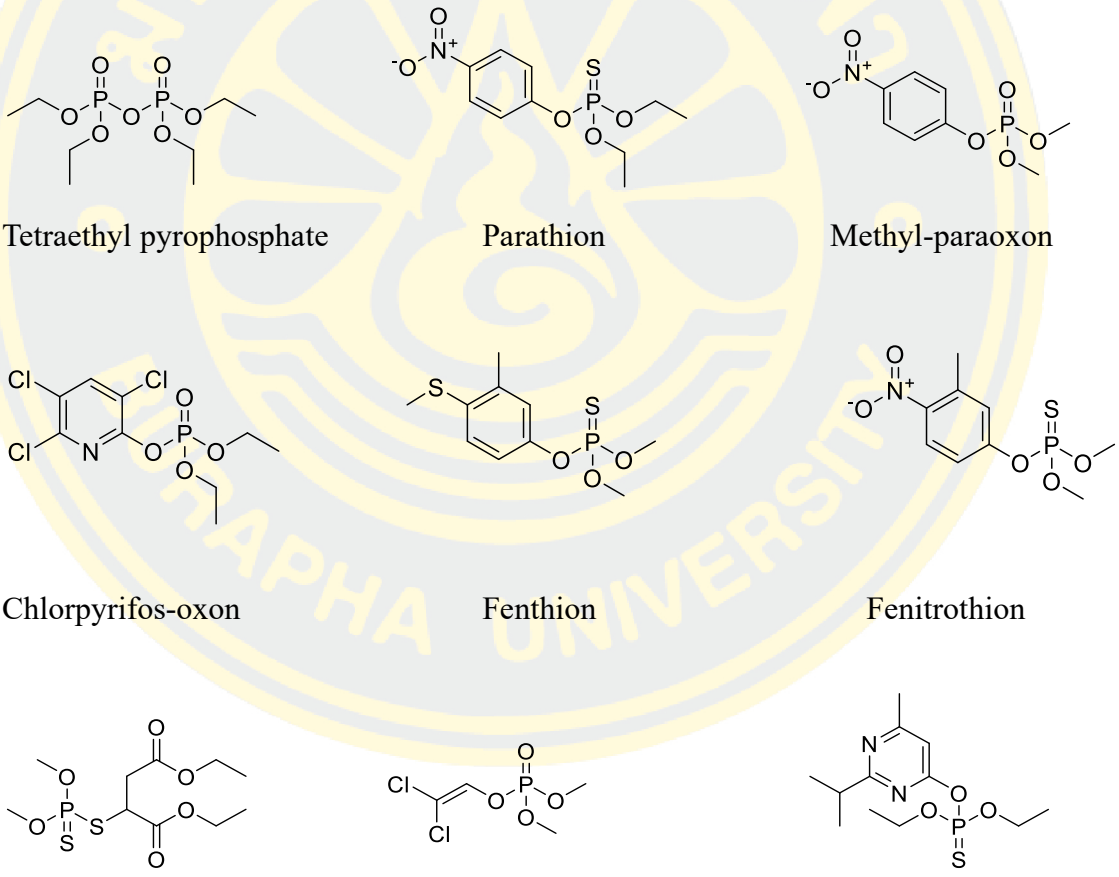

Figure 2-2 Examples of OP pesticides (Lorke & Petroianu, 2019)

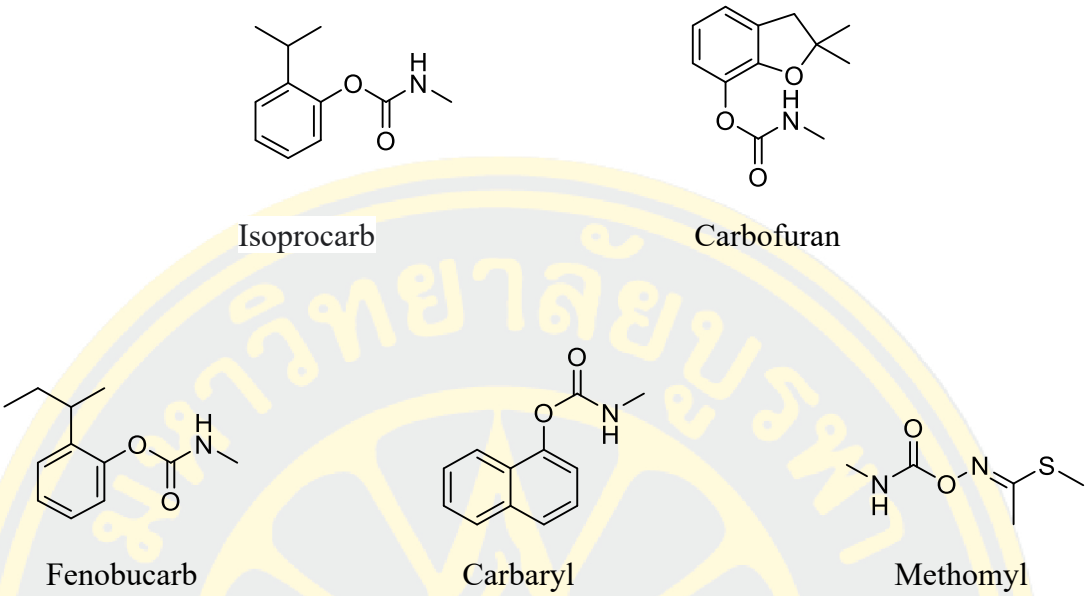

Figure 2-3 Examples of CB pesticides (Mustapha, Halimoon, Johar, & Abd Shukor, 2019)

2.2 Toxicity of OP pesticides

OP (OPs) compounds are derivatives of phosphoric, phosphonic, and phosphenic acids, in the form of amide, ester or thiol. The general formula of OP compounds is show in Figure 2-4 (Carullo, Cetrangolo, Mandrich, Manco, & Febbraio, 2015).

Molecular formula of organophosphorus compounds	
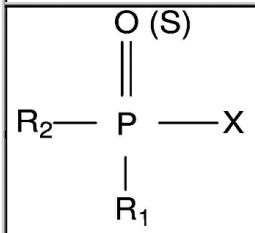	R_1 and R_2 are most commonly alkoxy groups, through other chemical substitutes are also possible; either an oxygen or a sulphur atom are also attached to the phosphorus with a double bond.
	X is the so-called "leaving group", that is displaced when the OP phosphorylates acetylcholinesterase (AChE), and is most sensitive to hydrolysis

Figure 2-4 General chemical structure of OP compounds (Carullo, Cetrangolo, Mandrich, Manco, & Febbraio, 2015)

OP pesticides are toxic due to their irreversible and permanent inhibition of the cholinesterase (ChE) enzyme in the central nervous system and other organs. The body has two types of cholinesterase enzymes: acetylcholinesterase (AChE) and pseudocholinesterase. AChE is present in both nervous system tissue and red blood cells and breaks down acetylcholine (ACh) through its enzymatic activity as shown in Figure 2-5. Butyrylcholinesterase (BChE) is another important cholinesterase enzyme found in peripheral nervous system and serous tissues. Its primary role is to hydrolyze ACh and eliminate toxins (Colovic, Krstic, Lazarevic-Pasti, Bondzic, & Vasic, 2013). The irreversible inhibition of AChE and BChE in the central nervous system caused by OP pesticide s leads to the accumulation of a significant amount of ACh in the body, which can damage the nervous system, cause organ failure, and pose life-threatening risks (Nouanthavong, Nacapricha, Henry, & Sameenoi, 2016).

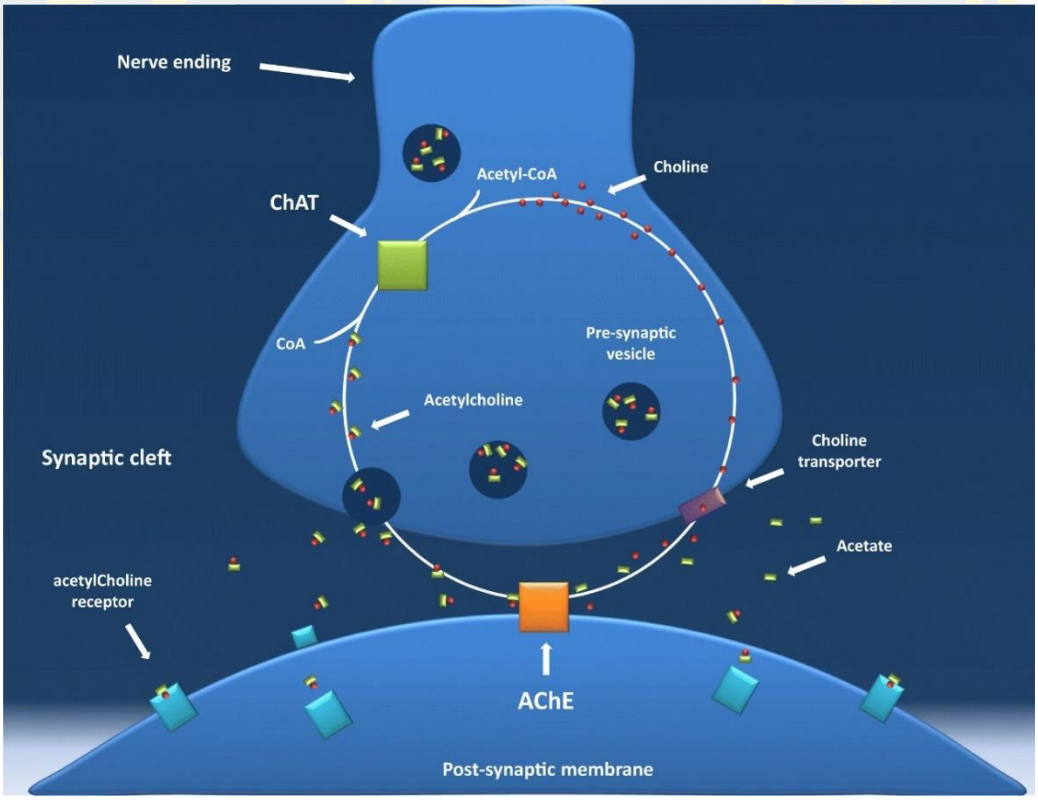

Figure 2-5 Catalytic mechanism of acetylcholinesterase enzyme (Assis et al., 2018)

2.2.1 Malathion (MAL)

Malathion (MAL) (*S*-(1,2-dicarboethoxyethyl)-*O*,*O*-dimethyl dithiophosphate) is a commonly used OP pesticide and is among the most frequently used pesticides today. Its chemical structure is shown in Figure 2-6. Because of its high efficiency and lower toxicity compared to other OP pesticides, it is widely used (Badr, 2020). Apart from its use as a pesticide, MAL has various other applications such as treating toenail infections, controlling mosquitoes, and eradicating head lice and nits.

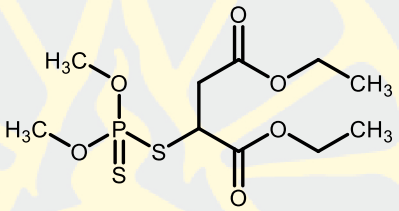

Figure 2-6 Chemical structure of MAL

The distillation method is widely used in the industry for producing MAL. (Flessel, Quintana, & Hooper, 1993). Refined MAL typically has a weight purity of 90-95%. Achieving a weight concentration of 100% for MAL is not feasible since it undergoes degradation upon exposure to oxygen. This oxidation process converts malathion to malaoxon, which is considered an impurity and can be found in the product of malathion, or potentially formed through the oxidation of malathion in air and soil, as shown in Figure 2-7 (Shamgsumova, Shurpik, Evtugyn, Stoikov, & Evtugyn, 2018).

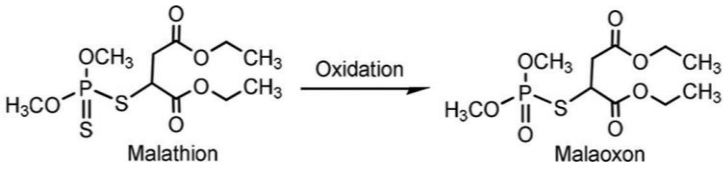

Figure 2-7 Oxidation reaction of malathion to malaoxon (Shamgsumova, Shurpik, Evtugyn, Stoikov, & Evtugyn, 2018)

The inhibition of the central nervous system enzyme AChE is the mechanism behind the toxicity of MAL in organisms, including humans (Badr, 2020). Ingesting MAL can cause acute toxicity leading to death or long-term effects such as psychosis, depression (Pereira et al., 2014), Alzheimer's and Parkinson's disease (Mohammadzadeh, Abnous, Razavi, & Hosseinzadeh, 2020). Reports suggest that there has been a rise in the level of MAL residues in the developing countries (Varol et al., 2015).

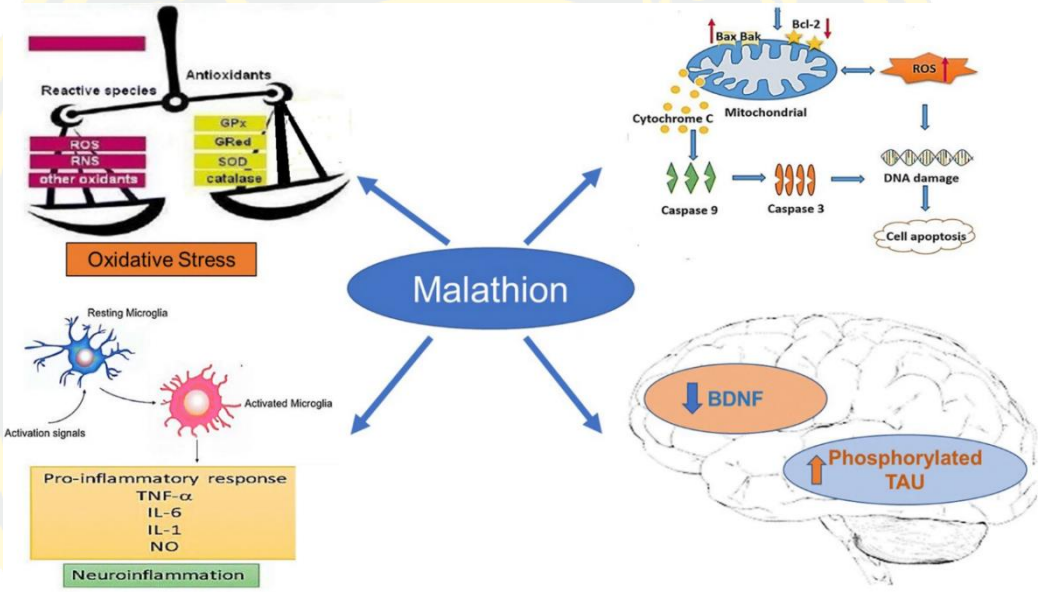

Figure 2-8 Non-cholinergic mechanism of malathion-induced neurotoxicity (Badr, 2020)

When MAL is applied to insects or agricultural areas, it can become airborne and pread over a wider area through the wind, potentially contaminating nearby water sources (LeNoir, McConnell, Fellers, Cahill, & Seiber, 1999). MAL undergoes efficient decomposition in alkaline water (pH > 7.0) with the presence of oxygen. In alkaline conditions, it undergoes hydrolysis shown in Figure 2-9 (Newhart, 2006). MAL does not cause any harm to plants, MAL can persist in fruits and vegetables even after being used as a pesticide. If large quantities of MAL are ingested by humans, it can harm the central nervous system. The maximum residue

limits (MRL) for MAL in cauliflower, cabbage, broccoli, citrus, chinese cabbage and kale were 0.5, 8, 5, 7, 8 and 3 mg/kg, respectively (ACFS, 2016).

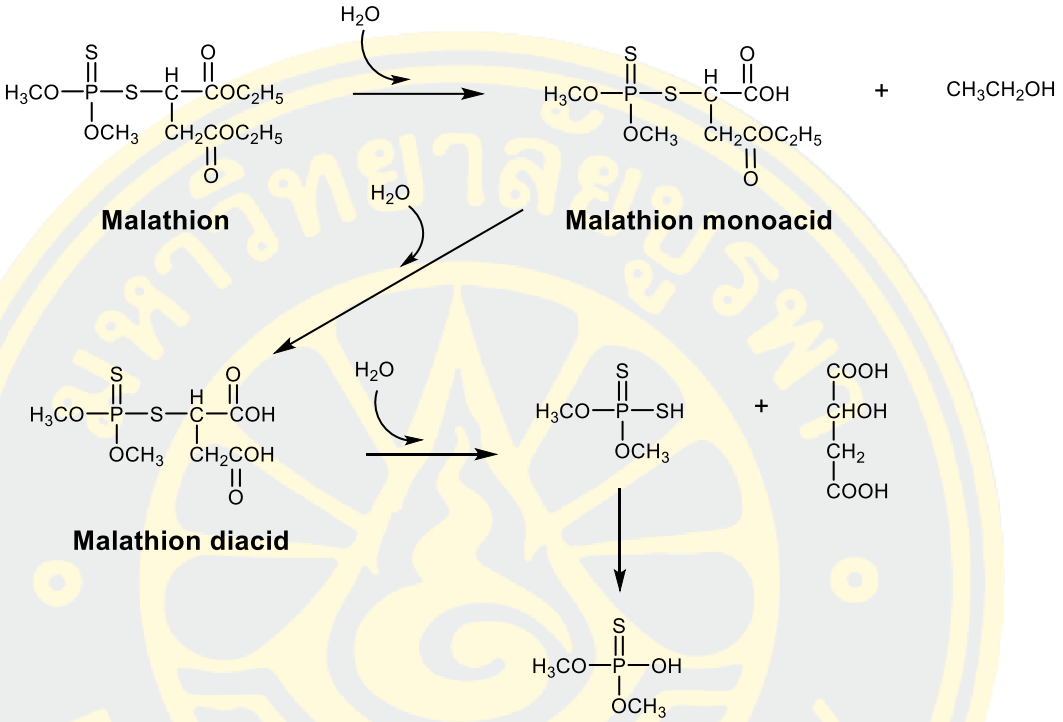

Figure 2-9 The decomposition of malathion by hydrolysis method in base water (Newhart, 2006)

2.2.2 Dichlorvos (DDVP)

Dichlorvos (DDVP) (2,2-dichlorovinyl dimethyl phosphate) is another OP pesticide that is considered the primary pesticide used for insect control in developing countries (Binukumar & Gill, 2010). DDVP is commonly used as pesticides in households and in residential areas. DDVP has a molecular mass of 220.98 g/mol and a molecular formula of $C_4H_7Cl_2O_4P$. The chemical structure of DDVP is shown in Figure 2-10. The World Health Organization classifies DDVP as a highly hazardous chemical, Category IB (WHO, 1995). One industrial method for producing DDVP involves the dehydrochlorination of trichlorfon in alkaline conditions at a temperature range of 40-50 °C (Fernandes et al., 2015).

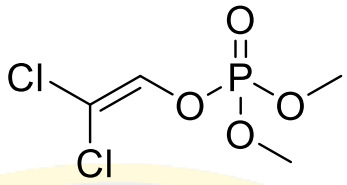

Figure 2-10 Chemical structure of DDVP

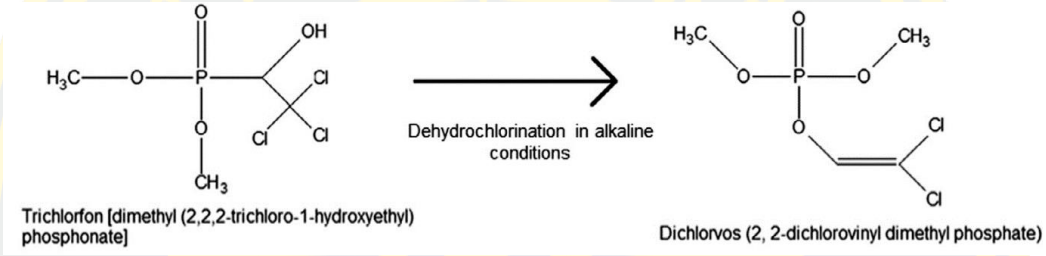

Figure 2-11 Dehydrochlorination reaction of trichlorfon (Fernandes et al., 2015)

The toxicity of DDVP to human health toxicity involves the mechanism of enzyme inhibition where irreversible inhibition of the central nervous system enzyme AChE causes slow heartbeat, nausea, vomiting, watery eyes, drooling, diarrhea, and possibly death (Deka & Mahanta, 2015; Okoroiwu & Iwara, 2018). DDVP does not undergo photolysis when it is dispersed in the environment and exposed to UV light wavelengths greater than 240 nm as it does not absorb such wavelengths. As a result, dichlorvos remains in the air for a long time until it comes into contact with water and decomposes by hydrolysis shown in Figure 2-12. DDVP is hydrolyzed into dichloroethanol, dichloroacetaldehyde, dichloroacetic acid, phosphate and eventually decomposes into carbon dioxide. The degradation of DDVP via hydrolysis is more pronounced under alkaline conditions. DDVP is rapidly excreted in the urine once ingested and is detoxified in the liver to be excreted as urea (Okoroiwu & Iwara, 2018). The maximum residue limits (MRL) for DDVP in citrus fruits, poultry and milk were 0.2, 0.05 and 0.02 mg/kg, respectively (ACFS, 2016).

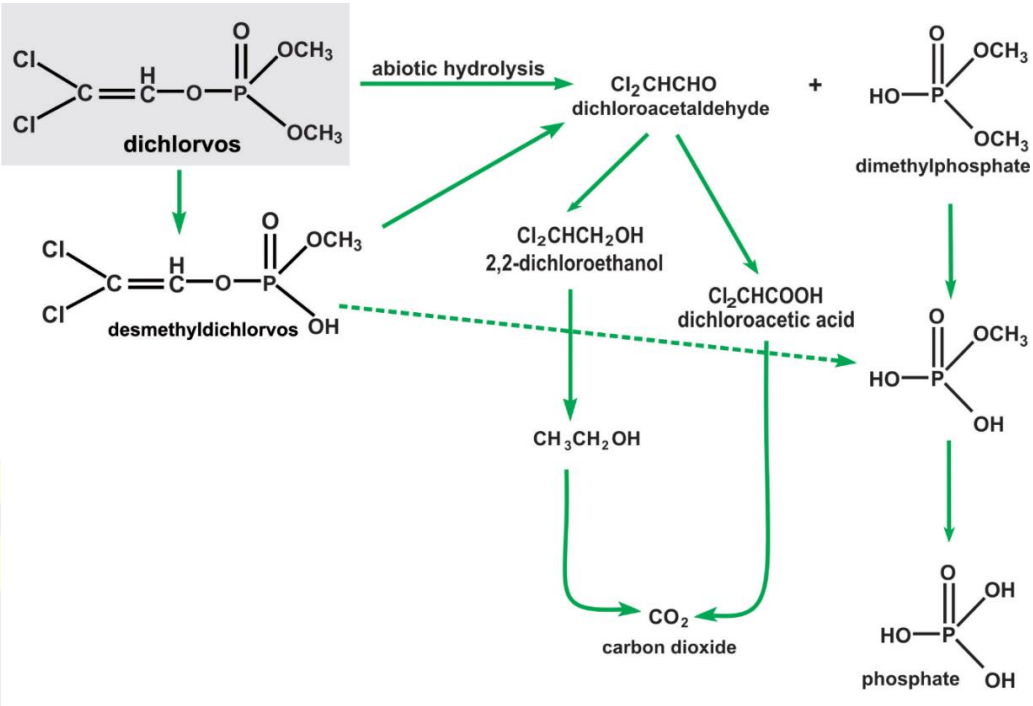

Figure 2-12 Hydrolysis mechanism of DDVP in water (Okoroiwu & Iwara, 2018)

2.3 Toxicity of CB pesticides

CB compounds (CBs) are carbamic acid derivatives (NH_2COOH). The general formula of CBs compounds is shown in Figure 2-13.

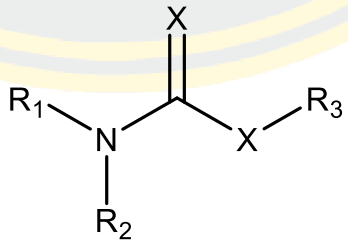

Figure 2-13 General chemical structure of CB compounds

From the CBs structure in Figure 2-13, groups R_1, R_2 and R_3 are alkyl or hydrogen groups, and X group can be either oxygen or sulfur atoms (Colovic et al., 2013). The toxicity of CBs pesticides is attributed to the inhibition of the enzyme

cholinesterase (ChE), which is a reversible process that occurs in the central nervous system and in the body's joints. The AChE inhibition mechanism CBs is similar to that of OPs by generating an accumulation of ACh but less amount than OPs. This is because the hydrogen bonding between the enzyme and CBs is less stable than that of the enzyme and OPs. As a result, CBs pesticides can be separated from the active site of AChE by decarboxylation reaction (Darvesh et al., 2008). Therefore, CBs pesticides are considered safer than OP pesticide s as they have a less stable mechanism for inhibiting AChE enzymes (Silva, Assis, Oliveira, Carvalho, & Bezerra, 2013).

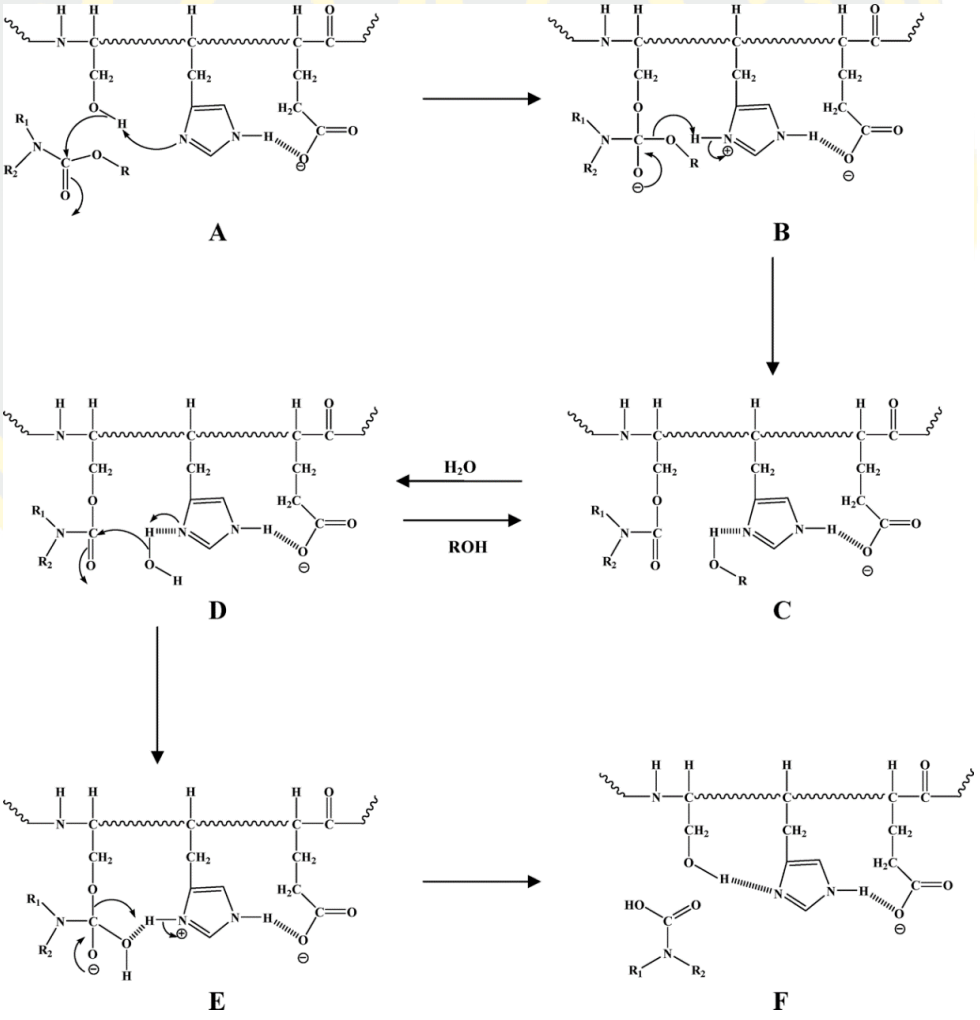

Figure 2-14 AChE inhibition mechanism and dissociation mechanism of CB pesticides (Darvesh et al., 2008)

2.3.1 Carbaryl (CAR)

Carbaryl (CAR) is known as Sevin (1-naphthyl-N-methyl CB) and its chemical structure is shown in Figure 2-15. CAR is a derivative of N-methyl carbamic acid (Mishra et al., 2021), its molecular weight is 201.22 g/mol and its molecular formula is $C_{12}H_{11}NO_2$. CAR is a type of CB pesticide that is widely used worldwide and is used as a replacement for OP pesticide s due to its residual toxicity in the environment less (Gunasekara, Rubin, Goh, Spurlock, & Tjeerdema, 2008).

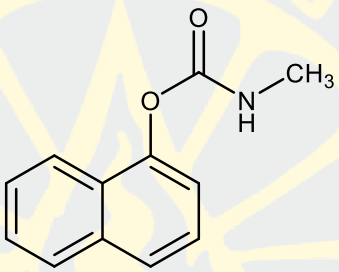

Figure 2-15 Chemical structure of CAR

CAR is commonly used for insect control in agricultural areas. There are two methods for producing CAR in the industry, both of which differ in the use of methyl isocyanate as demonstrated in Figure 2-16. In Figure 2-16A, methyl isocyanate is prepared first by reacting methyl amine with phosgene and then the obtained methyl isocyanate reacts with 1-naphthol to obtain CAR molecules. In Figure 2-16B, 1-naphthol was first reacted with phosgene to form 1-naphthyl chloroformate which subsequently reacted with methyl amine to form a CAR molecule. Processes without methyl isocyanate are more preferable because of lower toxicity.

The toxicity mechanism of CAR, a CBs pesticide, is similar to that of OP pesticide s which involves the inhibition of the AChE. This inhibition leads to an accumulation of ACh and acute toxicity in the body, resulting in convulsions, paralysis, and even death (Gunasekara et al., 2008). Unlike some other pesticides, CAR has a relatively low molecular weight, which makes it less likely to volatilize in the air, thus remaining in the atmosphere for an extended period after application.

Although CAR only decomposes via photolysis in the presence of free hydroxyl in the air, it can easily undergo hydrolysis in alkaline water, with 1-naphthol being the primary hydrolysis product (Mishra et al., 2021). The maximum residue limits (MRL) for CAR in citrus fruits, lychees, grapes and milk were 7, 1, 0.5 and 0.05 mg/kg, respectively (ACFS, 2016).

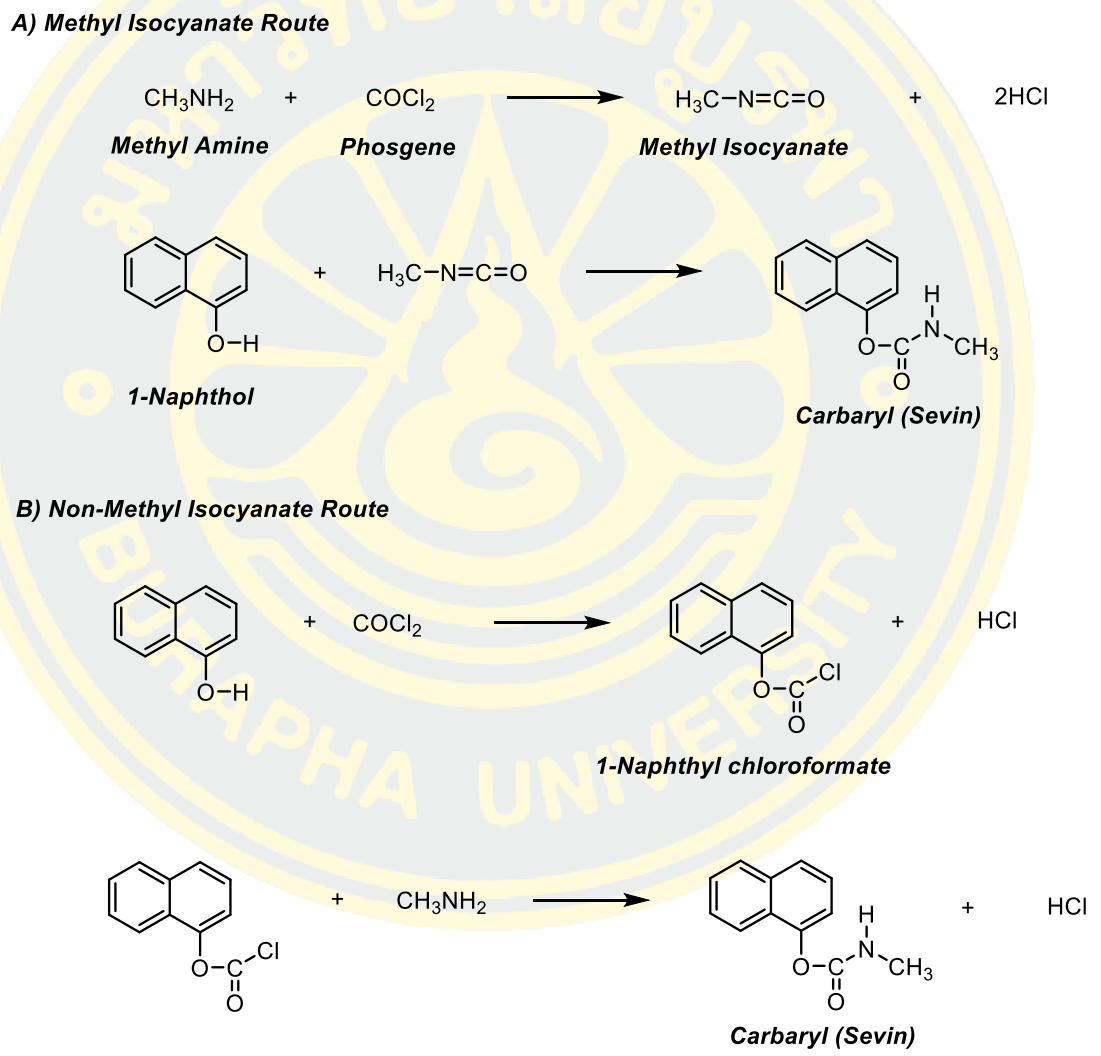

Figure 2-16 Industrial carbaryl production process, A) methyl isocyanate route and B) non-methyl isocyanate route (Gunasekara et al., 2008)

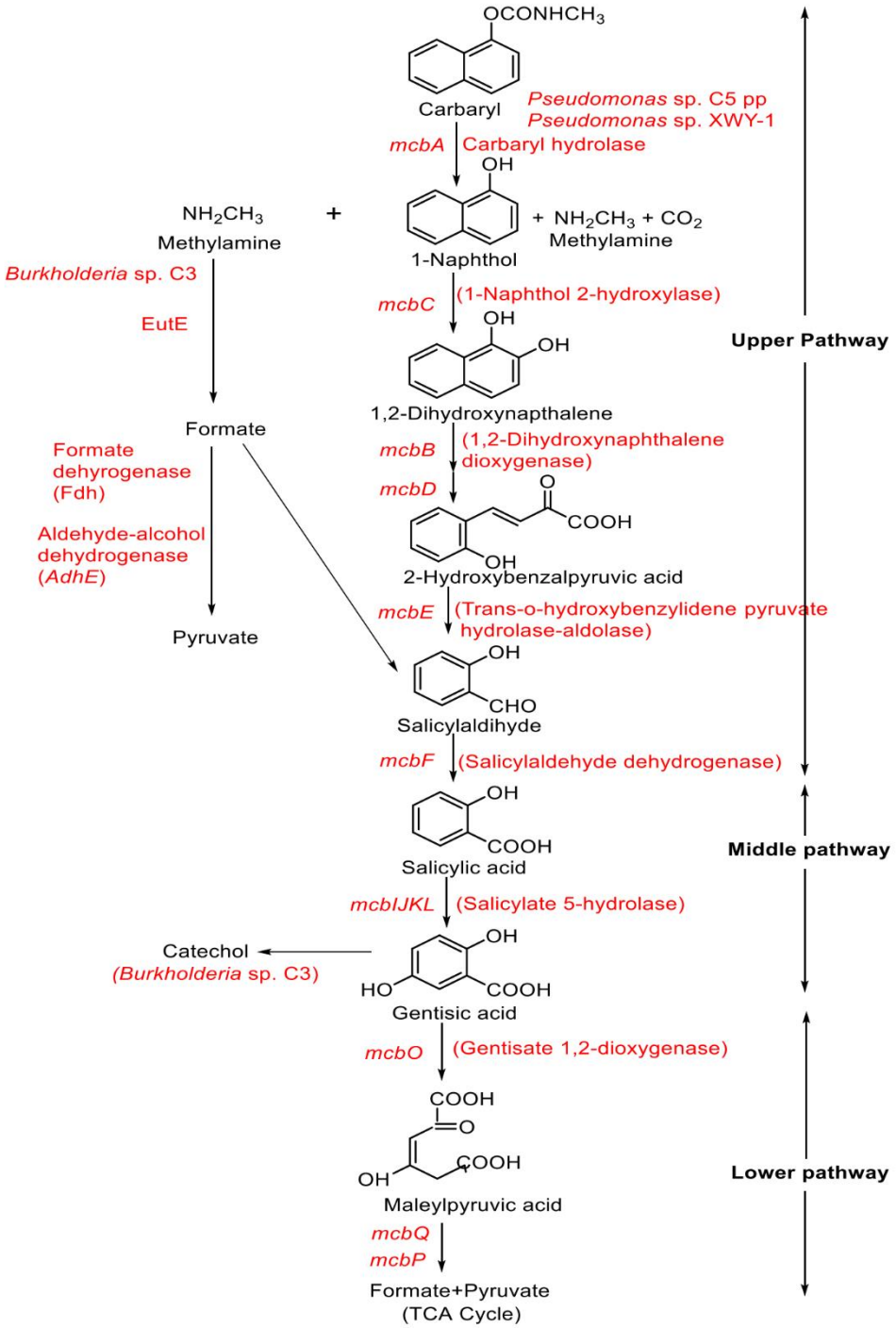

Figure 2-17 CAR degradation pathway (Mishra et al., 2021)

2.3.2 Carbofuran (CBF)

The structure of carbofuran (CBF) or (2,3-dihydro-2,2-dimethy-7-benzofuranyl-N-methylCB) is shown in Figure 2-18. It is a commonly used CBs in agricultural and residential areas, communities and in parks for insect control (Mishra et al., 2020). CBF has relatively good water solubility and can remain in the water and in the soil as well (Brkic, Vitorovic, Gasic, & Neskovic, 2008). It is classified as N-methyl CB type 1 pesticide with ester and amide linkage (Gupta, Rathour, Singh, & Thakur, 2019).

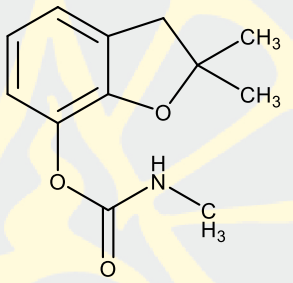

Figure 2-18 Chemical structure of CBF

Both liquid and tablet forms of CBF are available for commercial use, each with varying levels of risk and toxicity. Tablets are generally considered to be a safer option than liquids because they do not diffuse into the air, making them safe for both users and bystanders. However, CBF pellets, which are used in agriculture, can pose a threat to birds, as they may be mistaken for food and ingested, leading to potential mortality (Onunga et al., 2015). CBF induces toxicity via the inhibition of enzymes, especially AChE, which is comparable to other pesticides that affect the central nervous system. Ingestion of high doses of CBF can result in clinical symptoms such as fainting, loss of consciousness, tearing, drooling, diarrhea, muscle spasms, convulsions, and potentially death (HSDB, 2011). CBF decomposition occurs in air, water and soil similar to other pesticides by hydrolysis as shown in Figure 2-19. The maximum residue limits (MRL) for CBF in rice, cruciferous vegetables, citrus fruits and tomatoes were 0.1, 0.03, 0.02 and 0.1 mg/kg, respectively (ACFS, 2016).

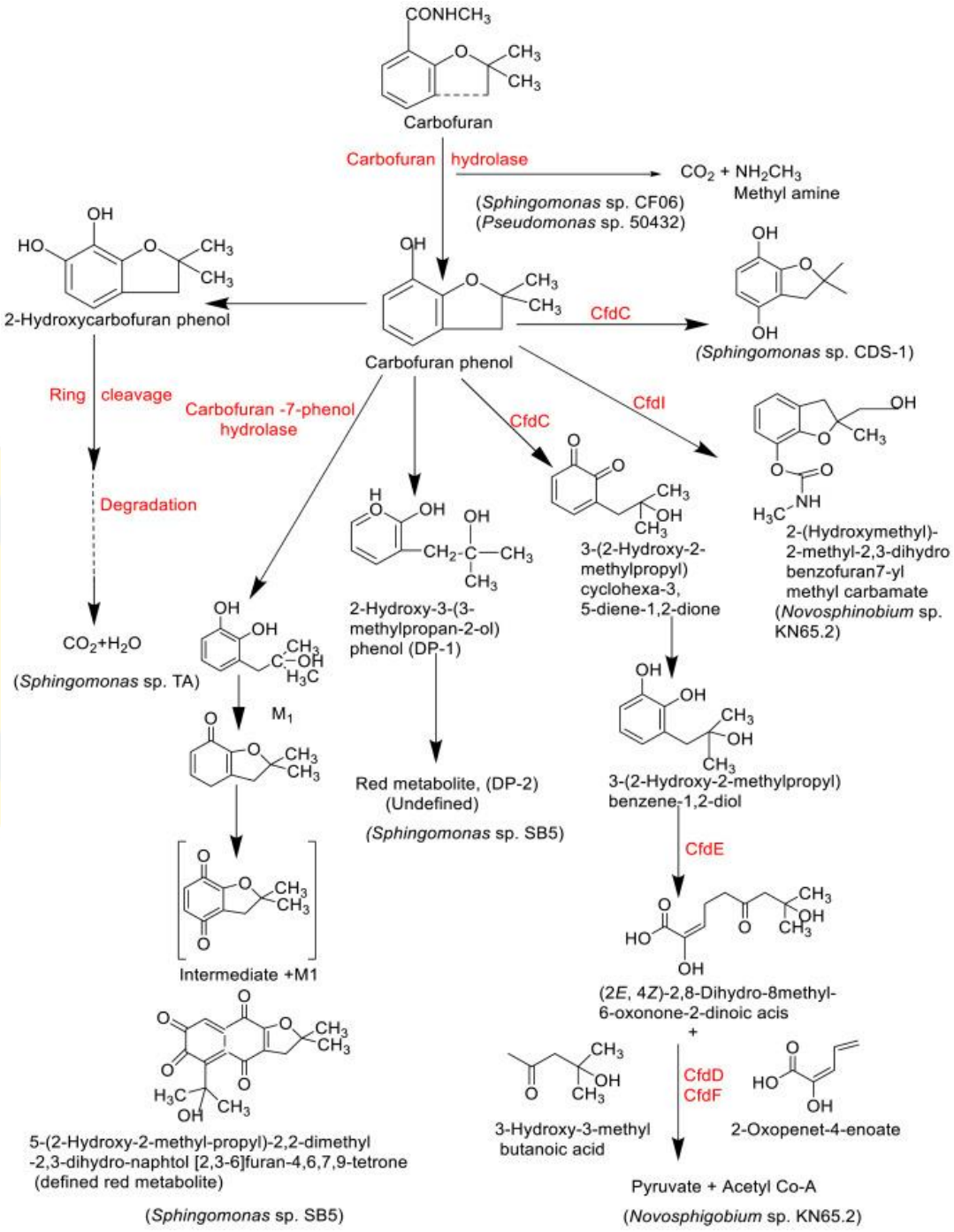

Figure 2-19 CBF degradation pathway by hydrolysis process in air, water and soil (Mishra et al., 2021)

2.4 Interaction between AChE and pesticides

The active site of the AChE molecule has an elliptical shape with narrow and deep channels, with a depth of 20 Å and a narrowest point of 4 Å. The Acyl pocket is formed by several aromatic residues located on the internal surface, such as Phe 297 and Phe 295. Trp 86 is a constituent of the choline binding site. Glu 534, His 447 and Ser 203 are constituents of the catalytic triad of AChE, organized as an esteric subsite where ACh is hydrolyzed to choline and acetate. It consists of three amino acid subunits: serine, histidine and glutamate. And Trp 286 and Asp 74 are components of the peripheral binding site located at the strait mouth (Colovic et al., 2013).

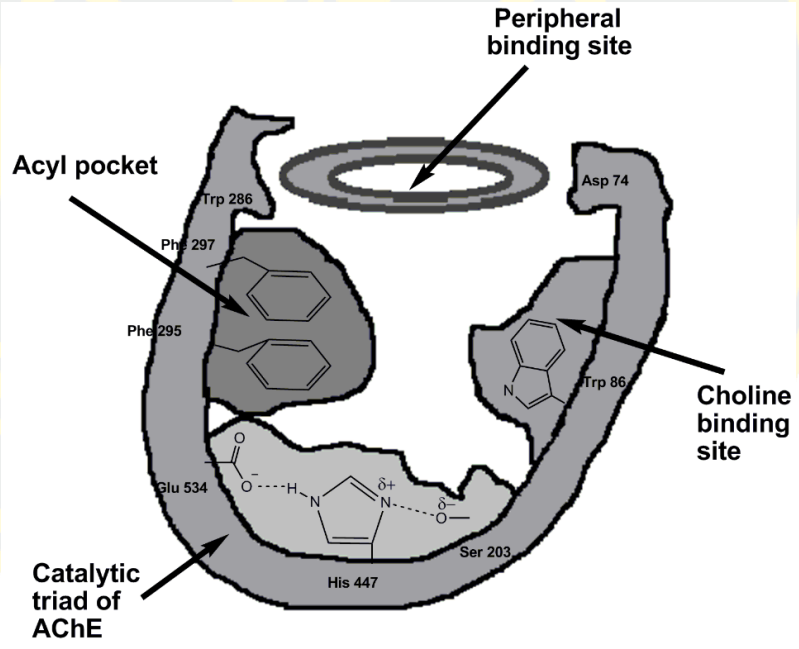

Figure 2-20 Schematic representation of AChE binding sites (Colovic et al., 2013)

OPs and CBs pesticides interact with the AChE enzyme at the esteric site, and the stability of the resulting complex is determined by the chemical structure of the pesticide (Assis et al., 2018). In the absence of pesticides, the negatively charged site of the AChE enzyme induces the ACh molecule at the positively charged quaternary amine region. Consequently, the carbonyl group of ACh moves closer to

the -OH group of serine at the esteric site in the presence of AChE enzyme, leading to the breakdown of ACh into Ch and acetic acid as shown in Figure 2-21A. When OP pesticide s are present, the positively charged alkyl group (R_L) of the pesticide is induced by the anionic site of the AChE enzyme. As a result, the phosphorus atom in the positive phosphate group moves closer to the -OH group of the negative serine as shown in Figure 2-21B. The R_L group forms a bond with the phosphorus atom, and simultaneously, the phosphorus atom of the phosphate group forms a new bond with the oxygen atom of serine, shown in Figure 2-21C. The OP pesticide binds to the -OH group of serine, blocking it at the esteric site and preventing it from decomposing ACh to Ch, as shown in Figure 2-21D.

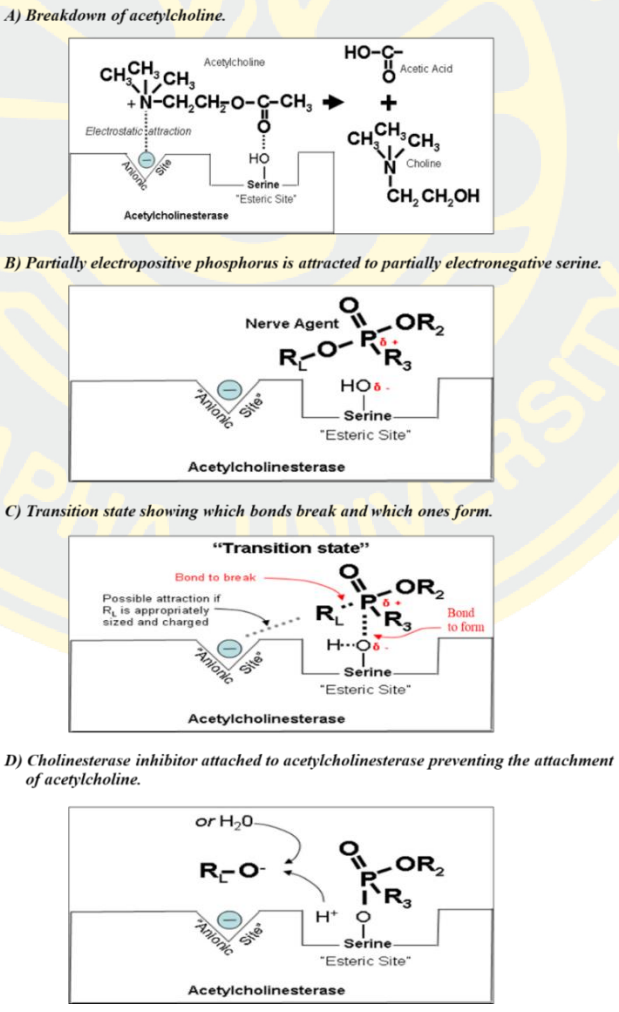

Figure 2-21 Interaction between AChE and pesticides (Health & Services, 1999)

2.5 Current methods for analysis of Pesticides

Currently, there are several methods have been developed to detect OPs and CBs pesticides in biological samples and environmental samples including gas chromatography (GC) (Theurillat, Dubois, & Huertas-Perez, 2021), high-performance liquid chromatography (HPLC) (Keikavousi Behbahan, Mahdavi, Roustaei, & Bagheri, 2021) gas chromatography-mass spectrometry (GC-MS) (Hosseini et al., 2021), liquid chromatography-mass spectrometry (LC-MS) (Gallo et al., 2021), enzyme linked immunosorbent assays (ELISA) (Yin, Qian, Wang, Wan, & Zhou, 2021) and enzyme inhibition assays (Habenschus et al., 2021). Of these methods, GC-MS and LC-MS seem to be the most effective method for pesticides detection due to its reproducibility and high analytical sensitivity. However, they still have some limitations. For example, they require expensive instrument-based analysis and well-trained personnel to operate resulting in high analytical costs per (S. Nouanthavong et al., 2016).

Some electrochemical techniques have also been developed for the analysis of pesticides such as cyclic voltammetry (CV) and amperometry (Tang & Wu, 2014). The use of traditional ELISA and enzyme inhibition techniques are an alternative method for pesticide determination due to its lower analytical cost and shorter analytical time. However, conventional enzyme inhibition methods require sophisticated techniques for determination such as spectrophotometry, fluorescence spectrophotometry and chemiluminescence spectrophotometry and electrochemistry. These detection methods require expensive equipment to operate, which makes them unsuitable for field testing of pesticides (S. Nouanthavong et al., 2016).

2.6 Enzyme inhibition assay

The principle of analyzing OPs and CBs pesticides using the enzyme inhibition test method is based on the inhibition of AChE activity. The AChE acts as a catalyst within the body to break down the neurotransmitter ACh into Ch and acetate as shown in Figure 2-22A. In the presence of OPs and CBs pesticides, the activity of AChE is inhibited and hence, reducing the capability to convert ACh shown in Figure 2-22B and Figure 2-22C.

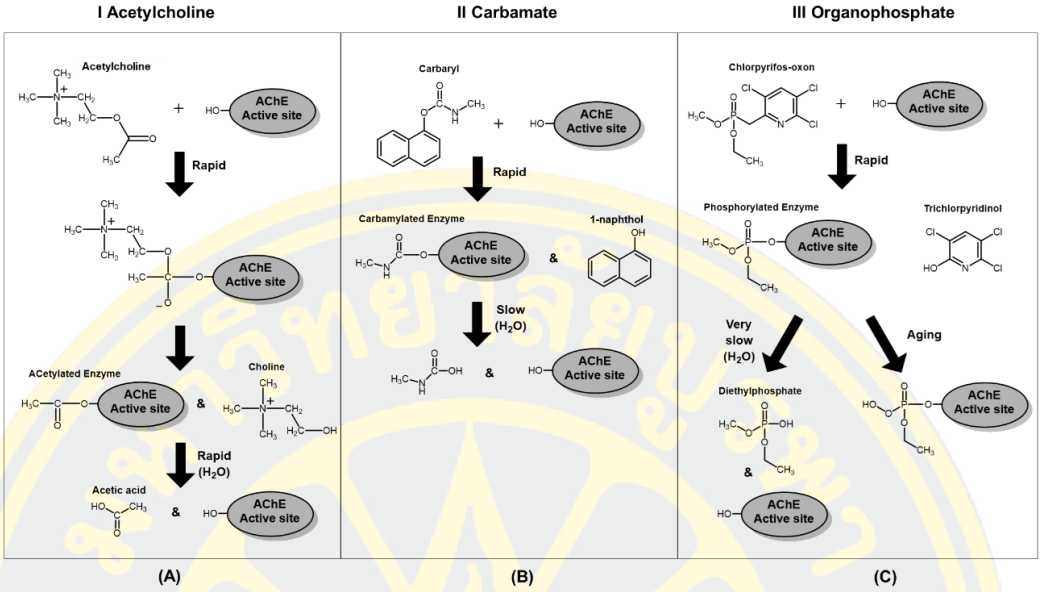

Figure 2-22 Schematic representation of the interaction of acetylcholine (A) and carbaryl, an CB pesticide (B) and chlorpyrifos-oxon, an OP pesticide (C) with the active site of AChE (TIMCHALK, 2006)

Based on previous research, the most commonly used methods for detecting pesticide involves measuring the amount of hydrogen peroxide (H_2O_2) produced from enzyme inhibition assay. The principle behind this assay is based on the catalytic activity of two enzymes, AChE and choline oxidase (ChOX) (S. Nouanthavong et al., 2016) as shown in Figure 2-23. The enzymes AChE and ChOX catalyze the production of H_2O_2 in the present of ACh. The quantity of H_2O_2 was subsequently measured by detecting the color change of nanoceria particles that were immobilized on a paper-based device, causing them to shift from white to yellow. In the samples containing pesticides, the activity of the AChE enzyme was reduced, which resulted in a lower production of H_2O_2 as a product. The detection signal generated by the nanoceria particles in response to H_2O_2 was inversely proportional to the pesticide concentration present in the sample. This method can be used to quantify the level of pesticide present in a given sample. However, the cost of this method is relatively high as it requires the use of two enzymes.

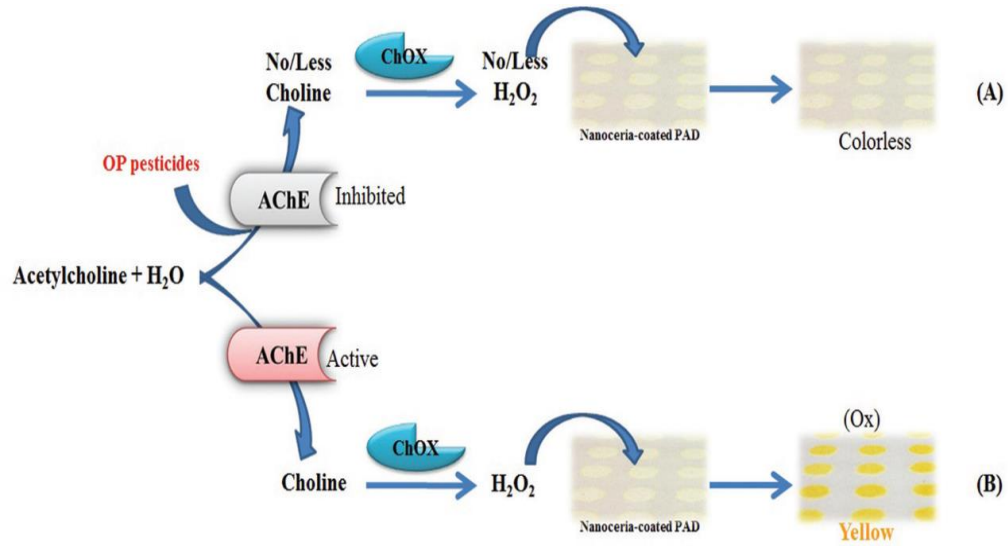

Figure 2-23 A paper-based device for the analysis of OP pesticides using enzyme assays and nanoceria particles and when the pesticides was added, the activity of AChE was inhibited, resulting in to have less H_2O_2 and make the color of nanoceria less (A) without the addition of pesticides, the activity of AChE is normally activated in the produced of H_2O_2 (B) (S. Nouanthavong et al., 2016)

This study aimed to develop a cost-effective approach for analyzing pesticides by modifying the method that uses only AChE and Acetylthiocholine (ATC) as the substrate, in combination with Ellman's reagent or DTNB (5,5'-dithiobis [2-nitrobenzoic acid]), instead of the two-enzyme method previously used. The reaction is shown in Figure 2-24.

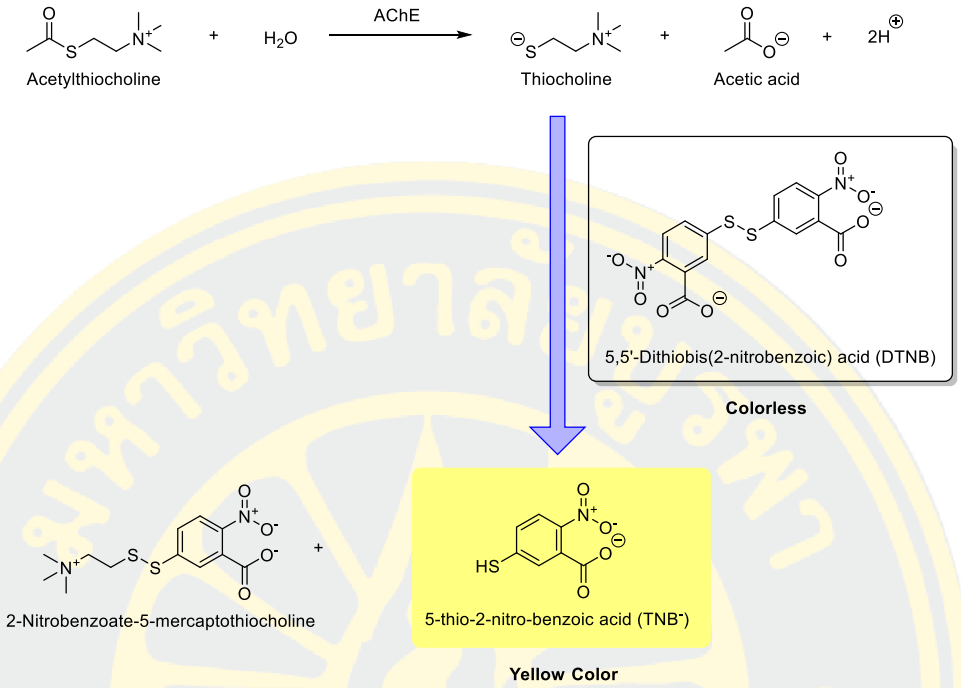

Figure 2-24 Catalytic hydrolysis of AChE in the reaction between ACh and thiocholine (TC) with Ellman's reagents

2.7 Paper-based device for pesticide analysis

Currently, microfluidic paper-based analytical devices (µPADs) are attractive to for chemical analysis as it is a portable and easy-to-use technology that allows for rapid analysis. µPADs have found applications in various fields, including environmental monitoring, food quality control and biological analysis (Cate, Adkins, Mettakoonpitak, & Henry, 2015; Hu et al., 2014; Yetisen, Akram, & Lowe, 2013). The paper-based device comprises two parts including a hydrophilic area and a hydrophobic area (Cate, Dungchai, Cunningham, Volckens, & Henry, 2013; Sameenoi et al., 2013). The pattern is formed by impregnating a hydrophobic material barrier on the paper, which guides the liquid in the desired direction and defines the region for the reaction to be detected shown in Figure 2-25.

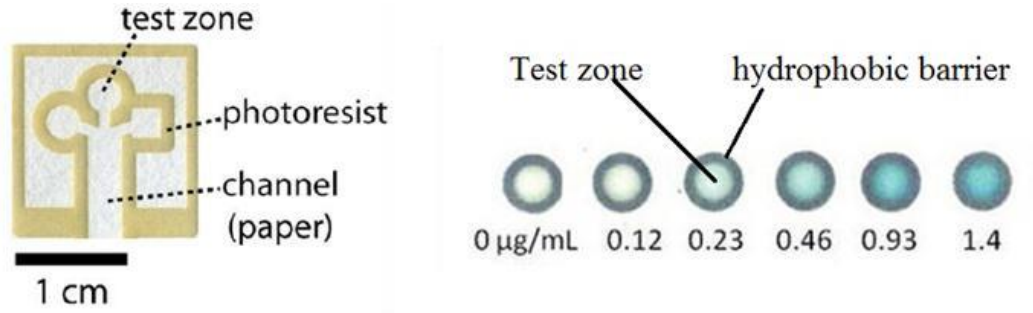

Figure 2-25 Typical µPADs with various test zone designs (Jokerst et al., 2012)

2.8 Related literature review

Nouanthavong et al. (2016) reported paper-based devices for OP pesticide analysis using enzymatic inhibition assay and nanoceria. The analysis is based on assay shown in Figure 2-23 by detecting H_2O_2 using nanoceria. H_2O_2 is produced in the presence of AChE and ChOX and detected a paper-based device coated with nanoceria, resulting in a yellow color. When there is the presence of OP pesticides, the AChE was inhibited, resulting in lesser formation of H_2O_2, and a decrease in the intensity of the yellow color on the paper-based device. This test can detect OP pesticides without requiring complex instrumentation, and the limit of detection for methyl-paraoxon was 18 ng/mL and for chlorpyrifos-oxon was 5.3 ng/mL shown in Figure 2-26. The samples were also analyzed by comparison using liquid chromatography-mass spectrometry (LC-MS) and the results obtained from the two methods were similar. This suggests that this approach is reliable and appropriate for the detection of pesticides in real samples.

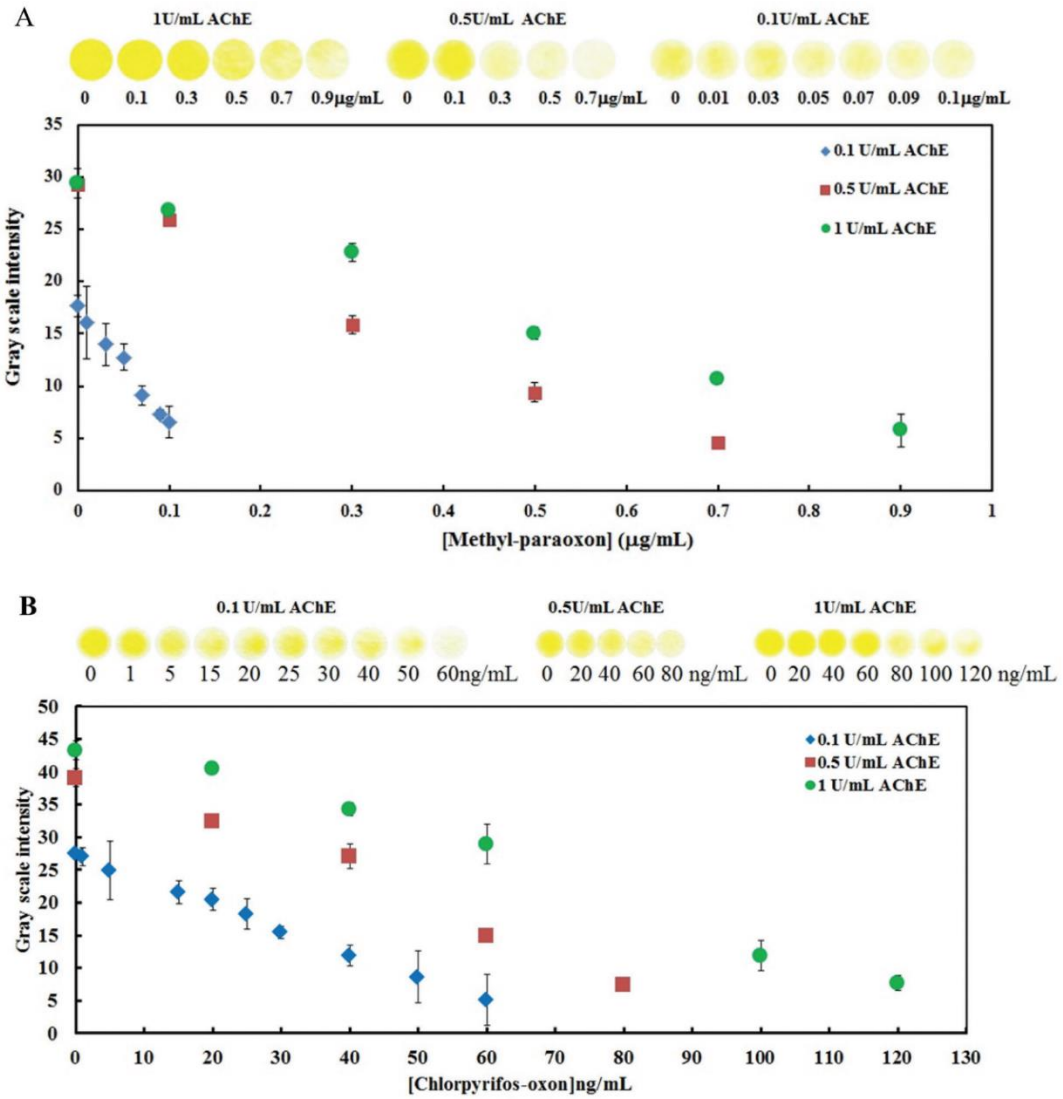

Figure 2-26 Graph showing the relationship between the detected color intensity and the concentration of the pesticide, methyl-paraoxon (A) and chlorpyrifos-oxon (B) (Nouanthavong et al., 2016)

Promphet et al. (2019) reported a textile-based color sensor developed for the simultaneous detection of both sweat pH and lactic acid. The reagents were immobilized by coating with three different bio-polymer layers to stabilize the reagents and increase assay sensitivity: 1) Chitosan (CS) 2) Sodium Carboxymethyl Cellulose (NaCMC) and 3) Indicator dye on the cloth. This sensor was then used to detect the pH and lactate concentration using the sweat sample. The color sensor

changes from red to blue when the pH in sweat increases, and the intensity of the purple color increases with the concentration of lactate in sweat shown in Figure 2-27.

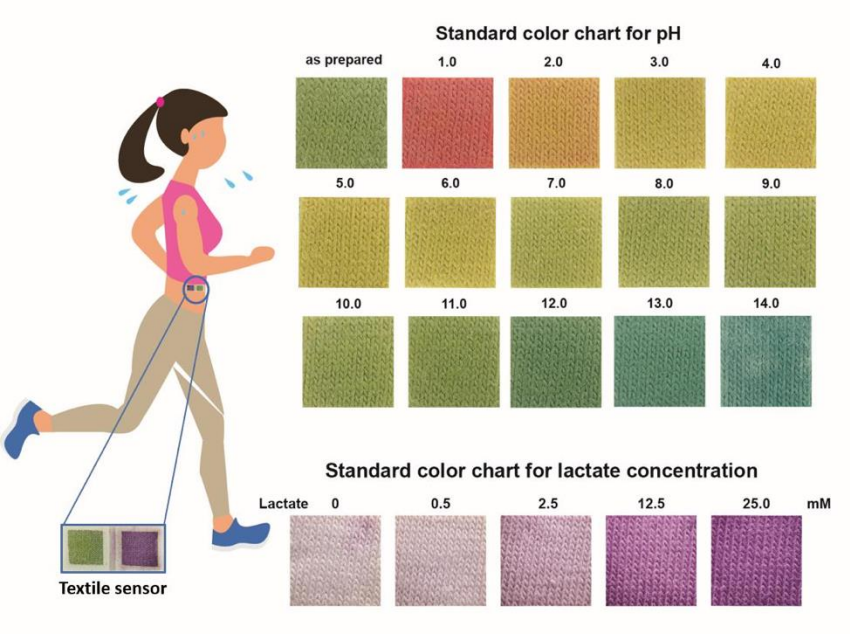

Figure 2-27 Standard color chart for of pH (top) and lactate concentration (bottom) (Promphet et al., 2019)

The process of reagent immobilization on the detection used in this work is as follows; Firstly, the chitosan solution (2 % (w/v)) prepared in 1 % (v/v) acetic acid under continued stirring and 5% (w/w) citric acid was coated on a cotton cloth and dried at 100 °C for 180 s. The next layer was employed by screen-printing the dye reagents for pH measurement including bromocresol green (BCG) and methyl orange (MO) prepared in CTAB and NaCMC was screen-printed on cotton coated with chitosan solution and heated at 170 °C for 150 s as shown in Figure 2-28. For the third layer, 2.5 % (w/v) NaCMC was dissolved using deionized water to coated the NaCMC-CTAB-indicator, then the cotton was then soaked with 0.25 % (w/v) $AlCl_3$ to construct the structure of NaCMC-Hydrogel by chemical crosslinking. After that, the cotton cloth was then immersed in deionized water at least three times to remove excess dye and $AlCl_3$. The sensor was dried at 100 °C for 300 s.

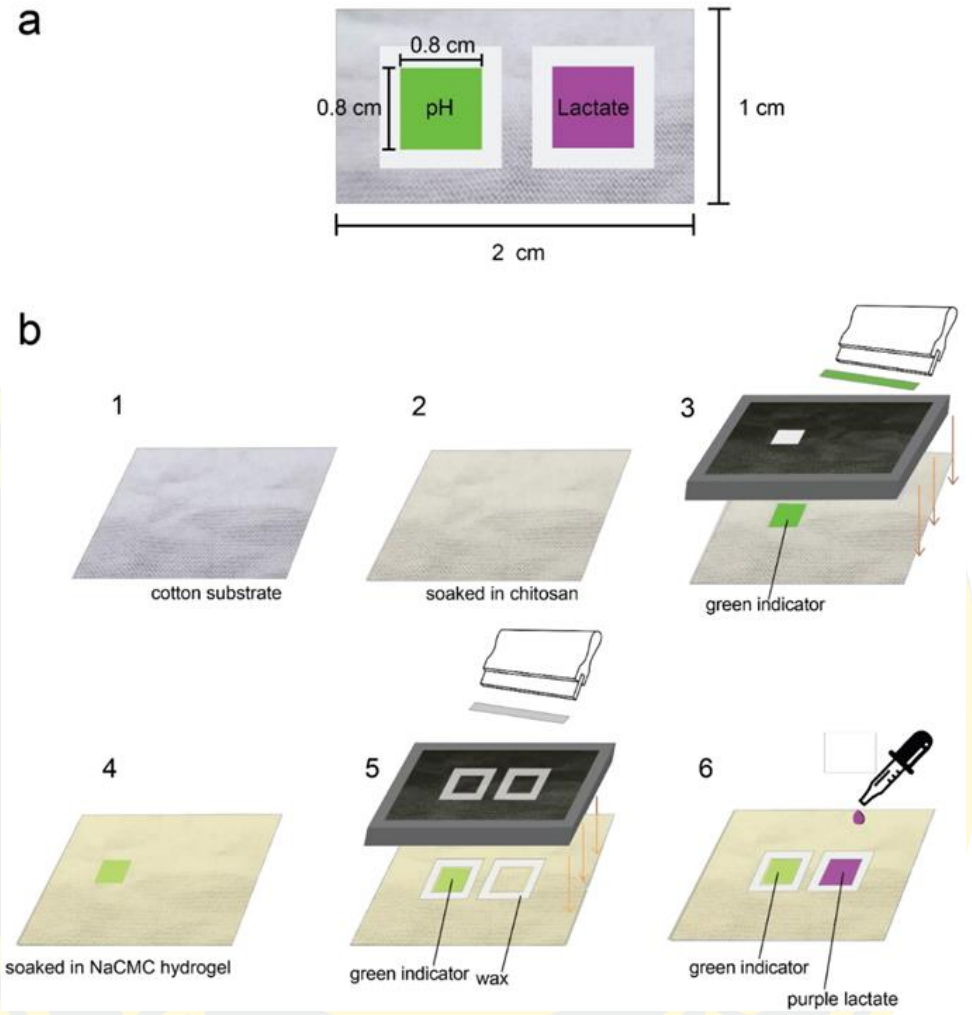

Figure 2-28 Production process of the detection zone for determination pH and lactate (Promphet et al., 2019)

Badawy & El-Aswad (2014) developed a bioactive paper-based sensor for detecting the levels of pesticide, OPs and CBs residues in food samples using AChE inhibition assay and Ellman's colorimetric test. The device was fabricated to have a dimension of 1 x 10 cm. Chitosan, a biopolymer, was used to immobilize AChE and DTNB, followed by chemical crosslinking using glutaraldehyde ($C_5H_8O_2$). Moreover, ATC was used as the endogenous reagent shown in Figure 2-29.

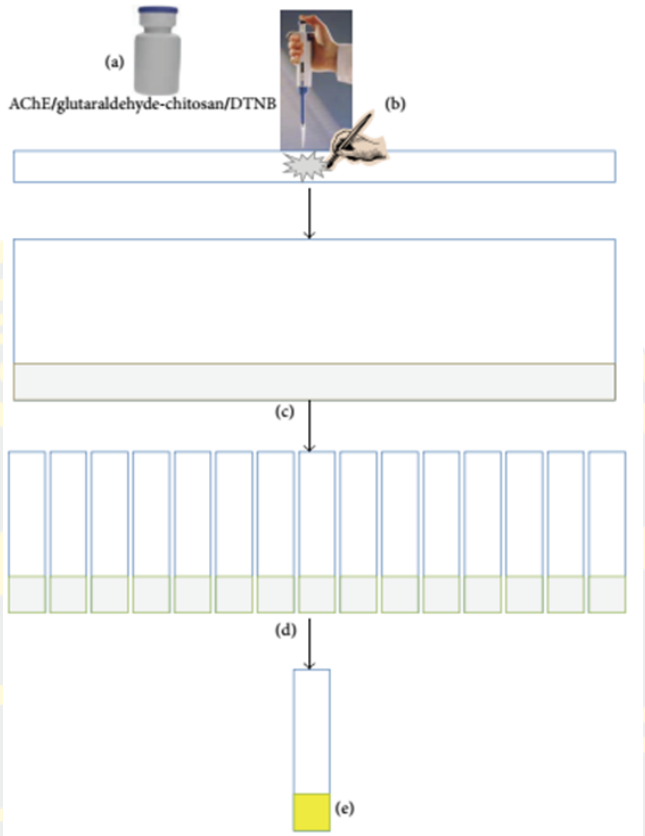

Figure 2-29 Schematic representation of the structure of a bioactive paper-based sensor (a) Gel containing AChE/glutaraldehyde-chitosan/DTNB (b) AChE/glutaraldehyde-chitosan/DTNB drops directly onto Canson paper and dried at 37 °C for 15 min. (c) A bioactive stripe sensor was applied to canson paper as a support material (d) The sheet of paper was cut into strips of size 1 × 10 cm (e) After the paper strips were immersed in ATC solution and heated at 37 °C for 5 min to produce yellow color (Badawy & El-Aswad, 2014)

The detection procedure was performed by immersing the detection zones in a solution containing pesticides. The ATC solution was then added to the detection zone to initiate the enzymatic hydrolysis reaction where AChE catalyzes the ATC solution resulting in a yellow change. The degree of AChE enzyme inhibition depending on amount of pesticide in the samples can be determined by the decrease in yellow color intensity. This biosensor exhibits good sensitivity and gives OPs and

CBs pesticides limits of detection of 6.16×10^{-4} mM for methomyl and 0.27 mM for profenofos shown in Figure 2-30 (Badawy & El-Aswad, 2014) and offers rapid analysis.

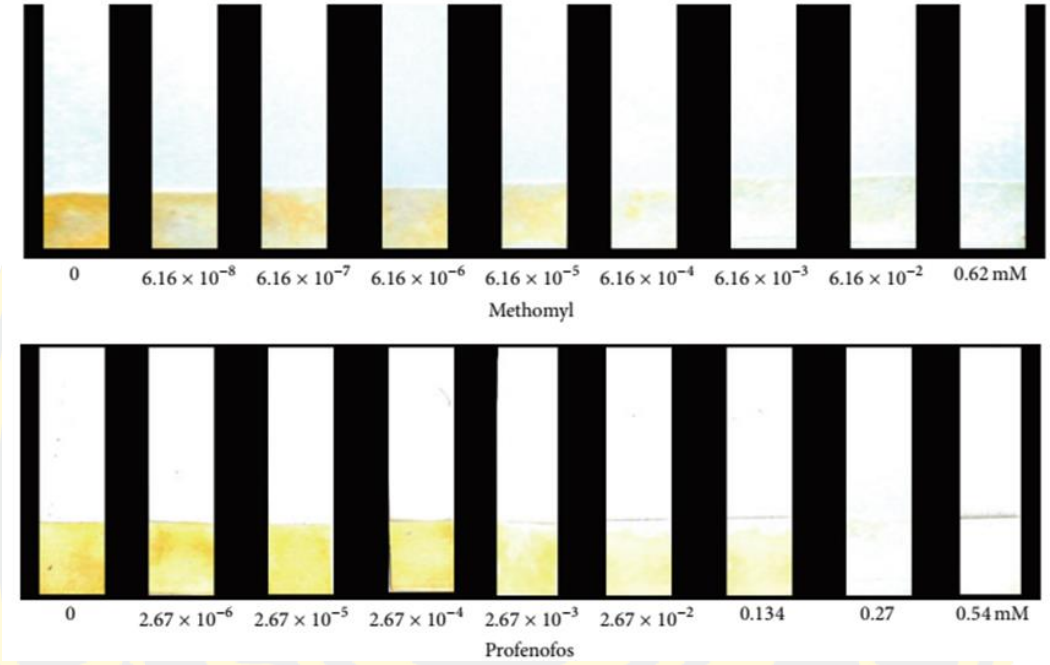

Figure 2-30 Relationship between AChE inactivation and different concentrations of methomyl and profenofos using a bioactive paper-based sensor (Badawy & El-Aswad, 2014)

Marques & Mitra (2021) developed a paper-based device as a low-cost, easy-to-use and rapid test for the determination of CBs and OP pesticide s in water samples. The device was designed as a "dip-and-fold" structure to allow for the analysis without further reagent and sample handling shown in Figure 2-31.

The analysis is based on a simple colorimetric method combined with AChE inhibition reaction and Ellman's method. In the absence of pesticides, the enzyme AChE catalyzed the formation of thiocholine (ThI) that reacts with DTNB to produce a yellow product (TNB). After incubation with pesticide, the activity of AChE was inhibited and produced less ThI, and hence, reduced yellow product shown in Figure 2-32. Pesticides including carbofuran, propoxur and chlorpyriphos were

used as model standards to demonstrate the applicability of the developed method to provide the detection in the range of 0.1 µM to 0.1 mM for colorimetric detection within 10 min.

In this research, chitosan is also used as a polysaccharide biopolymer with many good properties such as have good biocompatibility, non-toxic and low cost. In the structure of chitosan, there are hydroxyl groups (-OH) and amino groups ($-NH_2$). Having these functional groups, chitosan can be used as an intermediary in hydrogen bonding between paper cellulose fibers and AChE enzymes.

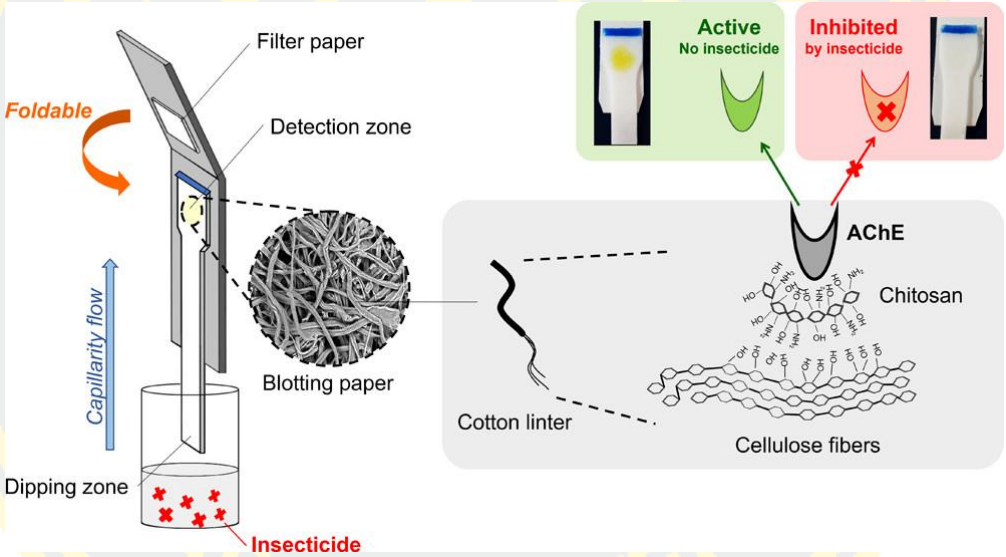

Figure 2-31 The structure design “dip-and-fold” of paper-based device (Marques & Mitra, 2021)

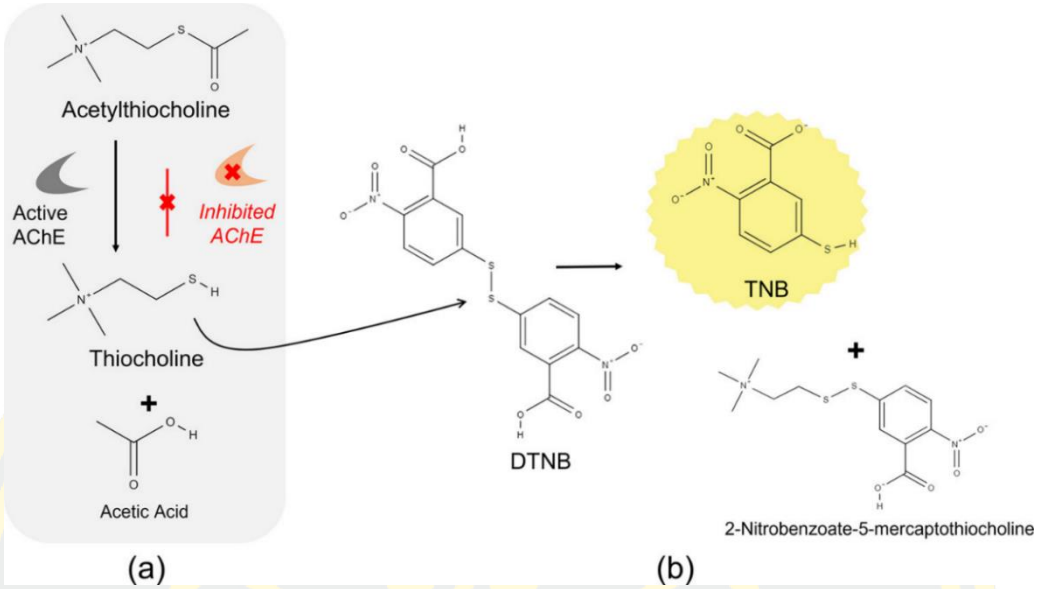

Figure 2-32 (a) Hydrolysis reaction of acetylthiocholine by AChE and (b) colorimetric reaction between thiocholine and DTNB (Marques & Mitra, 2021)

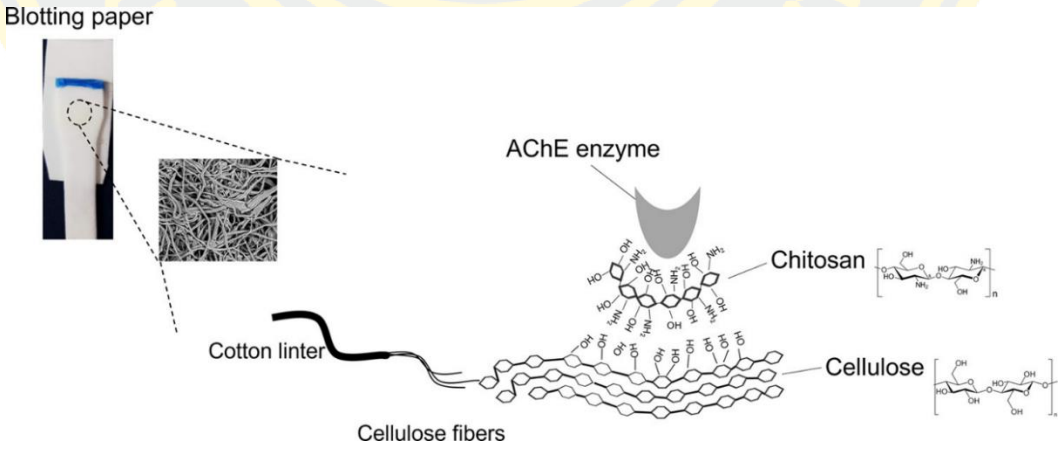

Figure 2-33 Schematic representation of AChE immobilization using chitosan as the principal for hydrogen bonding between cellulose fibers of paper and AChE enzyme (Marques & Mitra, 2021)

H. Liu, Yi, Shi, Liang, & Gao (2006) studied the substrate specificity of AChE in the brains of mature male and female *Carassius auratus*, and also investigated the sensitivity of brain AChE to CBs pesticides. The experiments conducted in this study were carried out in a controlled laboratory setting (in vitro). The study involved comparing the specificity of four substrates for AChE: acetylthiocholine iodide (ATCh), β-methylthiocholine iodide (β-MTCh), propionylthiocholine iodide (PrTCh), and butyrylthiocholine iodide (BuTCh). The structures of all 4 types of precursors are shown in Figure 2-34.

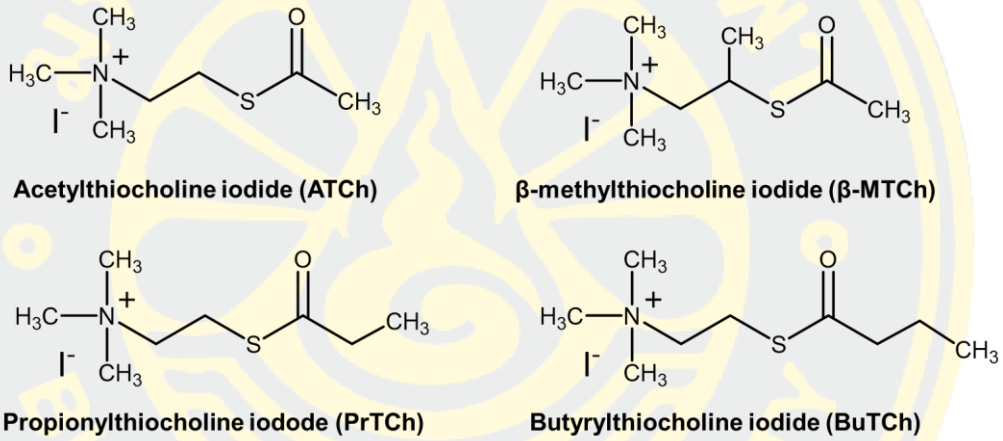

Figure 2-34 Structure of all 4 types of precursors (H. Liu, Yi, Shi, Liang, & Gao, 2006)

From the results of the investigation of the specificity of these 4 substrates towards AChE, it was found that the tendency of AChE degradation towards all 4 substrates tended in the same direction with increasing concentration. It was observed that the concentration of hydrolyzed precursors increased as the concentration of AChE in the brains of both male and female specimens increased. It was determined that among the precursors tested, ATCh was the most extensively hydrolyzed. In contrast, BuTCh was found to be a substrate with very low hydrolysis activity. The order of hydrolysis of the four substrates by AChE enzymes was ATCh > β-MTCh > PrTCh > BuTCh shown in Figure 2-35 (H. Liu, Yi, Shi, Liang, & Gao,

2006). Based on the aforementioned findings, it can be inferred that ATCh is the substrate with the most appropriate surface area, making it highly specific to AChE.

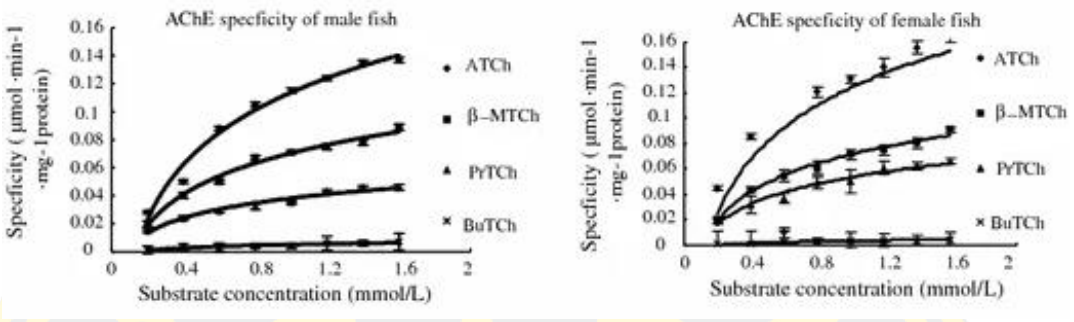

Figure 2-35 Trends of hydrolysis of four substrates by AChE enzymes (H. Liu, Yi, Shi, Liang, & Gao, 2006)

Upon analyzing the alkyl group sizes around the side chains of the four substrates, it was observed that their sizes followed this sequence: BuTCh > PrTCh > β-MTCh = ATCh (-C=O$CH_2CH_2CH_3$ > -C=OCH_2CH_3 > -C=OCH_3 = -C=OCH_3). The sizes of the alkyl groups of the four substrates were related to the trend curves in Figure 2-35. The smaller the alkyl group is in the structure, the stronger the binding to bind AChE enzyme. Thus, the surface structure of ATCh is comparatively smaller, leading to a stronger interaction between the carbonyl group of the substrate and the -OH group of serine on the esteric site. Consequently, ATCh exhibits the highest capacity to undergo hydrolysis by the AChE enzyme. In contrast, when the substrate contains a bulky alkyl group, its surface structure becomes larger, resulting in a weakened interaction between the carbonyl group of the substrate and the -OH group of serine on the esteric site. Therefore, BuTCh has the least ability to be hydrolyzed by the enzyme AChE. Then, the tendency of AChE inhibition was studied by using eserine, aldicarb and methomyl, representative insecticides of CBs. It was found that over time the inhibition of AChE activity decreased shown in Figure 2-36.

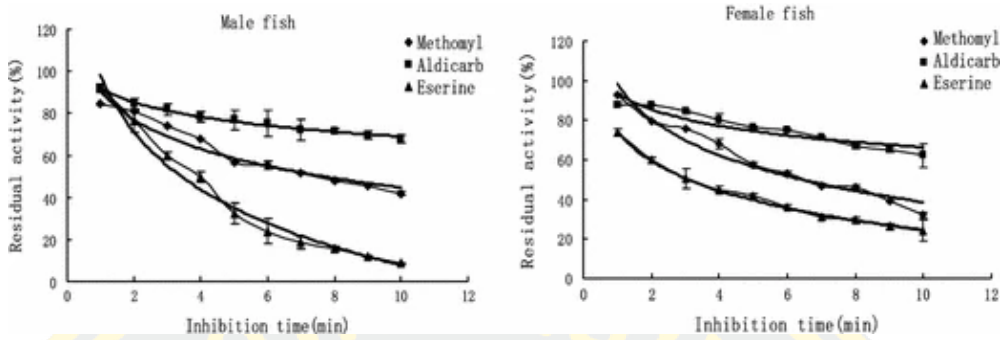

Figure 2-36 Effects of inhibition of AChE enzyme activity by various CBs pesticides (H. Liu, Yi, Shi, Liang, & Gao, 2006)

CHAPTER 3
METHODOLOGY

3.1 Materials and chemicals

3.1.1 Materials and Instruments

1. Wax-printer (Xerox Color Qube 8870-13, 9037 Flextronics Technology)
2. Scanner (CanoScan LiDE 110, Cannon Marketing Company Ltd, Thailand)
3. Filter papers Whatman No. 1 Sheet type 460 x 570 mm, Hole size 11 µm (GE Healthcare Company Ltd, China)
4. Oven (1375 FX, Delta Laboratory Company Ltd, Thailand)
5. 4-Digit Balance (MS, Mettler-Toledo Ltd., Thailand)
6. Micropipettes 100 – 1000 µL, 10 – 100 µL and 0.5 – 10 µL (Eppendorf Research, Eppendorf Thailand Co., Ltd, Germany)
7. Microcentrifuge tubes 250 µL and 1500 µL
8. Magnetic stirrer (C-MAG HS 7, IKA Works Co., Ltd, Thailand)
9. Clear tape Size 48 mm. x 40 m. (3M Scotch, 3M Thailand Ltd, Thailand)
10. Paintbrush NO. 6
11. Hair dryer (CKL-4000, Asawa Electric Group Co., Ltd, Thailand)
12. Attenuated Total Reflectance Fourier Transform Infrared Spectrometer (ATR- FTIR, model Frontier, PerkinElmer)
13. Scanning Electron Microscope-Energy Dispersive X-ray Spectro photometer (SEM-EDX, model LEO 1450 VP, Carl Zeiss)

3.1.2 Chemicals

1. Acetylcholine esterase (AChE) (E.C.3.1.1.7), 518 U/mg Solid and 3.9 mg solid, CAS: 9000-18-1 (Sigma-Aldrich, USA)
2. Acetylthiocholine iodide ($C_7H_{16}INOS$; ATC) MW: 289.18 g/mol, CAS: 1866-15-5, Analytical Grade (Acros Organics, Belgium)

3. DTNB (Ellman's reagent) (5,5-dithio-bis-(2-nitrobenzoic acid) ($C_{14}H_8N_2O_8S_2$; DTNB) MW: 396.35 g/mol, CAS: 69-78-3, Analytical Grade (Sigma-Aldrich, USA)
4. Malathion ($C_{10}H_{19}O_6PS_2$; MAL) MW: 330.36 g/mol, CAS: 121-75-5, (LGC Ltd, UK)
5. Dichlorvos ($C_4H_7Cl_2O_4P$; DDVP) MW: 220.98 g/mol, CAS: 62-73-7, (LGC Ltd, UK)
6. Carbaryl ($C_{12}H_{11}NO_2$; CAR) MW: 201.22 g/mol, CAS: 63-25-2, (LGC Ltd, UK)
7. Carbofuran ($C_{12}H_{15}NO_3$; CBF) MW: 221.25 g/mol, CAS: 1563-66-2, (LGC Ltd, UK)
8. Disodium Hydrogenphosphate (Na_2HPO_4) MW: 141.96 g/mol, (Ajax Finechem, Austria)
9. Sodium Dihydrogenphosphate ($NaH_2PO_4.2H_2O$) MW: 156.01 g/mol, (Ajax Finechem, Austria)
10. Chitosan ($C_{12}H_{24}N_2O_9$) (Sigma-Aldrich, USA)
11. Cetyltrimethylammonium bromide (CTAB) ($C_{19}H_{42}BrN$) MW: 364.46 g/mol, CAS: 57-09-0, Analytical Grade (Loba Chemie Pvt. Ltd, India)
12. Sodium carboxymethyl cellulose (NaCMC) ($C_8H_{15}NaO_8$) CAS: 9004-32-4, (Loba Chemie Pvt. Ltd, India)
13. Citric acid ($C_6H_8O_7.H_2O$) MW: 210.15 g/mol, CAS: 5949-29-1, (Fisher Scientific, England)
14. Polyethylene Glycol ($HO(C_2H_4O)_nH$; PEG) MW: 6000 g/mol, CAS: 25322-68-3, (Merck KGaA, Germany)
15. Aluminium Chloride Hexahydrate ($AlCl_3.6H_2O$) MW: 241.43 g/mol, CAS: 7784-13-6, Analytical Grade (QRëC (Quality Reagent Chemical), New Zealand)
16. Bovine Serum Albumin (BSA) MW: 66000 g/mol, CAS: 64-19-7, (Merck KGaA, Germany)
17. Acetic acid ($C_2H_4O_2$) MW: 60.05 g/mol, CAS: 5949-29-1, Analytical Grade, (RCI Labscan, Thailand)

18. Methanol (CH_4O) MW: 32.04 g/mol, CAS: 67-56-1, Analytical Grade, (RCI Labscan, Thailand)

3.1.3 Samples

Dried seafood product (DSPs) samples are bought from Markets in the area of Chon buri province, Thailand.

3.2 Research plan

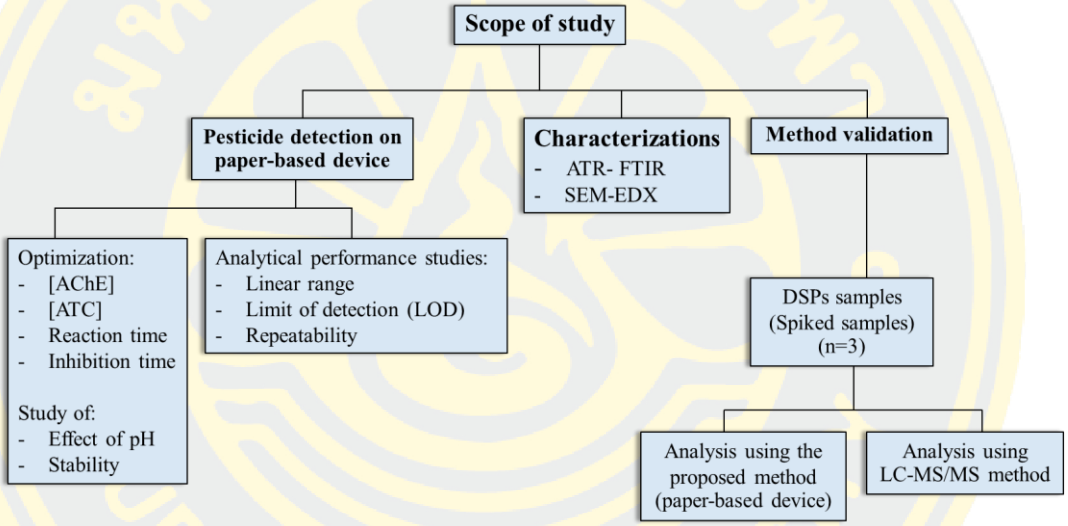

Figure 3-1 Scope of research

3.3 Experimental

3.3.1 Preparation of solution

3.3.1.1 Phosphate buffer pH 7.4, 0.1 M

The buffer was prepared by dissolving 1.5601 g NaH_2PO_4 in 100 mL deionized water and 6.3882 g Na_2HPO_4 in 450 mL deionized water, then the solutions were mixed. The pH of the solution was adjusted to 7.4 with 1 M HCl. The final volume was then adjusted to 1000 mL and the solution stored at 2-8 °C.

3.3.1.2 Acetylcholinesterase solution (AChE)

A stock solution of 1000 U/mL acetylcholinesterase (AChE) was prepared by dissolving 3.9 mg solids (518 U/mg solids) of AChE in 2000 µL 0.1 M phosphate buffer pH 7.4 and stored at -20 °C.

The stock acetylcholinesterase solution was diluted to the desired concentration using BSA solution (10 mg/mL BSA in 0.1 M phosphate buffer pH 7.4).

3.3.1.3 Acetylthiocholine iodide solution (ATC), 3 mM

The solution was prepared by dissolving 0.0087 g of ATCI in deionized water and the final volume was made up to 5 mL with deionized water.

3.3.1.4 Chitosan solution

Chitosan solution (2% w/v) was prepared by dissolving 0.2 g chitosan in 10 mL of 2% (v/v) acetic acid. Then 0.5 g citric acid was added into the chitosan solution.

3.3.1.5 NaCMC-CTAB-DTNB solution

Firstly, 10 mL of 5 mM DTNB was prepared by dissolving 0.0198 g DTNB in 10 mL of 0.1 M phosphate buffer pH 7.4. Then, a 0.05 g CTAB was added to the DTNB solution to obtain the DTNB-CTAB solution. Next, a 0.25 g NaCMC was added into the DTNB-CTAB solution followed by 0.5 g citric acid to obtain the NaCMC-CTAB-DTNB solution.

3.3.1.6 NaCMC solution

NaCMC solution was prepared by dissolving 0.25 g NaCMC in deionized water and the final volume was adjusted to 10 mL with deionized water.

3.3.1.7 Bovine serum albumin solution (BSA)

A 10 mg/mL BSA solution was prepared by dissolving 100 mg of BSA in 0.1 M phosphate buffer pH 7.4 and adjust the volume to 10 mL with 0.1 M phosphate buffer pH 7.4 and store the BSA solution at -20 °C until use.

3.3.1.8 Aluminium Chloride solution ($AlCl_3$)

A 0.25% (w/v) solution of $AlCl_3$ is prepared by dissolving 1.25 g of $AlCl_3$ in deionized water and the volume adjusted to 500 mL with deionized water.

3.3.1.9 Polyethylene Glycol solution (PEG)

A 1% (w/v) PEG solution is prepared by dissolving 5 g PEG in deionized water and the volume adjusted to 500 mL with deionized water. The solution was stored at 2-8 °C until use.

3.3.1.10 Pesticides solution

A stock solution of 50 mg/mL of malathion (MAL), 50 mg/mL of dichlorvos (DDVP), 50 mg/mL of carbaryl (CAR) and 50 mg/mL of carbofuran (CBF) was prepared by dissolving in methanol and stored at 2-8 °C.

A working solution is prepared by diluting the pesticide stock solution using 4% (v/v) methanol.

3.4 Fabrication of paper-based devices

The paper-based device was designed using Microsoft Word program to have a shape similar to a pH strip. The total length of the paper device was 7.5 cm long and 1 cm wide. It was designed to have two ends where one end was used as a control zone (C) and the other end was used as a test zone (T). The control and the test zones measure 1.5 cm in length. The typical device is shown in Figure 3-2

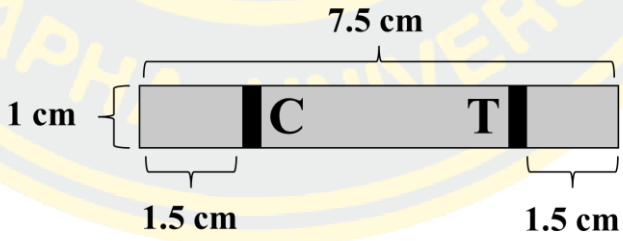

Figure 3-2 Typical paper-based test strip for pesticide analysis

Next, the paper-based device was fabricated using wax printing technique by printing the designed pattern using the wax-printer on the filter paper No. 1. The wax-printed paper was then heated at 150 °C in an oven for 30 seconds to allow the wax melt through the paper to form a hydrophobic barrier and create the test zones.

Then, the 3M clear tape was adhered to the back of the paper-based device to prevent the solution leakages. The fabrication process was shown in Figure 3-3.

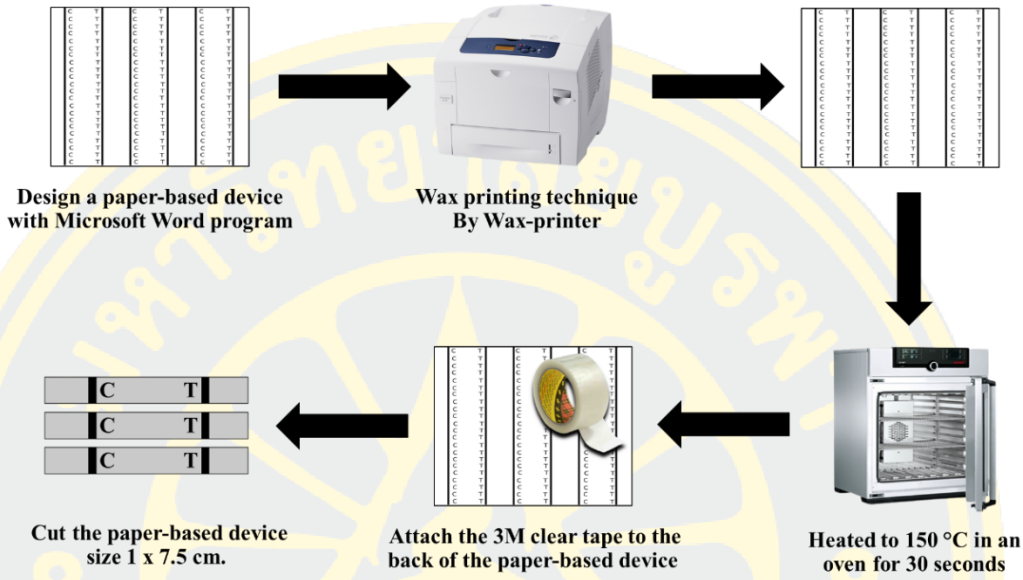

Figure 3-3 Fabrication process of a paper-based test strip for pesticide analysis

3.5 Reagents immobilization onto the paper-based test strip

The fabricated paper-based device was then employed for reagent immobilization for pesticide analysis according to the process shown in Figure 3-4. Initially, a chitosan solution was applied to the test zones of the device using a paintbrush, and subsequently left to dry at 35°C for 10 min. Next, a NaCMC-CTAB-DTNB solution was coated onto the device via a paintbrush and heated at 35°C in an incubator for another 10 min to allow for reagent absorption onto the surface of the device. The device was next coated with NaCMC solution using a paintbrush followed by incubating the device at 35°C for 10 min to dry and allow the NaCMC solution to absorb into the device, thus immobilizing it on the third layer. The three-layer reagent-coated paper-based device was then immersed in 0.25% (w/v) aluminum chloride solution for 10 min to form a hydrogel structure via chemical crosslinking. It was then heated at 35°C in an incubator for 20 min to dry the paper-based device. Next, the paper-based device was immersed in 1% (w/v) polyethylene glycol solution for 10 min to increase its hydrophilicity. It was then heated at 35°C in

an incubator for another 20 min to dry the device. Finally, 20 µL of acetylcholinesterase solution was added to the device and incubated at 35°C for 10 min to create a ready-to-use paper-based device.

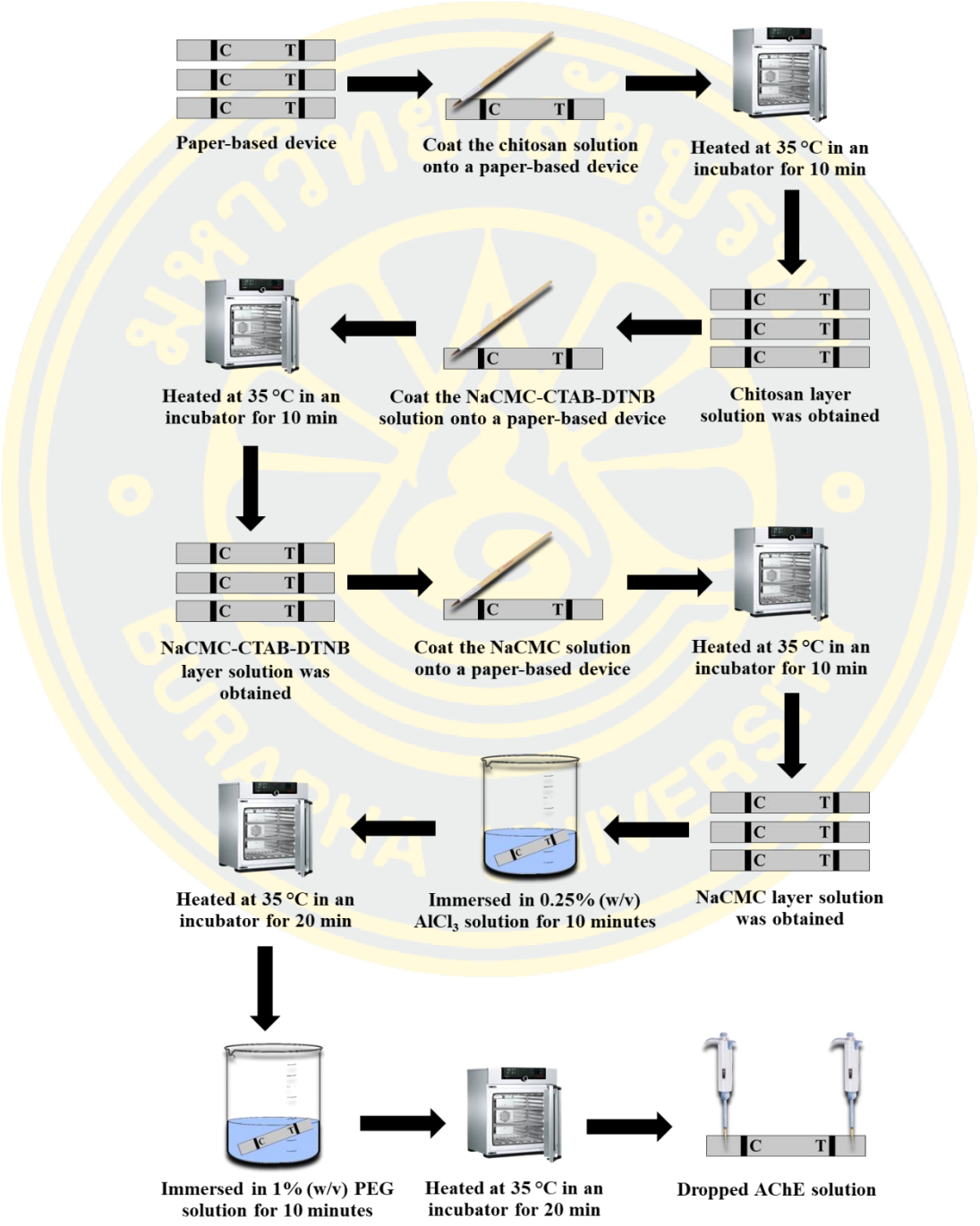

Figure 3-4 Process of reagent immobilization on the paper-based test strip for pesticide analysis

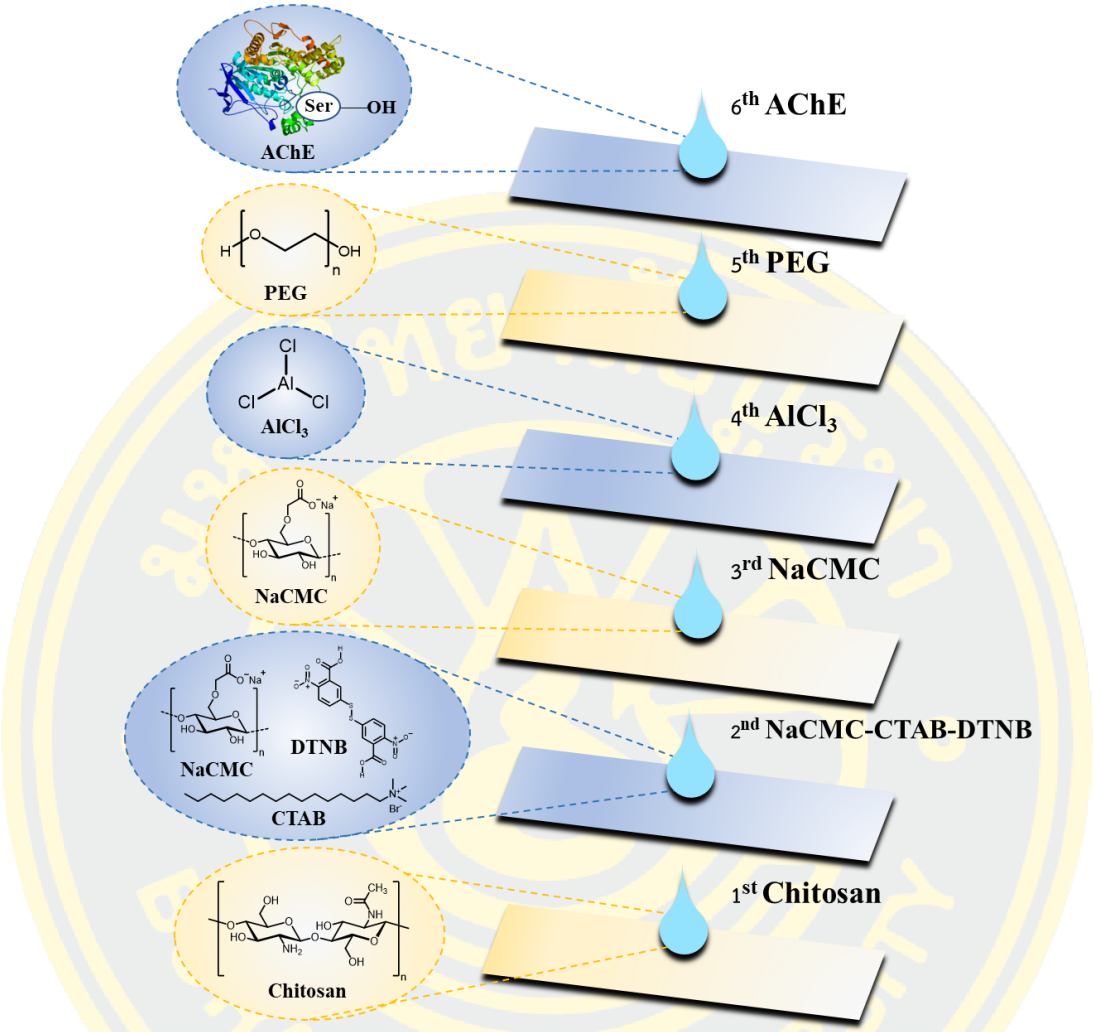

Figure 3-5 Order of reagent immobilization on paper-based devices

3.6 Pesticides detection on paper-based devices

To perform the test, 20 µL of a pesticide solution was dropped onto the T zone of the device, while a drop of a 4% (v/v) methanol (blank solution) was applied to the C zone. An enzyme inhibition reaction was allowed to occur at the T zone for 5 min. Subsequently, 20 µL of ATC solution was added to both ends of the device until yellow coloration appeared on both the T and C zones. In the absence of pesticides in the sample, the color intensity displayed on the T and C zones would be similar. However, if the sample contains pesticides, the color intensity on the T zone is less than that on the C zone, which can be observed by the naked eye. The color intensity

can be quantitatively analyzed by capturing images of the device using a scanner or camera and analyzing the color intensity using software such as ImageJ.

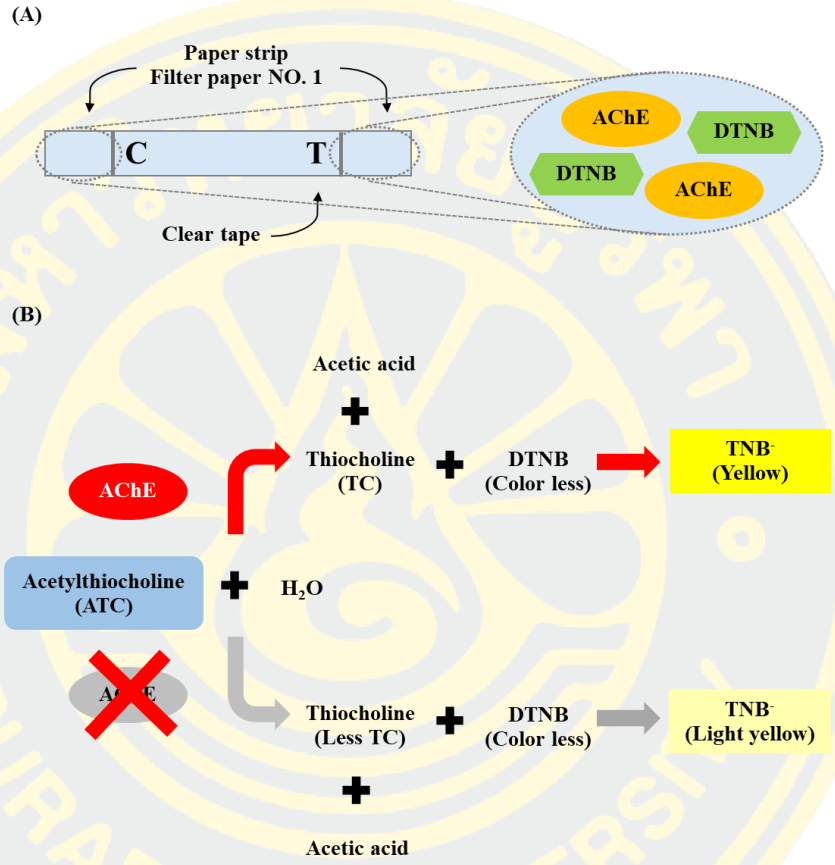

Figure 3-6 Characteristics of (A) the colorimetric paper-based test strip assay for pesticide analysis and (B) the principle of pesticide detection by enzyme inhibition assay

3.7 Color intensity analysis by ImageJ

1. Open the ImageJ program: select → Start or double-click the program icon on the computer desktop. Then the box below will appear.

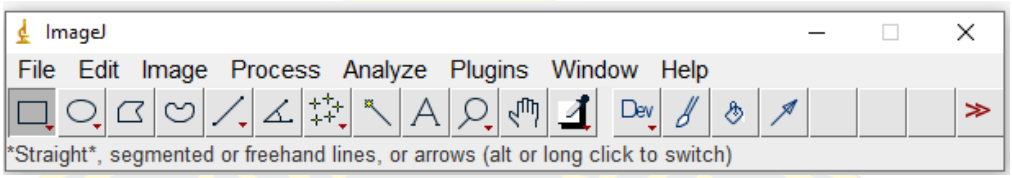

2. Select an image to measure color intensity: select File → Open and choose the image that is needed to analyze.

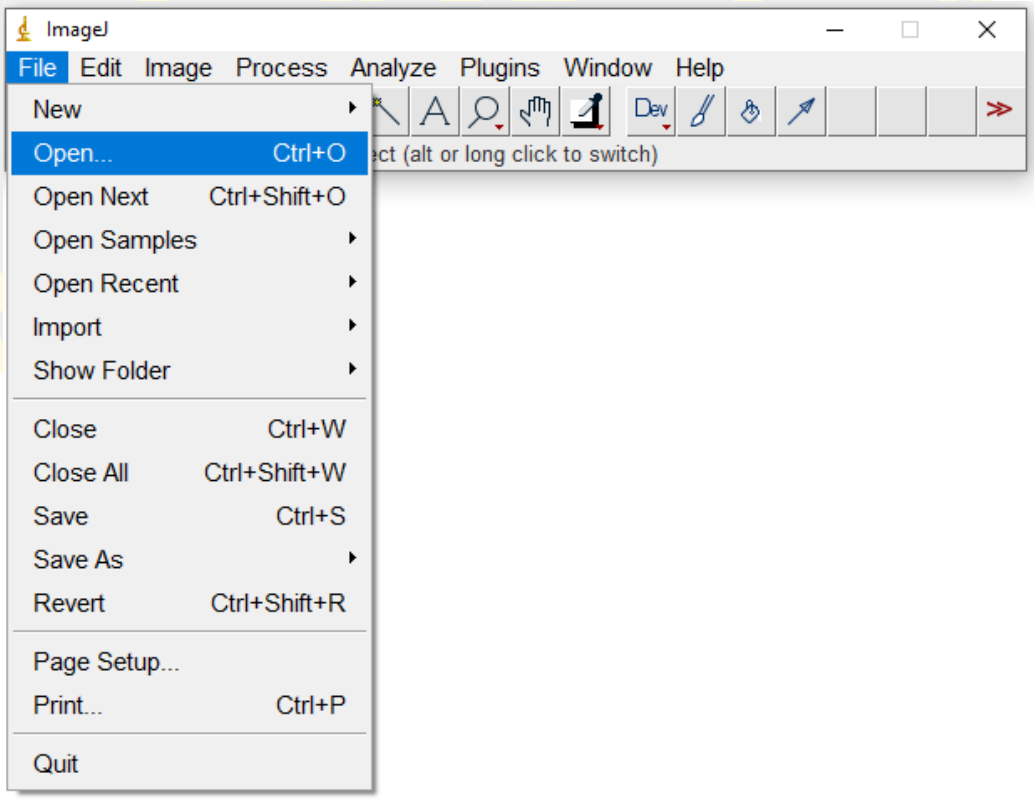

3. Adjust the image to only the area to be measured: select Image ⟶ Adjust ⟶ Color Threshold. Then the Threshold Color's window will appear.

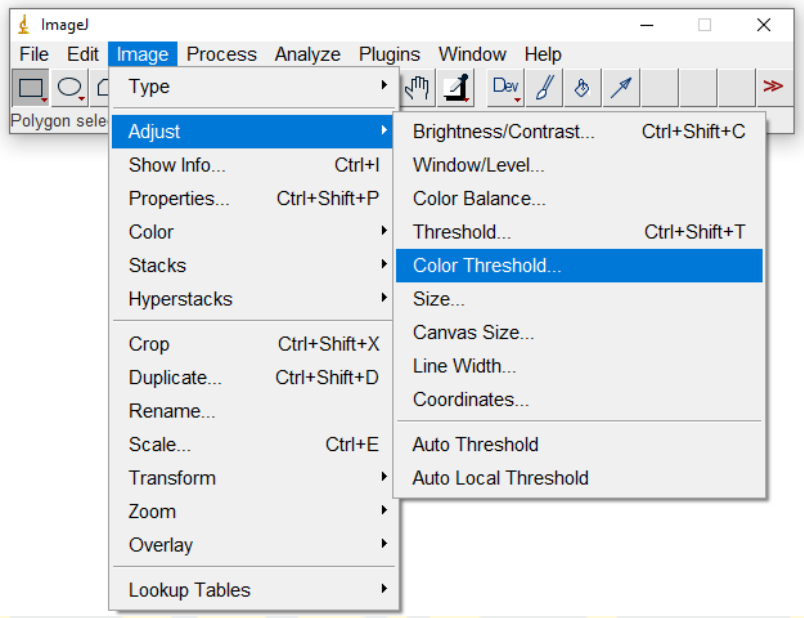

When the bar pops up select all “passes”, select Color space: Lab, Threshold color: White, Thresholding method: Default Then adjust the values of L*, a* and b* as shown.

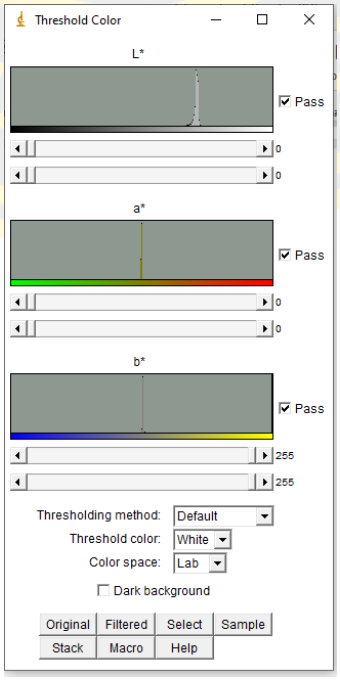

4. Setting gray scale: select Image ⟶ Type ⟶ 8-bit. Then the image will be converted as shown below.

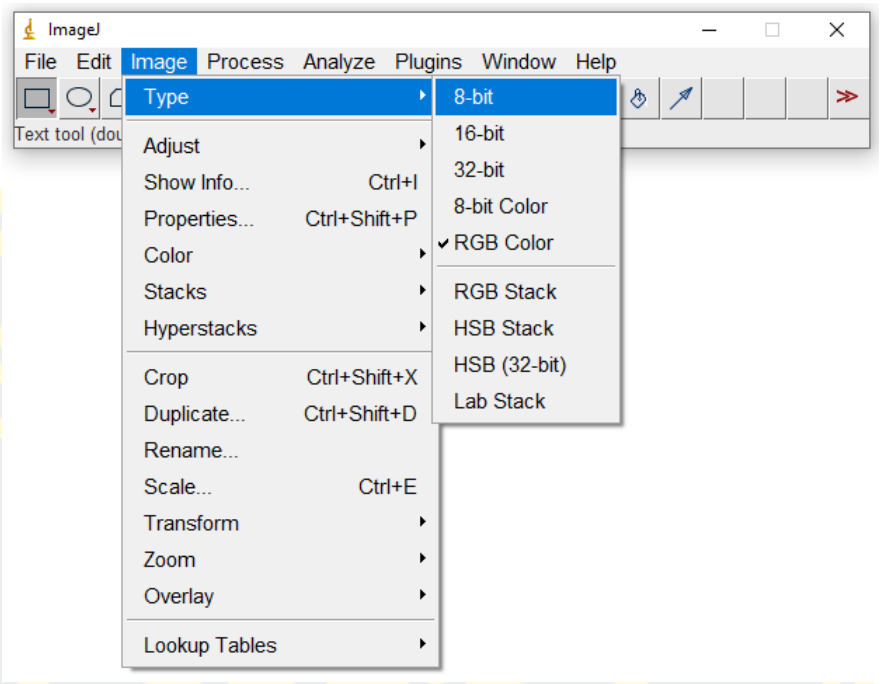

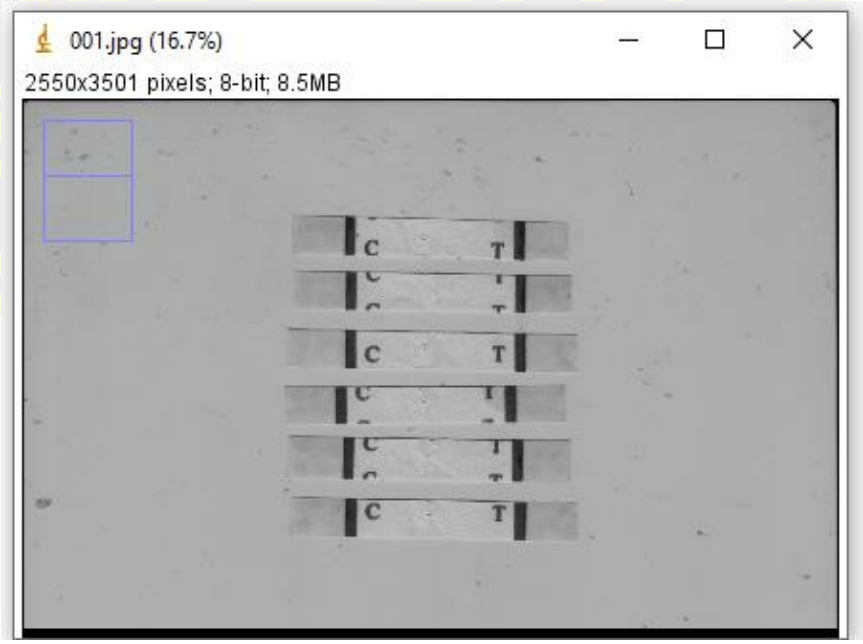

5. Adjust to gray intensity: select Edit ⟶ Invert

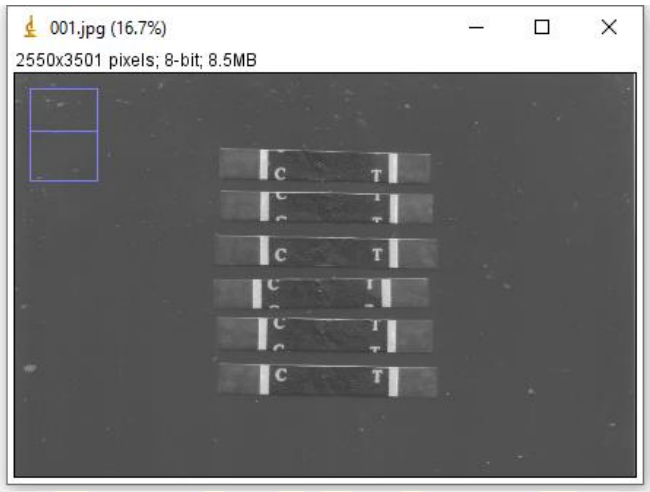

6. Select the color intensity measurement area: select Ctrl+M or M. A display window of color intensity will appear.

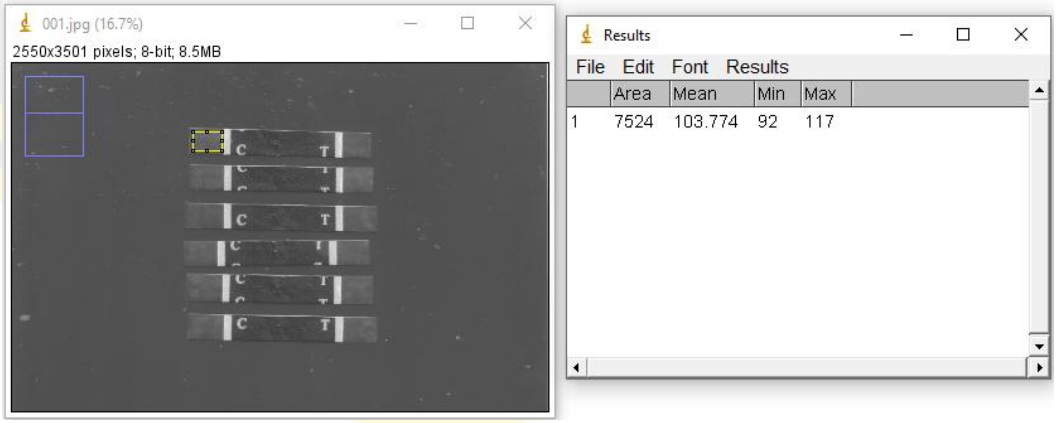

3.8 Characterizations of biopolymers on the paper-based test strip

This study was done to ensure that the biopolymer immobilized on the paper-based test strip remains on the surface of the paper-based test strip until the pesticide determination. The characterization was conducted using ATR- FTIR and SEM-EDX techniques.

3.9 Optimizations

3.9.1 Concentration of AChE

The initial concentration of AChE used in the enzyme activity inhibition assay plays an important role in the analytical sensitivity for pesticide analysis. The appropriate AChE concentration should lead to a high signal intensity in the absence of pesticides, while in the presence of pesticides, it should result in a lower signal intensity. The concentrations of AChE tested were 0.5, 1, 2, 3, 4 and 5 U/mL (n=3). The 20 µL of each AChE concentration was applied to the test area of the fabricated paper-based and color intensity was measured using ImageJ program according to the method described above.

3.9.2 Concentration of ATC

The concentration of ATC used in the assay is another important parameter affecting the analysis as a substrate for the reaction. ATC concentrations were studied in the concentration range of 0.5 to 15 mM to determine the optimal concentration of ATC used in the analysis. A graph showing the relationship between ATC concentration and color intensity was studied. In this experiment, no pesticides were added. The ATC concentrations used for testing were 0.5, 1, 3, 5, 10 and 15 mM (n=3). A 20 µL of each ATC concentration was applied on the paper-based devices according to the process described above.

3.9.3 Reaction time

The assay reaction time of catalytic reaction of acetylthiocholine by AChE for TNB^- formation plays an important role in determining the sensitivity of the assay. Different reaction time (1, 3, 5, 7, 10 and 15 min) was investigated (n=3). To identify the optimal reaction time, a graph between color intensity as a function of

reaction time was plotted. Notably, this experiment was conducted without the presence of pesticides.

3.9.4 Inhibition time

Assay sensitivity significantly relies on the inhibition time of AChE by pesticides. In order to observe a reduction in color, the time that AChE is inhibited by pesticides must be evaluated. An investigation was carried out (n=3) by varying inhibition times (3, 5, 7, 10, 15, 20, 25 and 30 min). This experiment was conducted with the presence of malathion pesticides. Other experimental parameters were similar to the method described above.

3.10 Effect of pH on the developed assay

The effects of sample pH were studied in range of 4-9 as this may result in the performance of the AChE enzyme being disturbed by these pH levels. The solution was prepared in the studied pH range and the solution was tested for its effect to the assay.

3.11 Stability of the biopolymer coated paper-based test strip

The stability of the developed paper-based test strip was evaluated and compared to non-biopolymer-coated paper-based test strips. The biopolymer coating was prepared using the methods described in the experimental section above, while the non-biopolymer-coated paper-based test strip was prepared by directly dropping the DTNB and AChE solution onto the test zones and allowing them to dry. All test strips were prepared simultaneously, kept in sealed aluminum foil bags containing 1-gram silica gel bags, and stored in the refrigerator (4°C) and at ambient temperature (25-36°C). A freshly prepared 3 mM ATC solution was tested using the evaluated paper-based test strips every 3-7 days (n=3).

3.12 Analytical Features

3.12.1 Linearity

Paper-based device prepared under optimal conditions were used to analyze pesticides. Four pesticide standards were used in this study including MAL, DDVP, CAR and CBF. Stocks pesticides (MAL, DDVP, CAR and CBF) were diluted to the desired concentrations using a 4% (v/v) methanol solution. The linear range was studied by applying 20 µL of each different concentration of MAL, DDVP, CAR and CBF and allowing to react for 5 min. Next, a 20 µL of 3 mM ATC solution was added and let the reaction continue for another 5 min. The color intensity was then scanned with a paper-based device using an imager program as described above. The average color intensity obtained from ImageJ program was used to plot calibration curves between the difference of inhibition level and the pesticide concentration of MAL, DDVP, CAR and CBF. The difference in inhibition levels, defined as the difference between the color intensity from the pesticide test at the T zone and that of the control obtained from the C zone of the same test strip, was calculated using Equation (1) where I_0 and I_C are the yellow color intensities of the control region and the test region, respectively.

$$\text{Difference of inhibition level} = I_0 - I_C \qquad (1)$$

3.12.2 Reproducibility

The reproducibility for the analysis of pesticides by the developed test was carried out by replicate analysis of the pesticide with concentration in the linear range (n=3). The reproducibility can be determined by calculating the percent relative standard deviation (%RSD) of the developed method according to Figure 3-7.

$$\%\text{RSD} = \frac{\text{SD}}{\bar{x}} \times 100$$

Figure 3-7 Equation for determining the percentage of the relative standard deviation (%RSD)

3.12.3 Limit of detection (LOD)

The experiment was similar to the linearity study in topics 3.9.1 by analyzing the color intensity of the blank solution (n=8) and then using the data obtained to determine the LOD according to Figure 3-8.

$$LOD = \frac{3SD}{Slope}$$

Figure 3-8 Equation for determining the limit of detection (LOD)

3.13 Method Validation

3.13.1 Sample preparation

To assess the method accuracy, the analysis of CBs and OP pesticides in spiked DSP samples was conducted using the developed assay and the conventional LC-MS/MS method (Paradis, Bérail, Bonmatin, & Belzunces, 2014). The laboratory-based sample preparation was carried out in similar procedure as the method previously described (Souksanh Nouanthavong, Duangjai Nacapricha, Charles S Henry, & Yupaporn Sameenoi, 2016). Firstly, the DSP sample was cut and homogenized using a blender. Next, a 5 g of homogenized samples were then placed into a 50 mL centrifuge tube and spiked with an CBs and OP pesticide s standard which were dichlorvos and carbofuran, respectively. The mixture was shaken for 1 min and left in the dark for 15 min. Next, a 20 mL of methanol was added, and the mixture was shaken for 30 min and then, centrifuged at 4000 rpm for 10 min. Then, a 1.5 mL of supernatant was added into a 2 mL micro-centrifuge tube of dispersive SPE containing 25 mg C18 and 150 mg $MgSO_4$ used for sample clean up and to remove residual water. The mixture was vortexed for 30 min and centrifuged at 4000 rpm for 10 min. Then, the supernatant was collected and dried under the hood. Finally, the extracted residue was reconstituted in 1 mL of 4% methanol for analysis using the developed paper-based device assay, and in 100% methanol for LC-MS/MS analysis. The traditional method, LC-MS/MS, was conducted at the Chachoengsao branch of Central Laboratory (Thailand) Co., Ltd.

CHAPTER 4
RESULTS AND DISCUSSION

4.1 The principle of the assay

Detection of OP and CB pesticides on paper-based test strip is based on the inhibition reaction of the AChE enzyme. Firstly, a paper-based test strip was created by immobilizing the AChE enzymes and DTNB onto the measurement area of the paper-based test strip using biopolymer as stabilizing agents. In the absence of pesticides, the AChE enzyme catalyzes the hydrolysis reaction of ATC to produce TC that reacts with DTNB to produce a yellow product (TNB^-), as shown in Figure 4-1. In the presence of OPs and CBs pesticides, the activity of the AChE enzyme is inhibited, resulting in less activity to catalyze the conversion from ATC to TC. Therefore, less TC was generated to react with DTNB and a reduced yellow color was obtained. The amount of pesticides detected can be monitored by measuring decrease of color intensity using the ImageJ program.

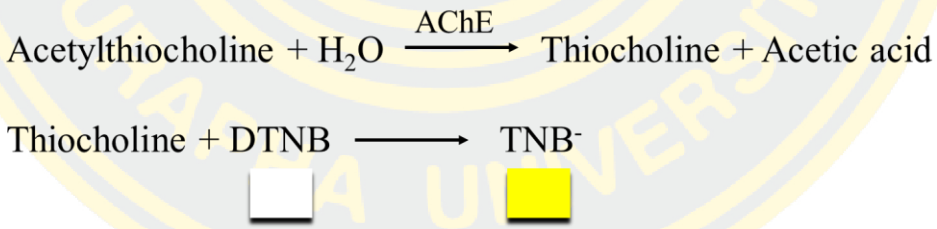

Figure 4-1 Hydrolysis reaction of ATC to TC catalyzed by the AChE enzyme and the TC produced reacted with DTNB to produce yellow color TNB^-

4.2 Characterization of biopolymers on the paper-based test strip

Biopolymers were employed to stabilize the key regents associated with the enzyme inhibition assay including DTNB and AChE on the paper-based test strip to increase their shelf life at various storage conditions. As shown in Figure 3-5, the first

layer was coated with chitosan, acting as the polymer with a positive charge to facilitate adsorption on the negatively charged cellulose. Moreover, chitosan also has antibacterial effects, which can extend the shelf life of paper-based test strip.(Fei Liu, Lin Guan, Zhi Yang, Li, & De Yao, 2001; Li & Zhuang, 2020) The next layer was coated with CTAB-DTNB-NaCMC. NaCMC is a negatively charged polymer used to stabilize DTNB since it is poor stability and sensitive to light. (Marques & Mitra, 2021; Yang, Chen, & Chen, 2018) Moreover, NaCMC hydrogel is responsible for maintaining the activity of the AChE enzyme, allowing it to adhere more efficiently to the paper-based test strip. CTAB is a cationic surfactant forming a micelle structure that could help stabilize the TNB^- color product from the reaction of DTNB and thiocholine in the enzyme inhibition assay on the paper-based test strip.(Lai et al., 2019; Mukdasai, Uppachai, & Srijaranai, 2019; Pungjunun et al., 2020; Shao et al., 2015) The next layer was coated by $AlCl_3$ solution acting as a chemical crosslinker to make all layers of the coated chemicals adhere together more tightly (Thom, Lewis, DiTucci, & Phillips, 2013). PEG was then coated to increase hydrophilicity. Finally, the AChE enzyme was dropped on the paper-based test strip. (Kaneko, Hara, Nishino, & Maruyama, 2020; Sundar, Stanley, Kumar, Keerthana, & Kumar, 2021; Tao, Yen, Liu, & Chen, 2016; H. Zhang, Smith, Zhang, & Zhou, 2019) Therefore, the chemical and physical properties of each biopolymer coating layer on the paper-based test strip was first characterized using AIR-FTIR and SEM-EDX.

4.2.1 Chemical characterization of the test strip layers

An ATR-FTIR spectrophotometer was used to characterize each layer of the paper-based test strip in the range 400-4000 cm^{-1} (Figure 4-2). The FTIR spectrum of unmodified paper substrate shows a characteristic peak of cellulose as the main component of the paper surface at 3264, 2938 and 1449 cm^{-1} corresponding to the O-H, C-H and CH_2 stretching vibrations, respectively (Promphet et al., 2019). The chitosan coated layer shows a characteristic chitosan peak at 3330 cm^{-1}, corresponding to the N-H stretching vibration peak and absorption bands at 1053 and 1028 cm^{-1}, which correspond to the stretching vibration peaks of the hydroxyl functional groups of the secondary and primary alcohols, respectively. The NaCMC

spectrum obtained by coating a NaCMC-CTAB-DTNB solution onto a paper-based test strip previously coated with a chitosan solution shows a O-H stretching vibration peak at 3271 cm^{-1}. While the peaks at 1725 and 1426 cm^{-1} show asymmetric and symmetric stretching vibrations of the -coo- group, respectively. The peak at 1028 cm^{-1} shows the vibration of -COC- in the NaCMC structure on the surface of the paper substrate (Wang et al., 2020). Finally, the NaCMC layer gave similar spectrum to the NaCMC-CTAB-DTNB layer. The chemical structure of chitosan, NaCMC, CTAB and DTNB are shown in Figure 4-3.

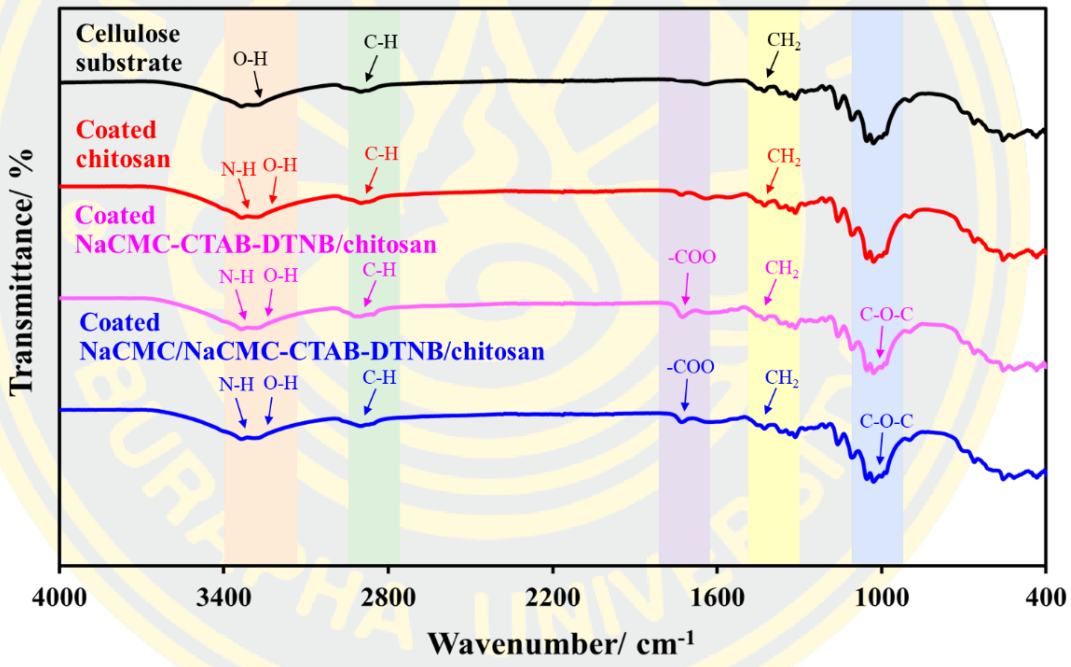

Figure 4-2 ATR-FTIR spectra of different biopolymers in paper-based test strip

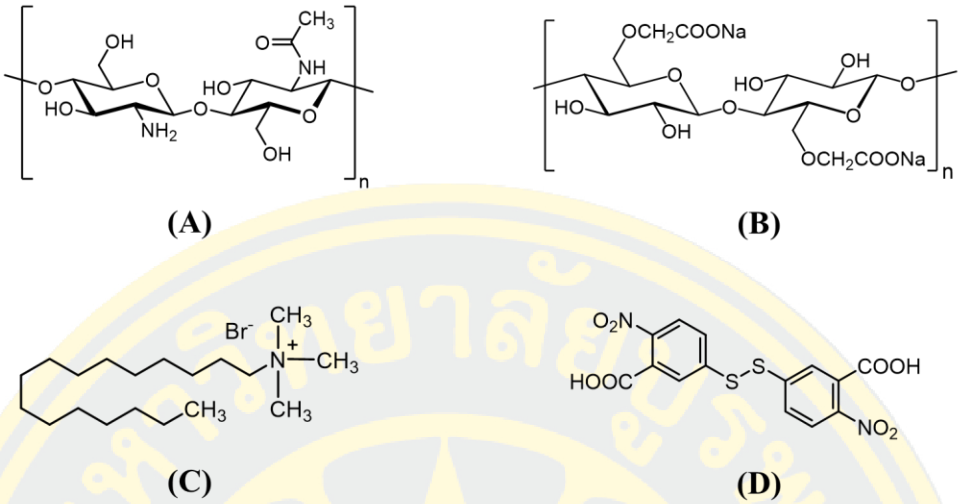

Figure 4-3 The chemical structure of (A) chitosan, (B) NaCMC, (C) CTAB and (D) DTNB

4.2.2 Physical characterization of each coating layer using SEM-EDX analysis

SEM-EDX technique was used to investigate the morphology and elemental composition of the filter paper coated with different layer of biopolymer (Figure 4-4). The morphology of the unmodified filter paper (Whatman No. 1) (Figure 4-4A) shows the porous structure of the pure cellulose microfibers. EDX analysis shows no trace elements except carbon and oxygen, which are the elements found in pure cellulose (Bennis, Benslimane, Vicini, Mairani, & Princi, 2010; Malekghasemi, Kahveci, & Duman, 2016; Yan et al., 2012). The SEM image of the chitosan-coated paper layer demonstrates that the paper was completely covered with chitosan, as reduced porosity in the paper fiber was observed (Figure 4-4B). The elemental composition also shows nitrogen, in addition to carbon and oxygen, which are elemental components of chitosan (Jia et al., 2020; Kopacic, Walzl, Zankel, Leitner, & Bauer, 2018). The layers of paper coated with chitosan/CTAB-DTNB-NaCMC and paper coated with chitosan/CTAB-DTNB-NaCMC/NaCMC (Figure 4-4C and 4-4D) exhibited a similar morphology, showing small flakes of the NaCMC hydrogel coated on the paper-based test strip. From the EDX results, in addition to carbon and

oxygen, there were sulfur, sodium, and additional %wt nitrogen from DTNB, NaCMC, and CTAB, respectively. The layer coated with chitosan/CTAB-DTNB-NaCMC/NaCMC/$AlCl_3$ shows aluminum and chlorine atoms in addition to the aforementioned layer, as the $AlCl_3$ was added to provide crosslinking for the NaCMC polymer (Figure 4-4E). Finally, the layer coated with PEG and AChE enzyme (Figure 4-4F and 4-4G) shows an increasing amount of carbon compared to the aforementioned layer, as it is the main composition of PEG and the enzyme. This result confirms that all the layers are adhered together and do not leach out even after multiple coating steps.

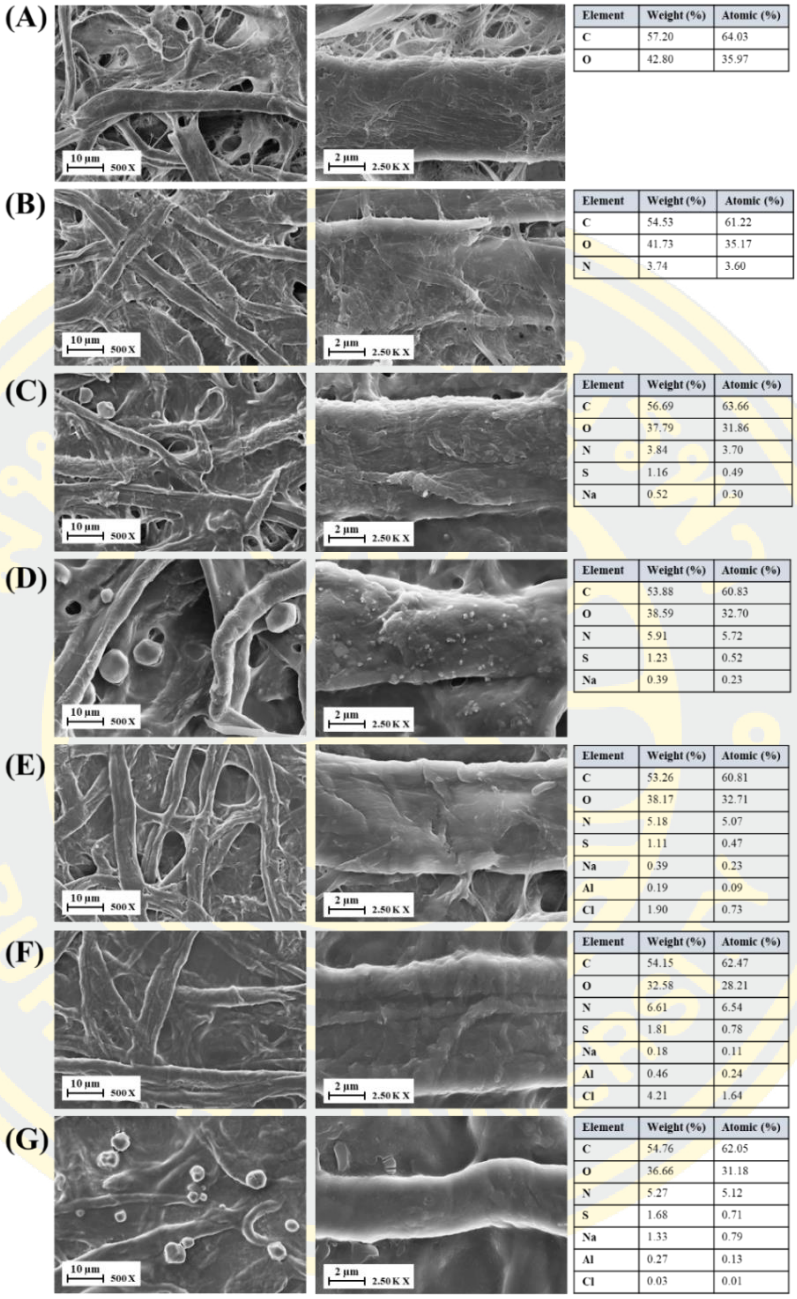

Figure 4-4 SEM-EDX analysis of paper-based test strip that was (A) unmodified cellulose, (B) coated with chitosan, (C) coated chitosan/ CTAB-DTNB-NaCMC (D) coated chitosan/ CTAB-DTNB-NaCMC/ NaCMC (E) coated chitosan/ CTAB-DTNB-NaCMC/ NaCMC/ $AlCl_3$ (F) coated chitosan/ CTAB-DTNB-NaCMC/ NaCMC/ $AlCl_3$/ PEG and (G) coated chitosan/ CTAB-DTNB-NaCMC/ NaCMC/ $AlCl_3$/ PEG/ AChE

4.3 Optimization of the enzyme inhibition assay for OP and CB pesticide analysis on the paper-based test strip

To achieve sensitive analysis with a low limit of detection for pesticides, the assay was optimized for several parameters, including AChE concentration, ATC concentration, reaction time, and inhibition time. All optimizations were performed without pesticides, except for inhibition time.

4.3.1 Concentration of acetylcholine esterase

In this work, the CB and OP pesticides were measured by observing the sensitive reduction in yellow color resulting from the inhibition of AChE enzyme activity by the pesticides. Therefore, the initial concentration of AChE enzyme immobilized on the paper-based test strip is an important parameter that could affect the performance of the assay in determining pesticides and hence was evaluated first. The AChE enzyme concentration in the range of 0.5-5 U/mL was studied and the results are shown in Figure 4-5.

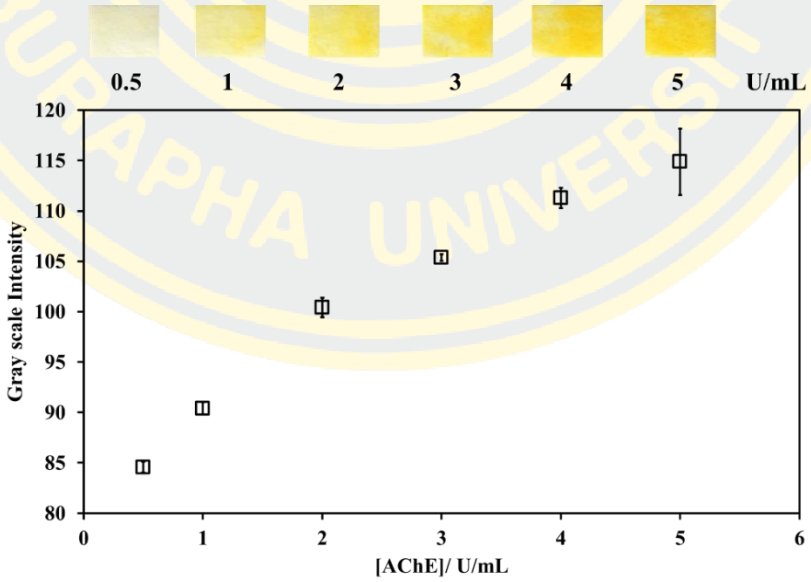

Figure 4-5 Plot of gray scale intensity as a function of AChE concentration. Experimental conditions: *DTNB* 5 mM, *ATC* 1 mM and *reaction time* 5 min (*n=3*)

The intensity of yellow color increased with the concentration of the AChE enzyme and tended to increase continuously. However, the concentration of 2 U/mL of AChE enzyme was selected and used throughout the experiment because it could allow for a sensitive response to the analysis of pesticides where AChE activity is inhibited, resulting in a reduction in color intensity.

4.3.2 Concentration of acetylthiocholine

The ATC concentration was optimized as it affected assay sensitivity. The results showed that the intensity of the yellow color increased as the ATC concentration increased and reached saturation at 5 mM (Figure 4-6). Therefore, an ATC concentration of 3 mM was selected as an optimal concentration to obtain a sensitive-response analysis of pesticides and was used for further experiments.

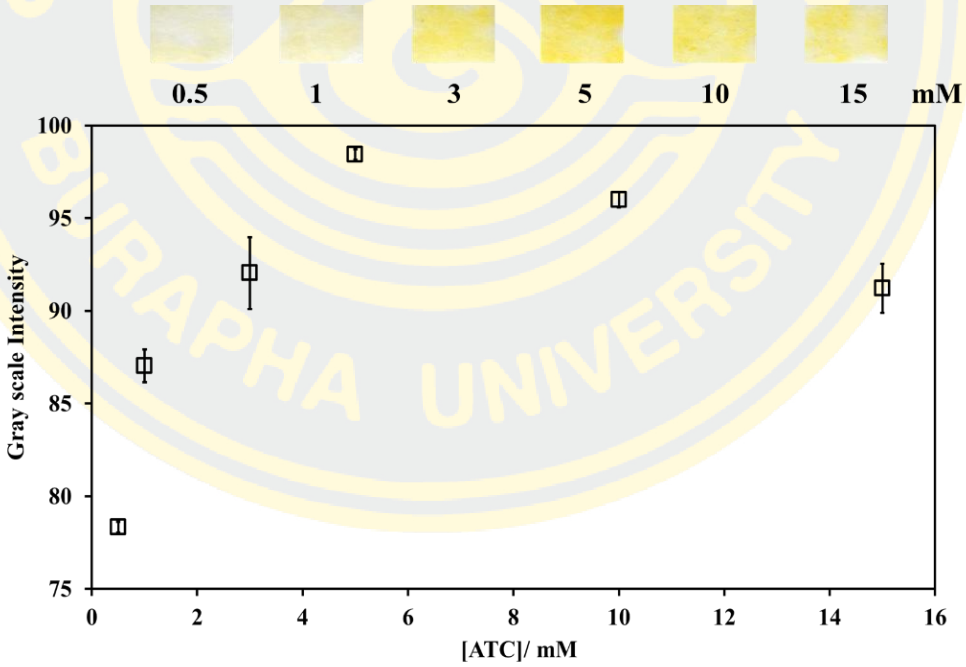

Figure 4-6 Plot of gray scale intensity as a function of ATC concentration. Experimental conditions: *DTNB* 5 mM, *AChE* 2 U/mL and *reaction time* 5 min (*n=3*)

4.3.3 Effect of reaction time

The reaction time of the catalytic hydrolysis reaction of AChE and ATC was then optimized in the range of 1-15 min. As shown in Figure 4-7, the yellow color intensity continued to develop increasingly from 1 to 15 min. A reaction time of 5 min was selected to allow for sensitive dose-response analysis of pesticides.

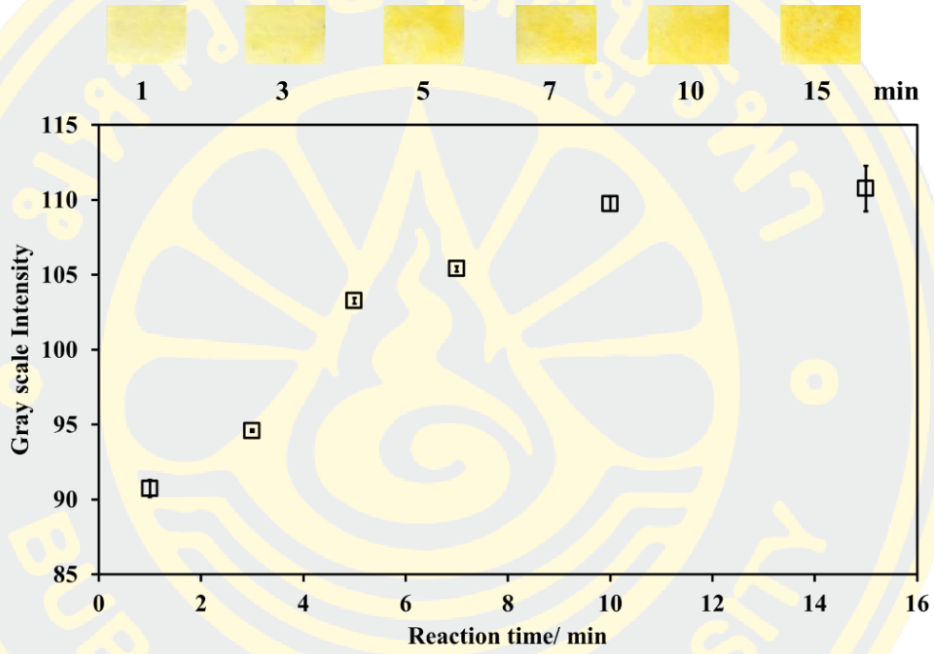

Figure 4-7 Plot of gray scale intensity as a function of reaction time. Experimental conditions: *DTNB* 5 mM, *AChE* 2 U/mL and *ATC* 3 mM (*n=3*)

4.3.4 Effect of inhibition time

The assay inhibition time of AChE enzyme activity by pesticide was optimized in the range of 3–30 min. When 20 µg/mL of malathion pesticide was added to the assay, the decrease in color intensity was rapidly observed within 3-5 min and remained constant up to 30 min, indicating the fast inhibition activity of the pesticide on the enzyme (Figure 4-8). Therefore, in this work, we chose an inhibition time of 5 min to provide a short analysis time with complete inhibition activity of the pesticide on the enzyme.

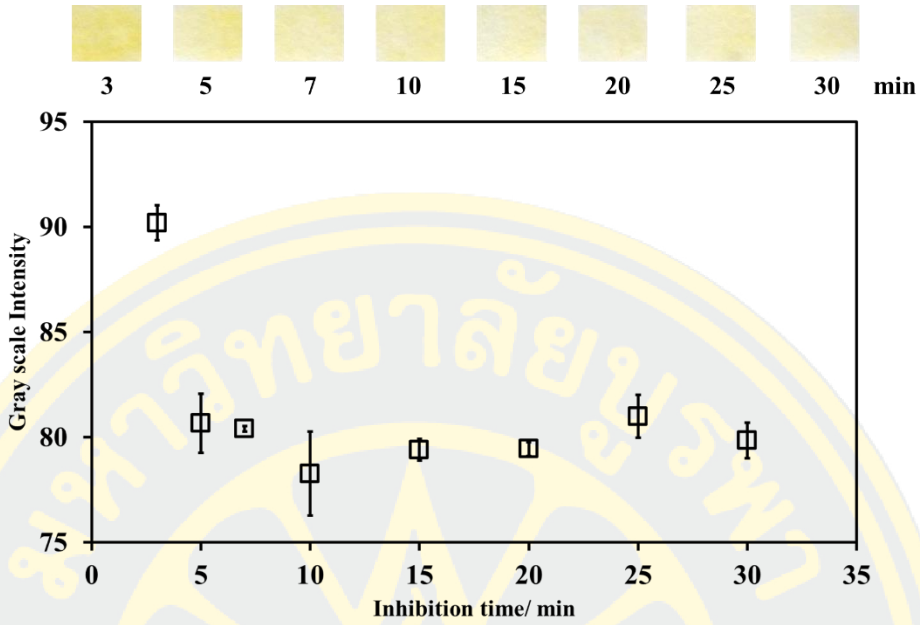

Figure 4-8 Plot of gray scale intensity as a function of inhibition time. Experimental conditions: *DTNB* 5 mM, *AChE* 2 U/mL, *ATC* 3 mM, *reaction time* 5 min and *malathion* 20 µg/mL (*n=3*)

Overall, the optimal conditions for pesticide analysis were 2 U/mL of AChE, 3 mM of ATC, with a 5-min reaction time and a 5-min inhibition time.

4.4 Effect of pH on the developed assay

The effect of pH on the developed pesticide assay was investigated in the pH range of 4-9, as pH also affects enzyme activity. Solutions containing different pH values were tested, and the results were compared to the control (4% methanol). As shown in Figure 4-9, all pH levels studied yielded yellow color intensities similar to that obtained from the control, indicating that the developed paper-based assay has a high tolerance for a wide range of pH values. Additionally, from the measurement of the DSPs-soaking solution pH (dried fish, dried squid, and dried shrimp), the solution pH fell within the range of 5-7 for all samples. Therefore, it should be anticipated that the pH of the DSP sample solution would not affect the developed pesticide assay.

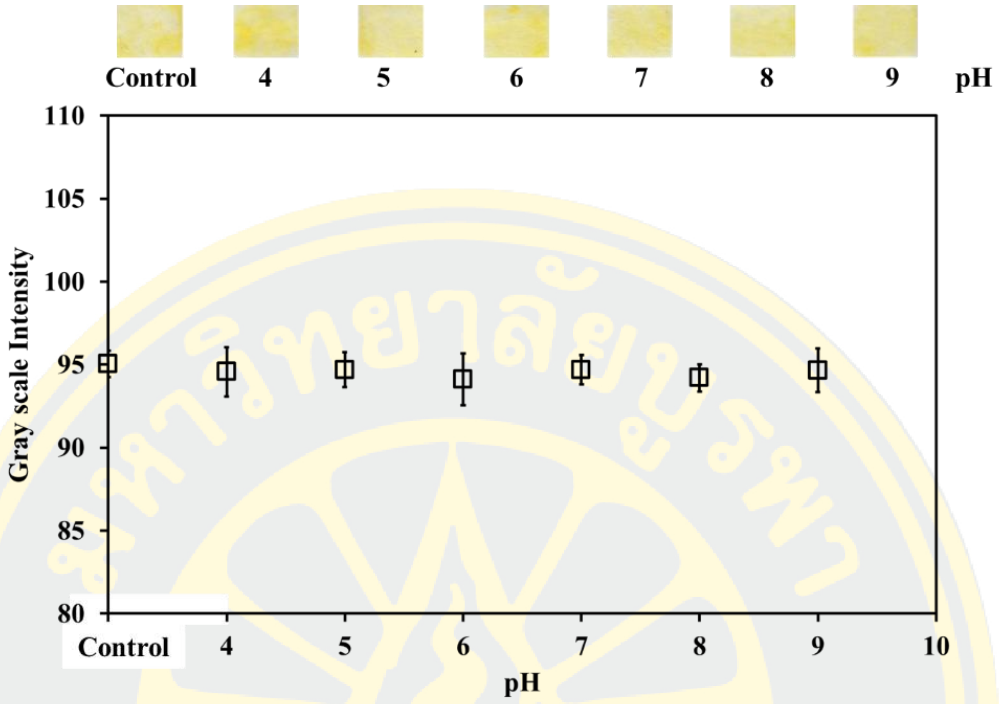

Figure 4-9 Study of the effect of pH on the paper-based assay for pesticide analysis. Experimental conditions: *DTNB* 5 mM, *AChE* 2 U/mL, *ATC* 3 mM and *reaction time* 5 min (*n=3*)

4.5 Stability of the biopolymer coated paper-based test strip

The stability of the developed paper-based test strip was evaluated and compared to non-biopolymer-coated paper-based test strips. The biopolymer coating was prepared using the methods described in the experimental section above, while the non-biopolymer-coated paper-based test strip was prepared by directly dropping the DTNB and AChE solution onto the test zones and allowing them to dry. All test strips were prepared simultaneously, kept in sealed aluminum foil bags containing 1-gram silica gel bags, and stored in the refrigerator (4°C) and at ambient temperature (25-36°C). A freshly prepared 3 mM ATC solution was tested using the evaluated paper-based test strips every 3-7 days (n=3). Real photographs of the stability test results of the paper-based test strip coated with biopolymer and the paper-based test strip without biopolymer coating are shown in Figures 4-10A and 4-10B, respectively. The percentage decrease in color intensity compared to that of freshly prepared test

strips was plotted against storage time for all storage conditions. The results show that the biopolymer-coated paper-based test strip exhibits excellent storage stability under both storage conditions for more than 63 days.

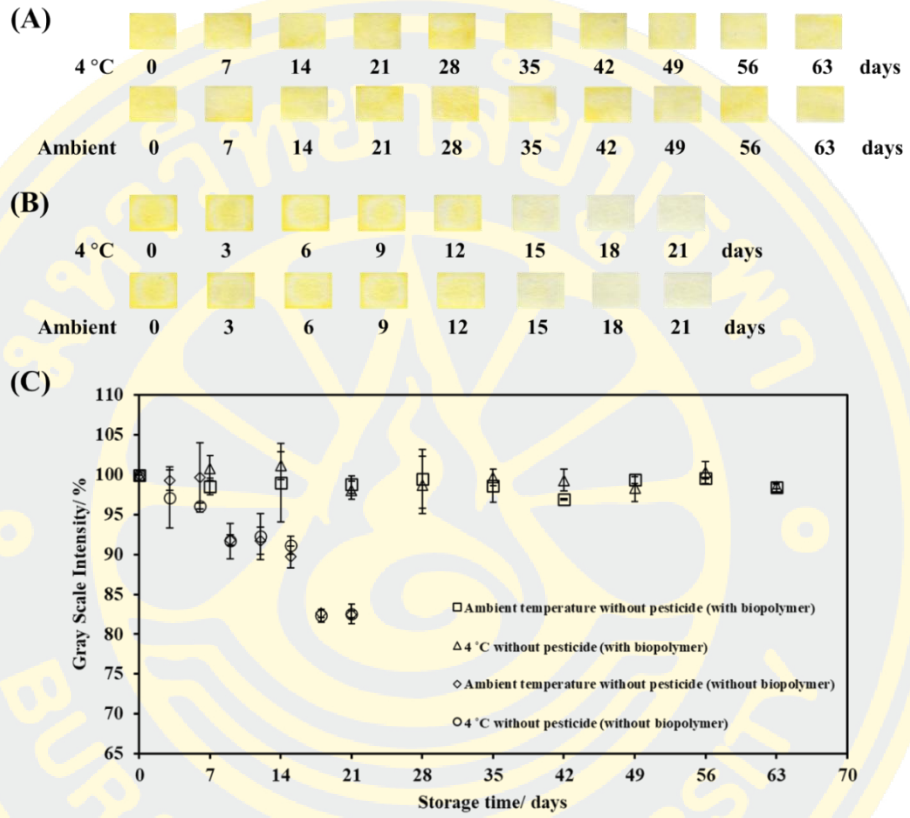

Figure 4-10 Storage stability of the developed paper-based test strip at different storage conditions including 4 °C (refrigerator) and at ambient temperature (A) the paper-based test strip coated with biopolymers, (B) the paper-based test strip without coating biopolymers and (C) The graph shows the %decrease in gray scale intensity over storage time at different storage condition. Experimental conditions: *DTNB* 5 mM, *AChE* 2 U/mL, *ATC* 3 mM and *reaction time* 5 min (*n=3*)

On the other hand, the paper-based test strip without biopolymer coating was found to lose stability under all storage conditions, as the percentage decrease in color intensity was reduced to 90% after only 7 days. This result confirms that the biopolymers

facilitate the preservation and stabilization of key reagents, including DTNB and AChE, on the paper-based test strips, making them suitable for further development into a commercially ready-to-use pesticide sensor where storage stability under various atmospheric conditions is required. Additionally, to the best of the knowledge, the developed paper-based test strip in this work has longest storage stability than the previous reported work developed for pesticide analysis using paper-based device as a detection platform (Hossain, Luckham, McFadden, & Brennan, 2009; Jing et al., 2021; J. Zhang et al., 2024).

4.6 Pesticide analysis using the paper-based test strip

OP and CB pesticides play an important role in foods and agricultural products. Agricultural use of pesticides leads to the accumulation of large quantities of pesticides in food and the environment and is of great danger to human health due to their high toxicity. Therefore, monitoring and determining the levels of these compounds in food is very necessary. In this work, malathion (MAL) and dichlorvos (DDVP) were chosen as representatives of OP pesticides (Figures 4-11A and 4-11B) and carbaryl (CAR) and carbofuran (CBF) are representatives of the CBs pesticides (Figures 4-11C and 4-11D). The analysis of these pesticides were performed under optimal conditions as summarized in Table 4-1.

Table 4-1 Optimal conditions for analysis of OPs and CBs pesticides on a paper-based test trip using enzyme inhibition assay

Conditions studied	Optimal conditions
concentration of AChE	2 U/mL
concentration of ATC	3 mM
reaction time	5 min
inhibition time	5 min

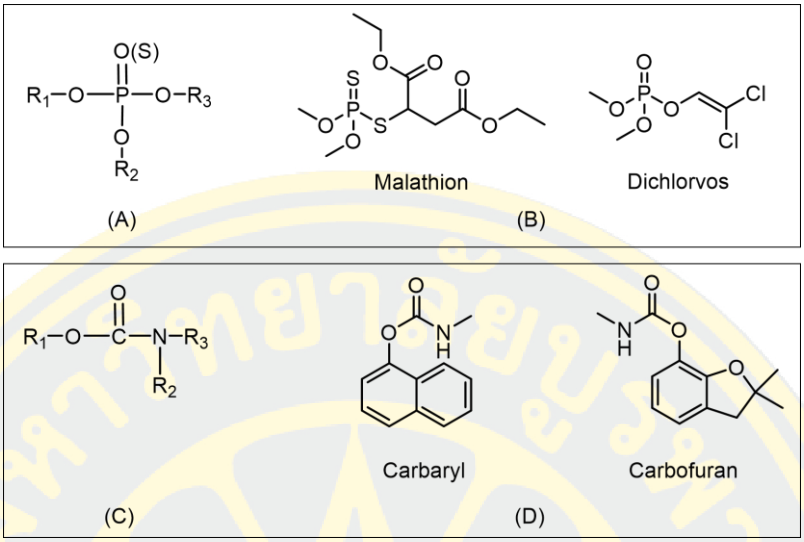

Figure 4-11 (A) General structure of OP compounds. (B) Structure of MAL and DDVP. (C) General structure of CB compounds. (D) Structure of CAR and CBF

4.6.1 OP and CB pesticides analysis

4.6.1.1 Linearity

After obtaining the optimized conditions, the developed paper-based test strip was used to analyze the target pesticides CBs and OPs, with MAL and DDVP representing OPs standards, and CAR and CBF representing CBs standards. As shown in Figure 4-12 and 4-13 respectively, the yellow color intensity decreased as the concentration of pesticide increased for all investigated pesticide standards. The difference in inhibition levels, defined as the difference between the color intensity from the pesticide test at the T zone and that of the control obtained from the C zone of the same test strip.

Calibration curves plotted between the difference of inhibition level and the pesticide concentration of MAL, DDVP, CAR and CBF are shown in Figures 4-12A,4-12B, 4-13A and 4-13B, respectively. The plots shows that the increasing in difference of inhibition level was observed as the concentration of pesticide increased. The assay provided the analysis of different pesticides in different working ranges and sensitivities, depending on their ability to inhibit AChE. For analysis of real-world

samples, this is still acceptable, however, because the system can be normalized to overall AChE inhibition. The linear ranges and sensitivities obtained from the analysis of each pesticide are summarized in Table 4-2.

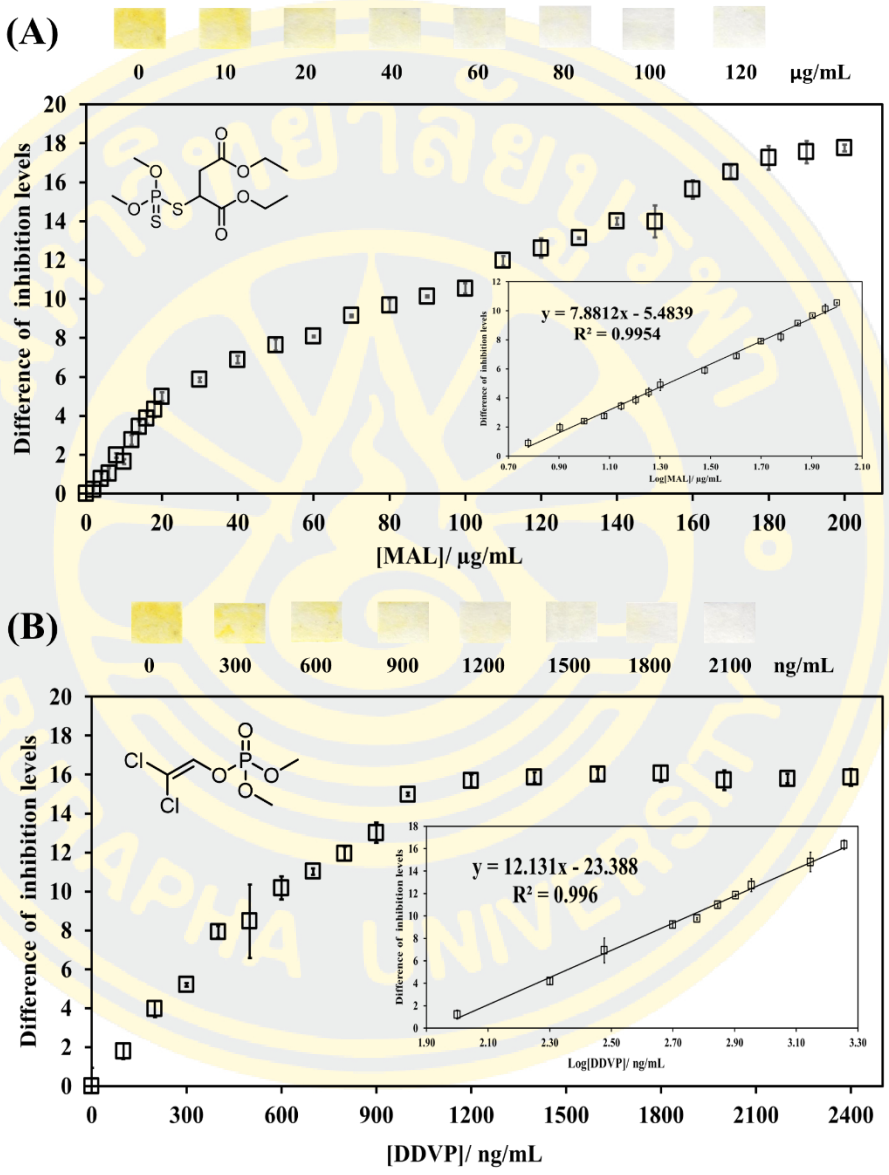

Figure 4-12 Standard curves for the detection of OP pesticide using the paper-based test strip by enzyme inhibition assays (A) MAL and (B) DDVP. Photographs of the actual responses are shown across the top of each plot. Insets of each plot is the linear range of calibration curve. Experimental conditions: *DTNB* 5 mM, *AChE* 2 U/mL, *ATC* 3 mM, *Inhibition time* 5 min and *reaction time* 5 min (*n=3*)

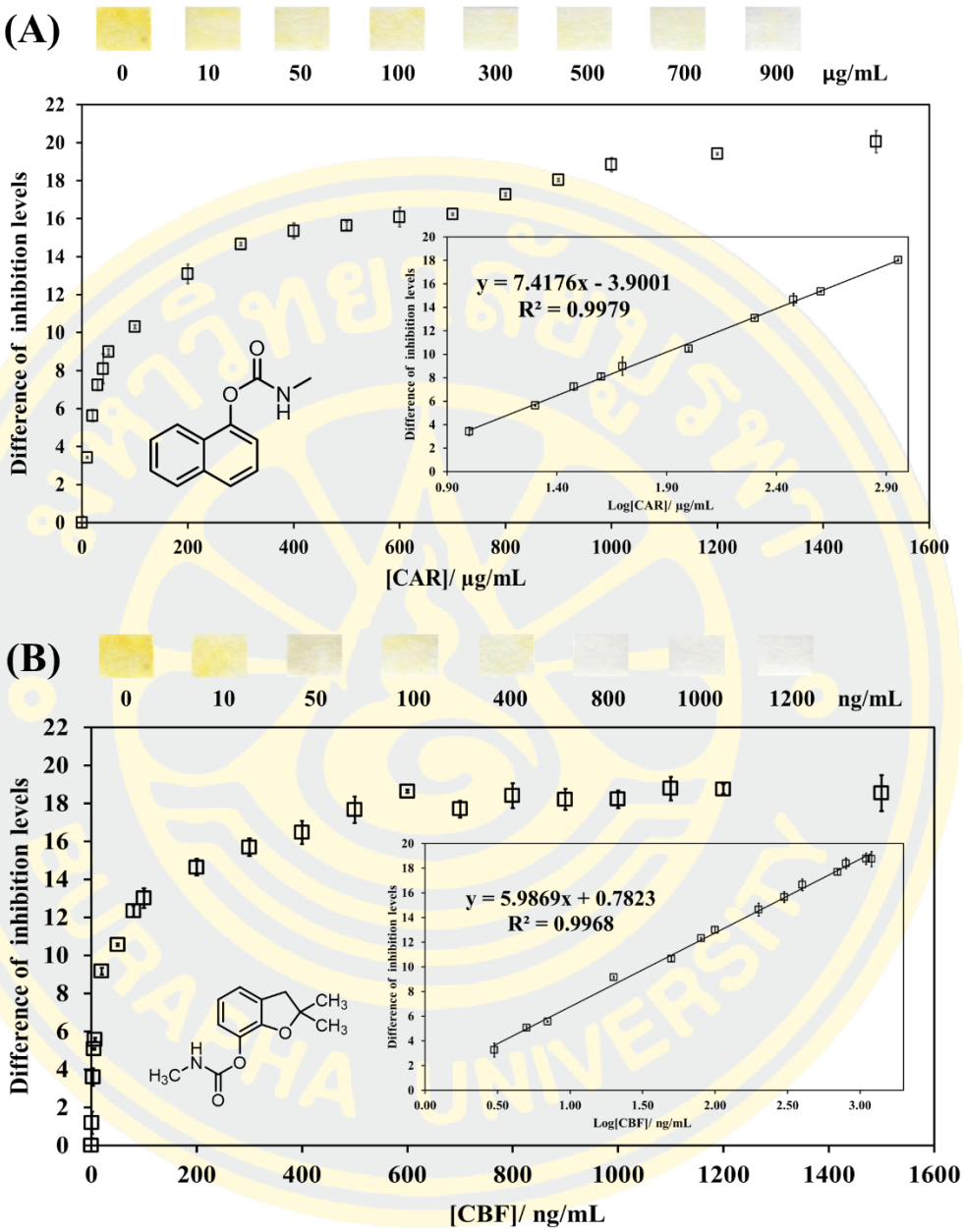

Figure 4-13 Standard curves for the detection of CB pesticide using the paper-based test strip by enzyme inhibition assays (A) CAR and (B) CBF. Photographs of the actual responses are shown across the top of each plot. Insets of each plot is the linear range of calibration curve. Experimental conditions: *DTNB* 5 mM, *AChE* 2 U/mL, *ATC* 3 mM, *inhibition time* 5 min and *reaction time* 5 min (*n=3*)

Table 4-2 Analytical figure of merit for CBs and OPs pesticide analysis with enzyme inhibition assay using paper-based test strip

Pesticide (type)	Linear range	R^2	Sensitivity	LOD	%RSD ($n=3$)
MAL (OPs)	6-100 µg/mg	0.9954	7.8812[a]	1.34 µg/mL	0.20-1.69
DDVP (OPs)	100-1800 ng/mL	0.9960	12.131[b]	1.21 ng/mL	0.46-5.41
CAR (CBs)	10-900 µg/mL	0.9979	7.4176[c]	1.36 µg/mL	0.16-3.47
CBF (CBs)	3-1200 ng/mL	0.9968	5.9869[d]	1.46 ng/mL	0.19-6.34

Unit of sensitivity: (*a*) Log[MAL, µg/mL]$^{-1}$, (*b*) Log[DDVP, ng/mL]$^{-1}$, (*c*) Log[CAR, µg/mL]$^{-1}$ and (*d*) Log[CBF, ng/mL]$^{-1}$.

4.6.1.2 Limit of detection (LOD) and repeatability

Limit of detection (LOD) is defined as the lowest pesticide concentration that can causes the signal intensity reliably difference from the blank signal and can be calculated by 3SD/slope where the SD is the standard deviation of the blank (n=8) and slope is the slope of the calibration plot. The LODs of the four pesticides were 1.36 µg/mL, 1.48 ng/mL, 1.34 µg/mL , and 1.21 ng/mL for CAR, CBF, MAL, and DDVP, respectively. This is sufficient to measure pesticide levels harmful to humans and MRL levels (Maximum Residue Limits for pesticide) found in foods such as CAR (cucumber is 3 mg/kg and grapes is 5 mg/kg), CBF (banana are 0.1 mg/mL and rice are 0.1 mg/kg), MAL (cabbages are 8 mg/kg and kale are 3 mg/kg) and DDVP (meat are 0.05 mg/kg and milks are 0.02 mg/kg).[24-27] Analytical figures for the analysis of the four different pesticides, CBs, and OPs are summarized in Table 4-2. All results show that the performance of the pesticide analysis is satisfactory, with excellent linearity range, low LOD and high repeatability expressed relative standard deviation (%RSD) for the analysis of CBs and OPs.

4.7 Analysis of OP and CB pesticides in real samples

4.7.1 Analysis of DDVP and CBF pesticides in dried seafood products

The developed paper-based test strip was further evaluated for its analytical performance in analyzing DDVP and CBF pesticides in real DSPs product samples, including dried fish, dried squid, and dried shrimp, as they have previously been reported to be contaminated with high levels of pesticides (Guo, Wu, Shen, & Zeng, 2010; Moon, Kim, Choi, Yu, & Choi, 2009). The validation procedure of the developed method involved spiking the samples with different concentrations of standard pesticide solutions. The sample extracts, prepared using the laboratory-based sample preparation method, were quantified for pesticides using the developed method and LC-MS/MS (Table 4-3). The measured pesticide concentrations obtained from the two methods for all samples were not statistically different at a 95% confidence level ($P > 0.05$ for all samples, all spiked concentrations and both pesticide standards), indicating that the developed paper-based test strip can provide measurements for the analysis of CB and OP pesticides in DSP samples as accurately as the traditional LC-MS/MS method. For dried fish and dried squid, the recoveries obtained from the two methods at every investigated concentration for both DDVP and CBF were in the range of 73-109%, which are acceptable according to AOAC standard (AOAC, 2018). However, the recoveries in dried shrimp samples were found to be very low when measured using both methods, indicating possible matrix interference in these samples and suggesting the unsuitability of the sample preparation method used in this work (Shewbart, Mies, & Ludwig, 1972). New sample extraction methods are currently being investigated for this type of sample.

Table 4-3 Results of determination of DDVP and CBF in spiked samples with paper-based test strip and LC-MS/MS method

Sample	Spiked pesticides (ng/mL)		Found (ng/mL) ± SD (*n*=3)		Recovery (%)		Real image
			This method	LC-MS/MS	This method	LC-MS/MS	
Dried fish	DDVP	0	ND	ND	-	-	
		100	109.35 ± 0.77	81.61 ± 8.67	109	82	
		500	478.65 ± 9.80	547.21 ± 17.66	96	109	
		1000	1072.13 ± 15.39	1035.95 ± 35.00	107	104	
	CBF	0	ND	ND	-	-	
		30	32.38 ± 1.99	22.04 ± 7.01	108	73	
		500	459.10 ± 31.82	548.34 ± 14.01	92	110	
		1000	1089.88 ± 20.21	1012.43 ± 28.03	109	101	
Dried squid	DDVP	0	ND	ND	-	-	
		100	108.60 ± 6.07	85.38 ± 8.58	109	85	
		500	457.16 ± 34.08	496.38 ± 17.39	91	99	
		1000	981.49 ± 20.46	1106.71 ± 35.40	98	111	
	CBF	0	ND	ND	-	-	
		30	32.61 ± 0.34	41.24 ± 7.01	109	137	
		500	470.41 ± 2.77	464.07 ± 14.01	94	93	
		1000	977.96 ± 18.98	1088.09 ± 28.03	98	109	
Dried shrimp	DDVP	0	ND	ND	-	-	
		100	34.63 ± 1.66	36.50 ± 8.80	35	37	
		500	227.66 ± 5.59	224.02 ± 17.01	46	45	
		1000	624.63 ± 3.59	580.16 ± 33.86	62	58	
	CBF	0	ND	ND	-	-	
		30	10.05 ± 0.90	11.02 ± 7.01	33	37	
		500	246.39 ± 6.35	256.58 ± 14.01	49	51	
		1000	744.62 ± 24.15	795.77 ± 28.03	74	79	

ND: not detecte

CHAPTER 5
CONCLUSIONS AND FUTURE PERSPECTIVES

5.1 Conclusions

This research has developed a method for analyzing OP and CB pesticides using a paper-based test strip based on the principle of enzyme inhibition assay. The advantages of this developed method are that it is simple analysis, rapid, cheap, uses a small amount of reagents on the sample and the analysis can be performed without the need for highly trained personnel. The biopolymers were employed to coat the paper-based test strip and found to be effective for reagent stabilization and increase storage shelf life.

From the optimization of enzyme inhibition assay on the paper-based test strip, the results showed that the optimal AChE enzyme concentration was 2 U/mL. ATC concentration was 3 mM with 5-min reaction time and 5-min inhibition time. Analysis of OPs and CBs pesticides was carried out under the above mentioned conditions and it was found that the color intensity decreased with increasing pesticide concentration. The four investigated pesticides including MAL, DDVP and CAR, CBF were successfully analyzed with low LOD and high repeatability.

Finally, the paper-based test strip was validated against LC-MS/MS method for analyzing DDVP and CBF spiked in DSP samples. The concentrations of DDPV and CBF in DSP samples obtained from both methods were similar which can indicate the accuracy of the developed method and can be used as an alternative for on-site food safety screening to determine the amount of pesticide contamination in food samples.

5.2 Future perspective

Future studies will focus on improving the stability of ATC, which acts as a substrate in the reaction as it might decompose over time. Moreover, the sample extraction methods suitable for complex matrix samples such as dried shrimp products will be studied.

APPENDIX A

Limit of detection (LOD)

(A) (B)

Figure A-1 (A) Color produced on a paper-based test strip from MAL analysis at a concentration of 0 µg/mL and (B) color produced on a paper-based test strip from MAL analysis at a concentration of 10 µg/mL

(A) (B)

Figure A-2 (A) Color produced on a paper-based test strip from DDVP analysis at a concentration of 0 ng/mL and (B) color produced on a paper-based test strip from MAL analysis at a concentration of 10 ng/mL

(A) (B)

Figure A-3 (A) Color produced on a paper-based test strip from CAR analysis at a concentration of 0 µg/mL and (B) color produced on a paper-based test strip from CAR analysis at a concentration of 10 µg/mL

(A) (B)

Figure A-4 (A) Color produced on a paper-based test strip from CBF analysis at a concentration of 0 ng/mL and (B) color produced on a paper-based test strip from CBF analysis at a concentration of 10 ng/mL

APPENDIX B

Relative standard deviation (%RSD)

Table B-1 Relative standard deviation of MAL analysis

MAL (µg/mL)	%RSD (*n=3*)
6	1.01
8	0.42
10	0.47
12	0.99
14	1.15
16	1.18
18	1.64
20	0.94
30	0.50
40	0.87
50	1.41
60	0.20
70	0.33
80	1.69
90	0.23
100	1.44

Table B-2 Relative standard deviation of DDVP analysis

DDVP (ng/mL)	%RSD (*n=3*)
100	1.33
200	1.04
300	4.64
500	1.37
600	0.46
700	0.68
800	0.60
900	3.16
1400	5.41
1800	2.96

Table B-3 Relative standard deviation of CAR analysis

CAR (µg/mL)	%RSD (*n=3*)
10	0.16
20	1.27
30	1.23
40	3.47
50	0.69
100	0.45
200	2.95
300	0.56
400	2.63
900	0.63

Table B-4 Relative standard deviation of CBF analysis

CBF (ng/mL)	%RSD (*n=3*)
1	2.10
3	1.85
5	0.19
7	0.39
20	0.92
50	0.37
80	1.70
100	3.32
200	3.17
300	3.59
400	4.98
700	3.94
800	6.34
900	5.24
1000	4.45
1100	6.21
1200	2.57

REFERENCES

ACFS. (2016). PESTICIDE RESIDUES: MAXIMUM RESIDUE LIMITS. *THAI AGRICULTURAL STANDARD*.

AOAC. (2018). Appendix F: Guidelines for Standard Method Performance Requirements.

Assis, C. R. D., Linhares, A. G., Cabrera, M. P., Oliveira, V. M., Silva, K. C. C., Marcuschi, M., . . . Carvalho, L. B., Jr. (2018). Erythrocyte acetylcholinesterase as biomarker of pesticide exposure: new and forgotten insights. *Environ Sci Pollut Res Int, 25*(19), 18364-18376. doi:10.1007/s11356-018-2303-9

Badawy, M. E., & El-Aswad, A. F. (2014). Bioactive paper sensor based on the acetylcholinesterase for the rapid detection of organophosphate and carbamate pesticides. *Int J Anal Chem, 2014*, 536823. doi:10.1155/2014/536823

Badr, A. M. (2020). Organophosphate toxicity: updates of malathion potential toxic effects in mammals and potential treatments. *Environ Sci Pollut Res Int, 27*(21), 26036-26057. doi:10.1007/s11356-020-08937-4

Bennis, H., Benslimane, R., Vicini, S., Mairani, A., & Princi, E. (2010). Fibre width measurement and quantification of filler size distribution in paper-based materials by SEM and image analysis. *J Electron Microsc (Tokyo), 59*(2), 91-102. doi:10.1093/jmicro/dfp051

Binukumar, B., & Gill, K. (2010). Cellular and molecular mechanisms of dichlorvos neurotoxicity: cholinergic, nonchlolinergic, cell signaling, gene expression and therapeutic aspects.

Brkic, D. V., Vitorovic, S., Gasic, S. M., & Neskovic, N. K. (2008). Carbofuran in water: Subchronic toxicity to rats. *Environ Toxicol Pharmacol, 25*(3), 334-341. doi:10.1016/j.etap.2007.11.002

Calista, N., Haikael, M. D., Athanasia, M. O., Neema, K., & Judith, K. (2022). Does Pesticide exposure contribute to the growing burden of non - communicable diseases in Tanzania. *Scientific African, 17*. doi:10.1016/j.sciaf.2022.e01276

Carullo, P., Cetrangolo, G. P., Mandrich, L., Manco, G., & Febbraio, F. (2015). Fluorescence spectroscopy approaches for the development of a real-time organophosphate detection system using an enzymatic sensor. *Sensors (Basel),*

15(2), 3932-3951. doi:10.3390/s150203932

Cate, D. M., Adkins, J. A., Mettakoonpitak, J., & Henry, C. S. (2015). Recent developments in paper-based microfluidic devices. *Anal Chem, 87*(1), 19-41. doi:10.1021/ac503968p

Cate, D. M., Dungchai, W., Cunningham, J. C., Volckens, J., & Henry, C. S. (2013). Simple, distance-based measurement for paper analytical devices. *Lab Chip, 13*(12), 2397-2404. doi:10.1039/c3lc50072a

Chau, N. D., Sebesvari, Z., Amelung, W., & Renaud, F. G. (2015). Pesticide pollution of multiple drinking water sources in the Mekong Delta, Vietnam: evidence from two provinces. *Environ Sci Pollut Res Int, 22*(12), 9042-9058. doi:10.1007/s11356-014-4034-x

Chau, N. D. G., Sebesvari, Z., Amelung, W., & Renaud, F. G. (2015). Pesticide pollution of multiple drinking water sources in the Mekong Delta, Vietnam: evidence from two provinces. *Environmental science and pollution research, 22*, 9042-9058.

Colovic, M. B., Krstic, D. Z., Lazarevic-Pasti, T. D., Bondzic, A. M., & Vasic, V. M. (2013). Acetylcholinesterase inhibitors: pharmacology and toxicology. *Current neuropharmacology, 11*(3), 315-335.

da Silva Sousa, J., do Nascimento, H. O., de Oliveira Gomes, H., & do Nascimento, R. F. (2021). Pesticide residues in groundwater and surface water: recent advances in solid-phase extraction and solid-phase microextraction sample preparation methods for multiclass analysis by gas chromatography-mass spectrometry. *Microchemical Journal, 168*. doi:10.1016/j.microc.2021.106359

Darvesh, S., Darvesh, K. V., McDonald, R. S., Mataija, D., Walsh, R., Mothana, S., . . . Martin, E. (2008). Carbamates with differential mechanism of inhibition toward acetylcholinesterase and butyrylcholinesterase. *J Med Chem, 51*(14), 4200-4212. doi:10.1021/jm8002075

Deka, S., & Mahanta, R. (2015). Dichlorvos toxicity on fish-a review. *European Journal of Biological Research, 5*(3), 78-85.

Fei Liu, X., Lin Guan, Y., Zhi Yang, D., Li, Z., & De Yao, K. (2001). Antibacterial action of chitosan and carboxymethylated chitosan. *Journal of Applied Polymer Science, 79*(7), 1324-1335.

Fernandes, L. S., Emerick, G. L., dos Santos, N. A., de Paula, E. S., Barbosa, F., Jr., & dos Santos, A. C. (2015). In vitro study of the neuropathic potential of the organophosphorus compounds trichlorfon and acephate. *Toxicol In Vitro, 29*(3), 522-528. doi:10.1016/j.tiv.2015.01.001

Flessel, P., Quintana, P., & Hooper, K. (1993). Genetic toxicity of malathion: a review. *Environmental and molecular mutagenesis, 22*(1), 7-17.

Gallo, V., Tomai, P., Gherardi, M., Fanali, C., De Gara, L., D'Orazio, G., & Gentili, A. (2021). Dispersive liquid-liquid microextraction using a low transition temperature mixture and liquid chromatography-mass spectrometry analysis of pesticides in urine samples. *Journal of Chromatography A, 1642*, 462036.

Gunasekara, A. S., Rubin, A. L., Goh, K. S., Spurlock, F. C., & Tjeerdema, R. S. (2008). Environmental fate and toxicology of carbaryl. *Rev Environ Contam Toxicol, 196*, 95-121. doi:10.1007/978-0-387-78444-1_4

Guo, J., Wu, F., Shen, R., & Zeng, E. Y. (2010). Dietary intake and potential health risk of DDTs and PBDEs via seafood consumption in South China. *Ecotoxicology and environmental safety, 73*(7), 1812-1819.

Gupta, J., Rathour, R., Singh, R., & Thakur, I. S. (2019). Production and characterization of extracellular polymeric substances (EPS) generated by a carbofuran degrading strain Cupriavidus sp. ISTL7. *Bioresour Technol, 282*, 417-424. doi:10.1016/j.biortech.2019.03.054

Habenschus, M. D., Carrao, D. B., de Albuquerque, N. C. P., Perovani, I. S., Moreira da Silva, R., Nardini, V., . . . Moraes de Oliveira, A. R. (2021). In vitro enantioselective inhibition of the main human CYP450 enzymes involved in drug metabolism by the chiral pesticide tebuconazole. *Toxicol Lett, 351*, 1-9. doi:10.1016/j.toxlet.2021.08.006

Health, U. D. o., & Services, H. (1999). Agency for Toxic Substances and Disease Registry-ATSDR.

Hossain, S. Z., Luckham, R. E., McFadden, M. J., & Brennan, J. D. (2009). Reagentless bidirectional lateral flow bioactive paper sensors for detection of pesticides in beverage and food samples. *Analytical chemistry, 81*(21), 9055-9064.

Hosseini, S. F., Nassehinia, H., Nazari, H., Dadban Shahamat, Y., Ghoraba, Z., &

Moeinian, K. (2021). Determination of diazinon concentration by Gas Chromatography - Mass Spectrometry in underground drinking water resources located near the rice fields, before and after the pesticide spraying. *Microchemical Journal, 170*. doi:10.1016/j.microc.2021.106600

HSDB, E. (2011). Biomonitorin PCBs. *Hazardous Substances Data Bank (HSDB)*.

Hu, J., Wang, S., Wang, L., Li, F., Pingguan-Murphy, B., Lu, T. J., & Xu, F. (2014). Advances in paper-based point-of-care diagnostics. *Biosens Bioelectron, 54*, 585-597. doi:10.1016/j.bios.2013.10.075

Jia, Z., Yang, C., Zhao, F., Chao, X., Li, Y., & Xing, H. (2020). One-Step Reinforcement and Deacidification of Paper Documents: Application of Lewis Base—Chitosan Nanoparticle Coatings and Analytical Characterization. *Coatings, 10*(12). doi:10.3390/coatings10121226

Jing, X., Wang, H., Huang, X., Chen, Z., Zhu, J., & Wang, X. (2021). Digital image colorimetry detection of carbaryl in food samples based on liquid phase microextraction coupled with a microfluidic thread-based analytical device. *Food Chem, 337*, 127971. doi:10.1016/j.foodchem.2020.127971

Jokerst, J. C., Adkins, J. A., Bisha, B., Mentele, M. M., Goodridge, L. D., & Henry, C. S. (2012). Development of a paper-based analytical device for colorimetric detection of select foodborne pathogens. *Anal Chem, 84*(6), 2900-2907. doi:10.1021/ac203466y

Kamel, F., & Hoppin, J. A. (2004). Association of pesticide exposure with neurologic dysfunction and disease. *Environ Health Perspect, 112*(9), 950-958. doi:10.1289/ehp.7135

Kaneko, K., Hara, M., Nishino, T., & Maruyama, T. (2020). One-Step Biotinylation of Cellulose Paper by Polymer Coating to Prepare a Paper-Based Analytical Device. *Anal Chem, 92*(2), 1978-1987. doi:10.1021/acs.analchem.9b04373

Keikavousi Behbahan, A., Mahdavi, V., Roustaei, Z., & Bagheri, H. (2021). Preparation and evaluation of various banana-based biochars together with ultra-high performance liquid chromatography-tandem mass spectrometry for determination of diverse pesticides in fruiting vegetables. *Food Chem, 360*, 130085. doi:10.1016/j.foodchem.2021.130085

Kopacic, S., Walzl, A., Zankel, A., Leitner, E., & Bauer, W. (2018). Alginate and Chitosan as a Functional Barrier for Paper-Based Packaging Materials. *Coatings, 8*(7). doi:10.3390/coatings8070235

Kumar, M., Yadav, A. N., Saxena, R., Paul, D., & Tomar, R. S. (2021). Biodiversity of pesticides degrading microbial communities and their environmental impact. *Biocatalysis and Agricultural Biotechnology, 31*. doi:10.1016/j.bcab.2020.101883

Lai, H., Li, Z., Zhu, S., Cai, L., Xu, C., & Zhou, Q. (2019). Naked-Eye Detection of Aluminum in Gastric Drugs on a Paper-Based Analytical Device. *Journal of Chemical Education, 97*(1), 295-299. doi:10.1021/acs.jchemed.9b00569

LeNoir, J. S., McConnell, L. L., Fellers, G. M., Cahill, T. M., & Seiber, J. N. (1999). Summertime transport of current-use pesticides from California's Central Valley to the Sierra Nevada Mountain Range, USA. *Environmental Toxicology and Chemistry: An International Journal, 18*(12), 2715-2722.

Li, J., & Zhuang, S. (2020). Antibacterial activity of chitosan and its derivatives and their interaction mechanism with bacteria: Current state and perspectives. *European Polymer Journal, 138*, 109984.

Liu, H., Yi, M., Shi, X., Liang, P., & Gao, X. (2006). Substrate specificity of brain acetylcholinesterase and its sensitivity to carbamate insecticides in Carassius auratus. *Fish Physiology and Biochemistry, 33*(1), 29-34. doi:10.1007/s10695-006-9114-5

Liu, X., Liu, Z., Bian, L., Ping, Y., Li, S., Zhang, J., . . . Wang, X. (2022). Determination of pesticide residues in chilli and Sichuan pepper by high performance liquid chromatography quadrupole time-of-flight mass spectrometry. *Food Chem, 387*, 132915. doi:10.1016/j.foodchem.2022.132915

Lorke, D. E., & Petroianu, G. A. (2019). Reversible cholinesterase inhibitors as pretreatment for exposure to organophosphates. A review. *J Appl Toxicol, 39*(1), 101-116. doi:10.1002/jat.3662

Malekghasemi, S., Kahveci, E., & Duman, M. (2016). Rapid and alternative fabrication method for microfluidic paper based analytical devices. *Talanta, 159*, 401-411. doi:10.1016/j.talanta.2016.06.040

Marques, F., & Mitra, S. K. (2021). Dip-and-Fold Device: A Paper-Based Testing Platform for Rapid Assessment of Insecticides in Water Samples. *ACS Appl Bio Mater, 4*(12), 8456-8465. doi:10.1021/acsabm.1c00986

Mishra, S., Pang, S., Zhang, W., Lin, Z., Bhatt, P., & Chen, S. (2021). Insights into the microbial degradation and biochemical mechanisms of carbamates. *Chemosphere, 279*, 130500. doi:10.1016/j.chemosphere.2021.130500

Mishra, S., Zhang, W., Lin, Z., Pang, S., Huang, Y., Bhatt, P., & Chen, S. (2020). Carbofuran toxicity and its microbial degradation in contaminated environments. *Chemosphere, 259*, 127419. doi:10.1016/j.chemosphere.2020.127419

Mohammadzadeh, L., Abnous, K., Razavi, B. M., & Hosseinzadeh, H. (2020). Crocin-protected malathion-induced spatial memory deficits by inhibiting TAU protein hyperphosphorylation and antiapoptotic effects. *Nutr Neurosci, 23*(3), 221-236. doi:10.1080/1028415X.2018.1492772

Moon, H.-B., Kim, H.-S., Choi, M., Yu, J., & Choi, H.-G. (2009). Human health risk of polychlorinated biphenyls and organochlorine pesticides resulting from seafood consumption in South Korea, 2005–2007. *Food and Chemical Toxicology, 47*(8), 1819-1825.

Mukdasai, S., Uppachai, P., & Srijaranai, S. (2019). A novel colorimetric paper sensor based on the layer-by-layer assembled multilayers of surfactants for the sensitive and selective determination of total antioxidant capacity. *RSC Adv, 9*(49), 28598-28608. doi:10.1039/c9ra05642d

Mustapha, M. U., Halimoon, N., Johar, W. L. W., & Abd Shukor, M. Y. (2019). An overview on biodegradation of carbamate pesticides by soil bacteria. *Pertanika Journal of Science & Technology, 27*(2).

Newhart, K. (2006). Environmental fate of malathion. *California Environmental Protection Agency, 11*, 1-20.

Nouanthavong, S., Nacapricha, D., Henry, C. S., & Sameenoi, Y. (2016). Pesticide analysis using nanoceria-coated paper-based devices as a detection platform. *Analyst, 141*(5), 1837-1846.

Nouanthavong, S., Nacapricha, D., Henry, C. S., & Sameenoi, Y. (2016). Pesticide analysis using nanoceria-coated paper-based devices as a detection platform.

Analyst, 141(5), 1837-1846. doi:10.1039/c5an02403j

Okoroiwu, H. U., & Iwara, I. A. (2018). Dichlorvos toxicity: A public health perspective. *Interdiscip Toxicol, 11*(2), 129-137. doi:10.2478/intox-2018-0009

Onunga, D. O., Kowino, I. O., Ngigi, A. N., Osogo, A., Orata, F., Getenga, Z. M., & Were, H. (2015). Biodegradation of carbofuran in soils within Nzoia River Basin, Kenya. *J Environ Sci Health B, 50*(6), 387-397. doi:10.1080/03601234.2015.1011965

Paradis, D., Bérail, G., Bonmatin, J.-M., & Belzunces, L. P. (2014). Sensitive analytical methods for 22 relevant insecticides of 3 chemical families in honey by GC-MS/MS and LC-MS/MS. *Analytical and Bioanalytical Chemistry, 406*, 621-633.

Pereira, E. F., Aracava, Y., DeTolla, L. J., Jr., Beecham, E. J., Basinger, G. W., Jr., Wakayama, E. J., & Albuquerque, E. X. (2014). Animal models that best reproduce the clinical manifestations of human intoxication with organophosphorus compounds. *J Pharmacol Exp Ther, 350*(2), 313-321. doi:10.1124/jpet.114.214932

Promphet, N., Rattanawaleedirojn, P., Siralertmukul, K., Soatthiyanon, N., Potiyaraj, P., Thanawattano, C., . . . Rodthongkum, N. (2019). Non-invasive textile based colorimetric sensor for the simultaneous detection of sweat pH and lactate. *Talanta, 192*, 424-430. doi:10.1016/j.talanta.2018.09.086

Pungjunun, K., Nantaphol, S., Praphairaksit, N., Siangproh, W., Chaiyo, S., & Chailapakul, O. (2020). Enhanced sensitivity and separation for simultaneous determination of tin and lead using paper-based sensors combined with a portable potentiostat. *Sensors and Actuators B: Chemical, 318*. doi:10.1016/j.snb.2020.128241

Sameenoi, Y., Panymeesamer, P., Supalakorn, N., Koehler, K., Chailapakul, O., Henry, C. S., & Volckens, J. (2013). Microfluidic paper-based analytical device for aerosol oxidative activity. *Environ Sci Technol, 47*(2), 932-940. doi:10.1021/es304662w

Shamgsumova, R. V., Shurpik, D. N., Evtugyn, V. G., Stoikov, I. I., & Evtugyn, G. A. (2018). Electrochemical Determination of Malathion on an Acetylcholinesterase-Modified Glassy Carbon Electrode. *Analytical Letters, 51*(12), 1911-1926.

doi:10.1080/00032719.2017.1396338

Shao, J., Tong, L., Tang, S., Guo, Z., Zhang, H., Li, P., . . . Yu, X. F. (2015). PLLA nanofibrous paper-based plasmonic substrate with tailored hydrophilicity for focusing SERS detection. *ACS Appl Mater Interfaces, 7*(9), 5391-5399. doi:10.1021/am508881k

Shewbart, K., Mies, W., & Ludwig, P. (1972). Identification and quantitative analysis of the amino acids present in protein of the brown shrimp Penaeus aztecus. *Marine Biology, 16*(1), 64-67.

Silva, K. C., Assis, C. R., Oliveira, V. M., Carvalho, L. B., Jr., & Bezerra, R. S. (2013). Kinetic and physicochemical properties of brain acetylcholinesterase from the peacock bass (Cichla ocellaris) and in vitro effect of pesticides and metal ions. *Aquat Toxicol, 126*, 191-197. doi:10.1016/j.aquatox.2012.11.001

Sinha, S. N., Kumar, K. R., Ungarala, R., Kumar, D., Deshpande, A., Vasudev, K., . . . Pokharakar, S. (2021). Toxicokinetic analysis of commonly used pesticides using data on acute poisoning cases from Hyderabad, South India. *Chemosphere, 268*, 129488. doi:10.1016/j.chemosphere.2020.129488

Skretteberg, L. G., Lyrån, B., Holen, B., Jansson, A., Fohgelberg, P., Siivinen, K., . . . Jensen, B. H. (2015). Pesticide residues in food of plant origin from Southeast Asia – A Nordic project. *Food Control, 51*, 225-235. doi:10.1016/j.foodcont.2014.11.008

Sundar, N., Stanley, S. J., Kumar, S. A., Keerthana, P., & Kumar, G. A. (2021). Development of dual purpose, industrially important PLA–PEG based coated abrasives and packaging materials. *Journal of Applied Polymer Science, 138*(21). doi:10.1002/app.50495

Tang, W., & Wu, J. (2014). Amperometric determination of organophosphorus pesticide by silver electrode using an acetylcholinesterase inhibition method. *Anal. Methods, 6*(3), 924-929. doi:10.1039/c3ay41932k

Tao, C., Yen, C.-S., Liu, J.-T., & Chen, C.-J. (2016). Analytical performance of paper electro-biosensor detection platform for point-of-care diagnosis. *Cellulose, 23*(6), 3799-3808. doi:10.1007/s10570-016-1046-3

Theurillat, X., Dubois, M., & Huertas-Perez, J. F. (2021). A multi-residue pesticide

determination in fatty food commodities by modified QuEChERS approach and gas chromatography-tandem mass spectrometry. *Food Chem, 353*, 129039. doi:10.1016/j.foodchem.2021.129039

Thom, N. K., Lewis, G. G., DiTucci, M. J., & Phillips, S. T. (2013). Two general designs for fluidic batteries in paper-based microfluidic devices that provide predictable and tunable sources of power for on-chip assays. *RSC Advances, 3*(19). doi:10.1039/c3ra40701b

TIMCHALK, C. (2006). Physiologically Based Pharmacokinetic Modeling of Organophosphorus and Carbamate Pesticides. *Toxicology of Organophosphate & Carbamate Compounds*, 103-125.

Varol, S., Başarslan, S., Fırat, U., Alp, H., Uzar, E., Arıkanoğlu, A., . . . Kıbrıslı, E. (2015). Detection of borderline dosage of malathion intoxication in a rat's brain. *Eur Rev Med Pharmacol Sci, 19*(12), 2318-2323.

Vuthijumnonk, J. T., & Shimbhanao, W. (2019). Insecticide Residue Removal by Microbubble Treatments in Fresh Consumed Agricultural Products: A Preliminary Study. *International Journal of Food Engineering, 5*(3).

Vuthijumnonk, J. T., & Shimbhanao, W. (2019). Insecticide Residue Removal by Microbubble Treatments in Fresh Consumed Agricultural Products: A Preliminary Study. *ETP International Journal of Food Engineering*, 205-208. doi:10.18178/ijfe.5.3.205-208

Wang, W., Hu, J., Zhang, R., Yan, C., Cui, L., & Zhu, J. (2020). A pH-responsive carboxymethyl cellulose/chitosan hydrogel for adsorption and desorption of anionic and cationic dyes. *Cellulose, 28*(2), 897-909. doi:10.1007/s10570-020-03561-4

WHO. (1995). *International Programme on chemical safety. WHO recommended classification of pesticide by hazards and guidelines to classification 1994–1995*. Retrieved from

Yadav, I. C., Devi, N. L., Syed, J. H., Cheng, Z., Li, J., Zhang, G., & Jones, K. C. (2015). Current status of persistent organic pesticides residues in air, water, and soil, and their possible effect on neighboring countries: a comprehensive review of India. *Sci Total Environ, 511*, 123-137. doi:10.1016/j.scitotenv.2014.12.041

Yan, J., Ge, L., Song, X., Yan, M., Ge, S., & Yu, J. (2012). Paper-based electrochemiluminescent 3D immunodevice for lab-on-paper, specific, and sensitive point-of-care testing. *Chemistry, 18*(16), 4938-4945. doi:10.1002/chem.201102855

Yang, C.-H., Chen, C.-A., & Chen, C.-F. (2018). Surface-modified cellulose paper and its application in infectious disease diagnosis. *Sensors and Actuators B: Chemical, 265*, 506-513. doi:10.1016/j.snb.2018.03.092

Yetisen, A. K., Akram, M. S., & Lowe, C. R. (2013). Paper-based microfluidic point-of-care diagnostic devices. *Lab Chip, 13*(12), 2210-2251. doi:10.1039/c3lc50169h

Yin, B., Qian, C., Wang, S., Wan, X., & Zhou, T. (2021). A Microfluidic Chip-Based MRS Immunosensor for Biomarker Detection via Enzyme-Mediated Nanoparticle Assembly. *Front Chem, 9*, 688442. doi:10.3389/fchem.2021.688442

Yin, X.-L., Liu, Y. Q., Gu, H.-W., Zhang, Q., Zhang, Z. W., Li, H., . . . Zhou, Y. (2021). Multicolor enzyme-linked immunosorbent sensor for sensitive detection of organophosphorus pesticides based on TMB2+-mediated etching of gold nanorods. *Microchemical Journal, 168*. doi:10.1016/j.microc.2021.106411

Zhai, R., Chen, G., Liu, G., Huang, X., Xu, X., Li, L., . . . Abd El-Aty, A. M. (2022). Enzyme inhibition methods based on Au nanomaterials for rapid detection of organophosphorus pesticides in agricultural and environmental samples: A review. *J Adv Res, 37*, 61-74. doi:10.1016/j.jare.2021.08.008

Zhang, H., Smith, E., Zhang, W., & Zhou, A. (2019). Inkjet printed microfluidic paper-based analytical device (muPAD) for glucose colorimetric detection in artificial urine. *Biomed Microdevices, 21*(3), 48. doi:10.1007/s10544-019-0388-7

Zhang, J., Li, Y., Zhang, T., Zheng, Z., Jing, H., & Liu, C. (2024). Improving pesticide residue detection: Immobilized enzyme microreactor embedded in microfluidic paper-based analytical devices. *Food Chem, 439*, 138179. doi:10.1016/j.foodchem.2023.138179

Zhao, Y., & Talha, M. (2022). Evaluation of food safety problems based on the fuzzy comprehensive analysis method. *Food Science and Technology, 42*. doi:10.1590/fst.47321

มหาวิทยาลัยบูรพา
BURAPHA UNIVERSITY

BIOGRAPHY

NAME	Mr.Wanchalearm Manchan
DATE OF BIRTH	05 December 1999
PLACE OF BIRTH	Nonthaburi, Thailand
PRESENT ADDRESS	106 Village No.5 Sub-district Thung Song Hong District Laksi Road Vibhavadi Rangsit Province Bangkok Postal Code 10210
AWARDS OR GRANTS	2018-2022 Bachelor Science of Chemistry (B.Sc), Faculty of Science, Burapha University, Thailand